THE UNIVERSITY OF CHICAGO

THE ROLE OF CUX1 IN ERYTHROPOIESIS

A DISSERTATION SUBMITTED TO

THE FACULTY OF THE DIVISION OF THE BIOLOGICAL SCIENCES

AND THE PRITZKER SCHOOL OF MEDICINE

IN CANDIDACY FOR THE DEGREE OF

DOCTOR OF PHILOSOPHY

COMMITTEE ON IMMUNOLOGY

BY

STEPHANIE NOEL KONECKI

CHICAGO, ILLINOIS

DECEMBER 2021

This thesis is dedicated to both Peter Koneckis.

TABLE OF CONTENTS

LIST OF FIGURES

LIST OF TABLES

ABBREVIATIONS

RBC: red blood cell

Epo: erythropoietin

BFU-E: burst forming unit-erythroid

CFU-E: colony forming unit-erythroid

CD71: TRFC, transferrin receptor

RI: pro-erythroblast

RII: basophilic-erythroblast

RIII: polychromatic-erythroblast

RIV: orthochromatic-erythroblast

PI3K: phosphoinositide 3-kinases

AKT: protein kinase B

MAPK: mitogen-activated protein kinase

FOG-1: Friend of GATA-1

HSPC: hematopoietic stem and progenitor cell

MDS: myeloid dysplastic syndrome

AML: acute myeloid leukemia

PBS: Phosphate-buffered saline

BSA: Bovine Serum Albumin

FcR: Fc receptor

FMO: full minus one

MEP: megakaryocyte-erythrocyte progenitor cell

ACK: Ammonium-Chloride-Potassium

CPM: counts per million

BP: base pairs

IMDM: Iscove's Modified Dulbecco's Medium

Pen/Strep: Penicillin Streptomycin

SCF: stem cell factor

RNP: ribonucleoprotein

NGS: next generation sequencing

GEO: gene expression omnibus

CUT&RUN: cleavage under targets and release using nuclease

BWA: burrows-wheeler aligner

MACS2: model-based analysis of ChIP-Seq 2

TSA: tichostatin A

FLIM: fluorescence lifetime imaging microscopy

SMD: single molecule detection

CRISPR: clustered regularly interspaced short palindromic repeat

SDS: sodium dodecyl sulfate

Kb: kilobase

GFP: green florescent protein

Ren: Renilla

HSC: hematopoietic stem cell

UTR: untranslated region

HOX: homeodomain

ELISA: enzyme-linked immunosorbent assay

SD: standard deviation

FDR: false discovery rate

PCA: priceable component analysis

FC: fold-change

ChIP-seq: chromatin immunoprecipitation sequencing

TSS: transcriptional start site

SEM: standard error mean

FSC-A: forward scatter area

IP: immunoprecipitation

GlyA: glycophorin A

ATAC-seq: assay for transposase-accessible chromatin using sequencing

GREAT: genomic regions enrichment of annotation tool

IGV: integrative genome browser

UCSC: University of California, Santa Cruz

LC-MS/MS: liquid chromatography with tandem mass spectrometry

ACKNOWLEDGEMENTS

First, I would like to thank my incredible mentor Dr. Megan McNerney. Dr. McNerney has the impossible task of conducting world class scientific research, teaching courses, serving as a physician, keeping the lab finically afloat, managing all the staff, reviewing scientific work, traveling to conferences, and mentoring (pesky) graduate students like myself. I don't know how she manages to do it all, but I'm exceedingly thankful that she does. Dr. McNerney truly is Wonder Woman and everyone in the lab is lucky to serve under her mentorship. I want to sincerely thank her for her scientific excellence, kindness, patience, and ever positive attitude. I would also like to specifically thank her for indulging in my desire to buy ridiculous hematopoietic themed cookies for the lab summer party. Dr. McNerney is an outstanding scientist and enthusiastic and engaged mentor. She provided feedback on each experiment and piece of writing. From my trepidation with mice, to my complete incomprehension of appropriate comma usage, Dr. McNerney has been the perfect blend of academically excellent and empathetic. I would be content to be a fraction of the scientist that she is. Beyond the bench Dr. McNerney taught me how to persist, ask for help, and stop needlessly apologizing. At the beginning of my graduate career she forbade my graduation if I did not stop my constant barrage of unnecessary apologies! This was an accurate and valuable ultimatum. I'm thankful to have had an advisor who truly cares about my development as a person. I hope reflecting back on my years in the lab she can see how much I have grown under her mentorship. I am eternally thankful, Dr. McNerney.

The entire McNerney lab deserves my deepest gratitude. I would like to personally thank Dr. Molly Imgruet for taking my frantic calls from the flow core at 10PM,

Dr. Ningfei An for teaching me everything I know, Saira Khan for her exceptional biochemistry skills (and the best smelling coffee anyone could ask for in an office-buddy), Dr. Jeff Kurkewich for making IP-injections less scary and forever making me laugh, Manisha Krishan for always being around for a snack and a chat and keeping it down to Earth, Weihan Liu for being my computational companion and sharing a love of cats, Dr. Madavi Senagolage for her sage advice (and great sense of humor), Henna Nam for being an absolute joy to teach, Tanner Martinez for being on team immunology, Matt Jottee for keeping the lab grounded and calm, Raven Watson for bringing new enthusiasm and life into the lab, and Dhivyaa Anadan for being the backbone of the CD34 crew. I believe science is a team sport, and I could not have asked for a better team. Thank you.

I would especially like to thank the members of my thesis committee: Dr. Barbara Kee, Dr. Amittha Wickrema, and Dr. Fotini Gounari for their time, thoughtful comments, scientific insight, and mentorship. Thank you for writing me letters of recommendation, supporting me at Works in Progress, and sharing fun red blood cell facts! It was a pleasure to grow as a scientist under your expert guidance.

Several collaborations were essential for the success of this project. First, the work of Dr. Vtyas Bindokas, expert on all things microscopy, was vital for the FLIM component of this work. Additionally, Julian Lutze connected me with the histone modification world at The University of Chicago and helped with confocal microscopy analysis. Dr. Angela Stoddard deserves my thanks for giving great feedback, always being available to talk science, and having an exceedingly cute dog. I need to personally thank the members of the flow cytometry core: Mandel Davis, Robert ‘Bert’

Ladd, Mike Olsen, and of course David Leclerc. Your cytometry expertise helped me keep my science at its best and the fun conversations we would have while sorting cells always lifted my spirits. I hope you enjoy seeing what happened to all of these red cells we sorted. I would also like to thank the members of the Animal Resources Center and Genomics Core Facility.

I would like to thank the Committee on Immunology for shaping me into a strong scientist. Particularly, Pete Savage for helping me take translate my obsessive note taking into tangible scientific understanding.

Very importantly, I would like to thank my friends and family for their unwavering support during the challenge that is graduate school. Thank you to my parents Karen and Peter Konecki for always believing in me. Thank you also for instilling the values of science, education, and curiosity into me at such a young age, and enabling me to believe I can make the world a better place through science. Those nights watching Star Trek certainly paid off. Thank you to my good friends preceding graduate school. In particular Dr. Hannah Stein and Dr. Maria Vercelli, and my oldest friend Monika Gaiser. Thank you to the dear friends I have made throughout this journey, specifically: Dr. Jill Rosenberg my microscope and plant care mentor and friend for life, and Elaine Kouame my fellow burger lover and immunology companion. I could not have done this without your friendship and support. Thanks most importantly to my caring and attentive partner AG Stephan. You've done more than your fair share of dishes while I'm at lab, ordered burritos for me on late-night-lab days, and encouraged me every step of the way. Thank you for your steadfast support, love, and assurance.

ABSTRACT

Anemia is a significant cause of morbidity and mortality in myeloid malignances. Cytogenetic changes are recurrent within malignant hematopoietic stem and progenitor cells, yet their role in anemia pathogenesis remains unknown. One recurrent karyotypic abnormality in myeloid neoplasms is the deletion of part or all of chromosome 7 [-7/del(7q)], which harbors the transcription factor and tumor suppressor gene, *CUX1*. CUX1 knockdown mouse models develop myeloid disease similar to that seen in humans, including a spontaneous, cell intrinsic, and lethal anemia that develops with age. Here, we elucidate the cellular and molecular mechanisms by which CUX1 regulates erythropoiesis. We demonstrate CUX1 knockdown mice have an aberrant stress erythropoiesis response and decreased survival after acute anemia induction. CUX1 insufficient erythroblasts undergo accelerated cell cycling and increased apoptosis. In line with these phenotypes, transcriptome profiling indicates that CUX1-knockdown elicits increased proliferation and decreased erythroid differentiation gene signatures. ATAC-sequencing demonstrated dramatic, global chromatin opening in CUX1-knockdown erythroblasts. As measured by fluorescence lifetime imaging microscopy, this increased chromatin accessibility is concomitant with a disruption in nuclear condensation, which is normally requisite in mammalian erythroblasts for nuclear eviction and terminal differentiation. Finally, we show that CUX1 mediates chromatin compaction by promoting histone deacetylation. Thus, our data implicate in an epigenetic regulatory role for CUX1 in erythropoiesis. Furthermore, these results suggest therapeutic targeting of epigenetic regulators, such as histone acetyl transferases, may have clinical benefit for the anemias associated with loss of CUX1.

CHAPTER 1: INTRODUCTION

This dissertation details the role of CUX1 in red blood cell development. The following section describes the need to understand the process of generating red blood cells, current status of the field, and identification of CUX1 as a potentially critical factor during erythropoiesis.

Red blood cell function and generation

Red blood cell function

The average human adult produces 200 billion red blood cells (RBCs) each day (Neildez-Nguyen et al. 2002). RBC generation is a massive enterprise; an estimated 70% of adult human cells are RBCs. Given their abundance, it is not surprising to find that RBCs carry out one of the most crucial tasks for multicellular survival: oxygen transport. RBCs that disseminate oxygen are ubiquitous across vertebrates (except for Channichthyidae: ice-water fish), and RBC composition is highly conserved, though RBC size varies greatly throughout vertebrata (G. K. Snyder and Sheafor 1999). In humans, RBCs disseminate an estimated 22 moles of dioxygen per day (Wagner, Venkataraman, and Buettner 2011) which are acquired from the lungs and distributed through capillaries across body. Transport is accomplished via oxygen packaging into hemoglobin contained within RBCs. Each cell in the human body, except ironically the RBC itself (which contain no mitochondria), requires oxygen for respiration (Wagner, Venkataraman, and Buettner 2011). Oxygen circulation is essential for survival. Indeed,

without sufficient oxygen circulation to the brain consciousness and then life itself is quickly lost (Lennox, Gibbs, and Gibbs 1935).

Further demonstrating the importance of RBCs, no RBC knockout mouse has generated viable pups. This is such an endemic problem in the field, investigators transplant fetal-liver stem and progenitor cells from such knockouts into adult mice to circumvent the moribund knockout pups. Examples of knockout mice with severe fetal anemia include *Gata-1*-/- (Y. Fujiwara et al. 1996), *Fog-1*-/- (Tsang et al. 1998), *Stat5a-/-5b*-/- (Socolovsky et al. 1999), *Lmo2*-/- (A. J. Warren et al. 1994), *Klf1*-/- (Nuez et al. 1995; Perkins, Sharpet, and Orkin 1995), and *Tmod3*-/- (Sui et al. 2014) mice. While non-erythroid hematopoietic cells are critically important, knock outs can be generated and produce viable litters as evinced by NSG (NOD *scid* gamma) mice (Ishikawa et al. 2005) commonly employed in humanized mouse models for their reduced endogenous immune function. Beyond mouse models, anemias and leukemias are devastating and prevalent human diseases with clear links to RBC dysfunction. However, the roots of many maladies have subtle connections to red cells, such as traumatic injury, cardiac arrest, and respiratory failure. The foundational problem in such ailments is insufficient oxygen circulation, and therefore could theoretically be circumvented by RBC transfer.

RBCs are vitally important because they transport life-sustaining oxygen. Therefore, understanding RBC composition and generation is of critical significance. RBCs are primarily hemoglobin. By weight hemoglobin comprises 96% of an individual RBC and an estimated ~35% of the average mammal (Goldman 2008). In human adults, hemoglobin is transcribed from 3 loci: *HBA1* and *HBA2* which encode the hemoglobin alpha subunit, and *HBB* encoding the beta subunit. One of each alpha

subunit and two beta subunits together each contain a heme group, which comes together to form hemoglobin which can bind 4 oxygen molecules (Schroeder and Cavacini 2010). To maximize room for hemoglobin, erythroblasts condense and expel their nucleus and degrade their organelles. Reticulocytes are thought to degrade their organelles and mitochondria through autophagy (Ney 2011), while nuclear extrusion is a complex process that will be outlined in more detail below. Thus, through removal of all excess components, the RBC comes to be 96% hemoglobin with a unique bi-concave disc shape. The compact size and unique shape of mammalian enucleated RBCs is thought to enable RBCs to traverse through tight capillaries and increase the cell volume dedicated to hemoglobin storage (Ji, Murata-Hori, and Lodish 2011). In fact, it is hypothesized that the unique structure and composition of enucleated mammalian RBCs, along with reduced oxygen availably during the Permian/Triassic period, enabled the evolution of endothermy (Soslau 2020).

Given the easy access and constant regeneration of RBCs, RBCs are an excellent model to study biological phenomenon at large. From the emergence of modern science to current clinical trials, RBCs have always been on the precipice of discovery. Following in the invention of the compound microscope in 1590, blood was one of the first tissues to be investigated in 1658 by Jan Swammerdam (Hajdu 2003). Throughout the 17th century ‘red corpuscles’ were described as the sole characteristic of peripheral blood under the first compound microscopes (Hajdu 2003). Many Nobel prizes can be attributed to work on RBCs. The Nobel Prize in Physiology or Medicine has been awarded for RBC research in 1902 (Ronald Ross – malaria), 1930 (Karl Landsteiner – human blood groups), 1934 (George Whipple, George Minot, William

Murphy – liver therapy for anemia), 2015 (Tu Youyou – malaria), and 2019 (William Kaelin, Peter Ratcliffe, and Gregg Semenza – erythropoietin and hypoxia), and the Nobel Prize in Chemistry in 1962 was awarded for the crystal structure of hemoglobin. More recently, RBCs remain on the cutting edge of science with sickle cell anemia disease at the forefront of gene editing therapy (Abraham and Tisdale 2021).

Red blood cell generation

Given the critical role for RBCs in mammalian survival and role in prominent scientific discoveries, how does one 'Turn [a] Cell Red' (Richmond, Chohan, and Barber 2005)? The process of red cell development can broadly be divided into two phases: 1) the proliferative phase and 2) terminal erythroid differentiation (Figure 1). During the proliferative phase erythroblasts are Erythropoietin (Epo) dependent. Here, Burst Forming Unit Erythroid (BFU-E) become Colony Forming Unit Erythroid (CFU-E) erythroblasts whose survival is directly dependent on Epo signaling (Lin et al. 1996; Wu et al. 1995). Epo is produced by kidney cells in response to hypoxic stress (Watowich 2011). Thus, this system allows the body to maintain a reserve of erythroblasts in case of sudden RBC loss. As cells transition from the Epo dependent proliferative phase into terminal erythroid differentiation surface expression of the Epo receptor is gradually lost (Jing Zhang et al. 2003). In the terminal phase, erythroblast cell cycle and differentiation are intimately connected. Transition through each of the four progenitors is linked with one iteration through the cell cycle (Hattangadi et al. 2015). CD71 (TRFC, transferrin receptor) and Ter119 (LY76) are used to mark murine erythroblasts throughout terminal erythroid differentiation (Figure 1). These markers delineate the four sequential

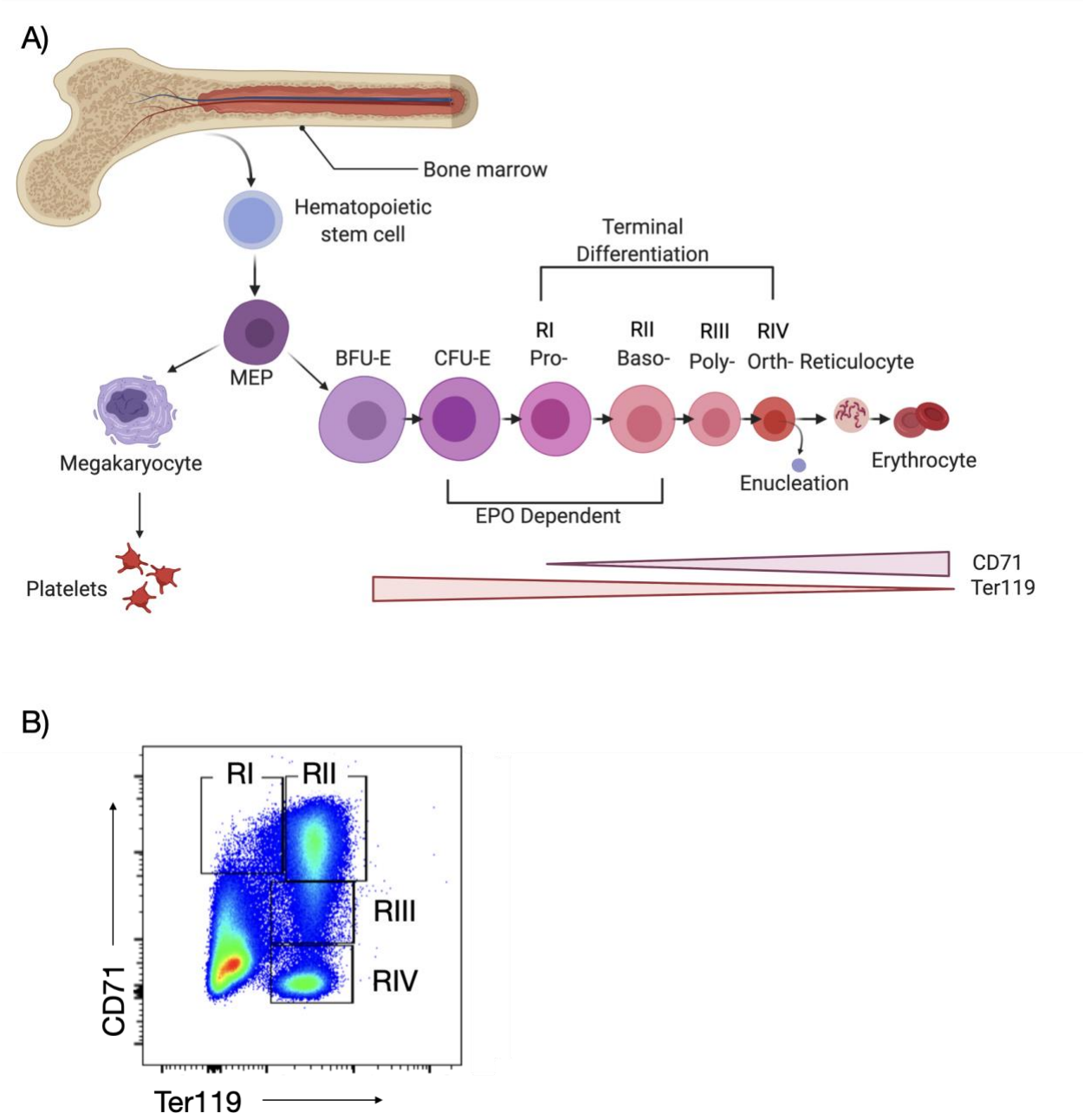

Figure 1. Red blood cell generation. (A) An overview of the generation of erythrocytes. Like all hematopoietic cells, RBCs originate from hematopoietic stem cells (HSCs). Commitment to the erythroid lineage occurs at the Burst Forming Unit-Erythroid (BFU-E) stage. Erythroblasts then become Colony Forming Unit-Erythroid (CFU-E) cells. Next, during terminal erythroid differentiation each progressive step through development is coupled with one iteration of the cell cycle. The progression begins with pro-erythroblasts (RI) and proceeds through basophilic-erythroblasts (RII), polychromatic-erythroblasts (RIII), and orthochromatic-erythroblasts (RIV). Throughout this process both nuclear and cellular size are dramatically reduced. This culminates in

Figure 1, continued

the nuclear ejection forming reticulocytes. These cells then migrate from the bone marrow and into the peripheral blood where they undergo final maturation into RBCs. **(B)** Maturation of erythroblasts can be mapped using the cell surface markers CD71 and Ter119, which correspond to RI-RIV erythroblasts as shown.

populations of erythroblasts: RI pro-erythroblasts, RII basophilic-erythroblasts, RIII polychromatic-erythroblasts, and RIV orthochromatic-erythroblasts. Orthochromatic-erythroblasts then enucleate and emigrate from the bone marrow into the peripheral blood where they become reticulocytes, and then fully developed RBCs.

As one might expect, many of the signaling cascades regulating the proliferative phase are Epo dependent. Following binding of Epo to Epo-Receptors on an erythroblast, several signaling cascades are activated including Stat5 (Klingmüller et al. 1996), PI3K/Akt (Ghaffari et al. 2006), and MAPK (Jing Zhang and Lodish 2007). Following binding, Jak2 kinase phosphorylates the intercellular region of the Epo-Receptor (Witthuhn et al. 1993). This leads to a conformational change recruiting Stat5 (Chin et al. 1996; Klingmüller et al. 1996) and the p85 subunit of PI3K (Damen et al. 1993, 1995) to the internal regions of the Epo-Receptor, thus beginning the signaling cascade. Stat5 regulates erythroblast survival through Bcl_{XL} (Socolovsky et al. 2001), and PI3K promotes erythroblast survival and proliferation though phosphorylation of AKT and subsequent inhibition of FOXO3a (Bouscary et al. 2003; Martelli et al. 2010; Sivertsen et al. 2006). MAPK has subtle effects on proliferation and differentiation through AKT, as demonstrated by *in vitro* mouse fetal liver systems (Jing Zhang and Lodish 2007). As erythroblasts progress through differentiation they downregulate the Epo-Receptor and transition from Epo dependence to fibronectin (Ji, Murata-Hori, and Lodish 2011). α4Bβ1 integrins expressed on late erythroblasts interact with fibronectin to support proliferation and suppress apoptosis, in part through Bcl_{XL} (Eshghi et al. 2007). These signaling cascades and subsequent induction of canonical erythroid transcription factors is summarized in Figure 2.

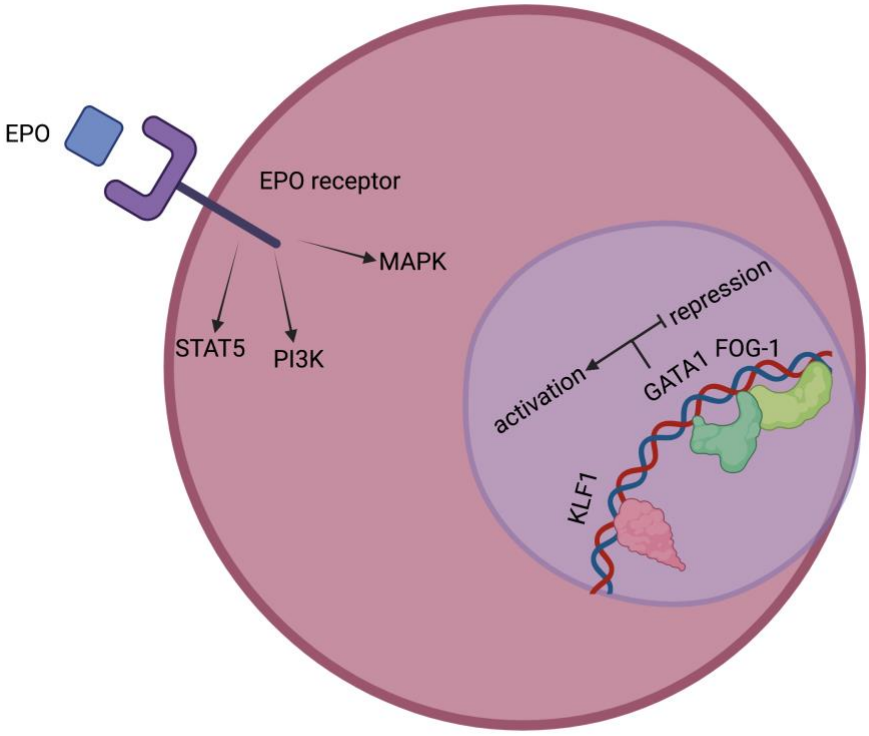

Figure 2. Summary of factors in erythropoiesis. During the EPO dependent phase, the EPO-receptor is expressed on the cell surface of erythroblasts. EPO binding the EPO-receptor signals erythroblast survival, proliferation, and differentiation through STAT5, PI3K, and MAPK. Several transcription factors required for erythropoiesis include KLF1, GATA-1, and FOG-1. GATA-1 can act both as a transcriptional activator and a repressor.

Transcriptional regulation of erythroblasts is orchestrated by several key lineage-restricted transcription factors including GATA-1, FOG-1, TAL1 (SCL), LMO2 (RBTN2), and KLF1 (ELKF) (Cantor and Orkin 2002). GATA-1, arguably the most recognizable erythroid transcription factor, contains two zinc fingers and binds its name granting (A/T)GATA(A/G) consensus sequence (Evans, Reitman, and Felsenfeld 1988). GATA-1 primarily binds distal regulatory regions (~85%), most of which are marked as enhancers by H3K4me1 (Yong Cheng et al. 2009), instead of promoters (~15%) (T. Fujiwara et al. 2009; Yu et al. 2009). Direct GATA-1 chromatin targets have both activated and repressed expression (Kerenyi and Orkin 2010). GATA-1 gene activation involves a complex of GATA-1, LMO2, LDB1, TAL1, and E2A (Cohen-Kaminsky et al. 1998; Wadman et al. 1997). The components of the repression complex are thought to include the NuRD complex (Hong et al. 2005; Rodriguez et al. 2005) and the LSD1-CoREST (Rodriguez et al. 2005) complex, or the polycomb repressive complex (Ross et al. 2012; Yu et al. 2009). As its name suggests, friend of GATA-1 (FOG-1) binds GATA-1 (Tsang et al. 1997), and *Fog-1* knockout mice (Tsang et al. 1998) suffer a similar embryonic anemia as *Gata-1* knockout mice (Y. Fujiwara et al. 1996). KLF1 is also an essential erythroid transcription factor that binds distal enhancers (Tallack et al. 2010). Although, findings suggest the role of KLF1 during erythropoiesis may be regulation of the cell cycle: enabling cell cycle exit for enucleation during terminal differentiation (Gnanapragasam et al. 2016).

Imaging cytometry of *ex vivo* differentiating erythroblasts showed *Klf1* knockout cells condense their nucleus but fail to enucleate (Gnanapragasam et al. 2016). The mechanism proposed to be responsible for the enucleation failure is insufficient

expression of the cell cycle inhibitors p18 and p27 (Gnanapragasam et al. 2016). There are many other examples of the interplay between the cell cycle and erythroblast differentiation. Knockout of *Rb*, the regulator between G1-to-S-phase, results in an erythropoietic block and anemia in mice (Sankaran, Orkin, and Walkley 2008). The Rb-regulated factor *E2f-2* is required for nuclear condensation and deletion results in anemia (Swartz et al. 2017). Knockout of *E2f-4* (Kinross et al. 2006) and D-Cyclins (Kozar et al. 2004) also leads to anemia. Taken together these studies indicate the inseparable connection between erythroblast proliferation and differentiation.

Red cell enucleation

The final cellular acts required of an erythroblast before enucleation is nuclear condensation and polarization. The nucleus of an erythroblast is condensed 10-fold in preparation for its extrusion (Mei, Liu, and Ji 2021). Several other cell types, namely skin keratinocytes and lens fiber cells, also remove their nuclei as a function of normal differentiation. However, the mechanisms governing this process appear to be distinct. While RBCs condense and expel their nucelli, skin keratinocytes and lens fiber cells are thought to internally degrade their nucleus (Rogerson, Bergamaschi, and O'shaughnessy 2018). The molecular mechanisms of enucleation in erythroblasts are just now coming into focus (reviewed in (Mei, Liu, and Ji 2021)). The process of enucleation can be broken down into three steps 1) nuclear condensation 2) nuclear polarity and 3) nuclear extrusion. These steps are summarized in Figure 3.

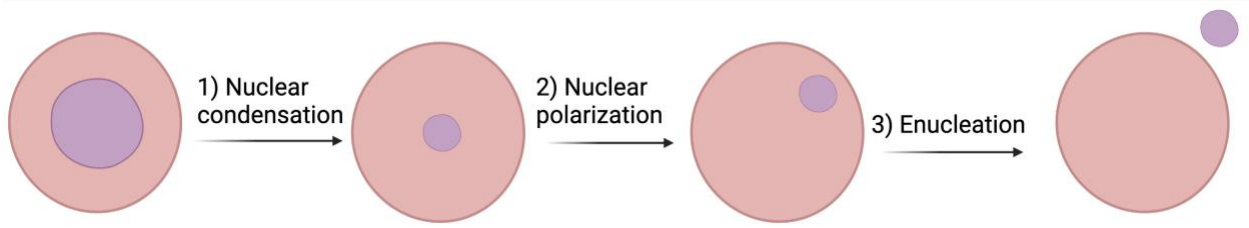

Figure 3. Overview of erythroblast enucleation. Nuclear condensation is achieved via epigenetic changes including histone deacetylation. Nuclear polarization and enucleation require synchronization of structural proteins culminating in the formation of an actin contractile ring during enucleation.

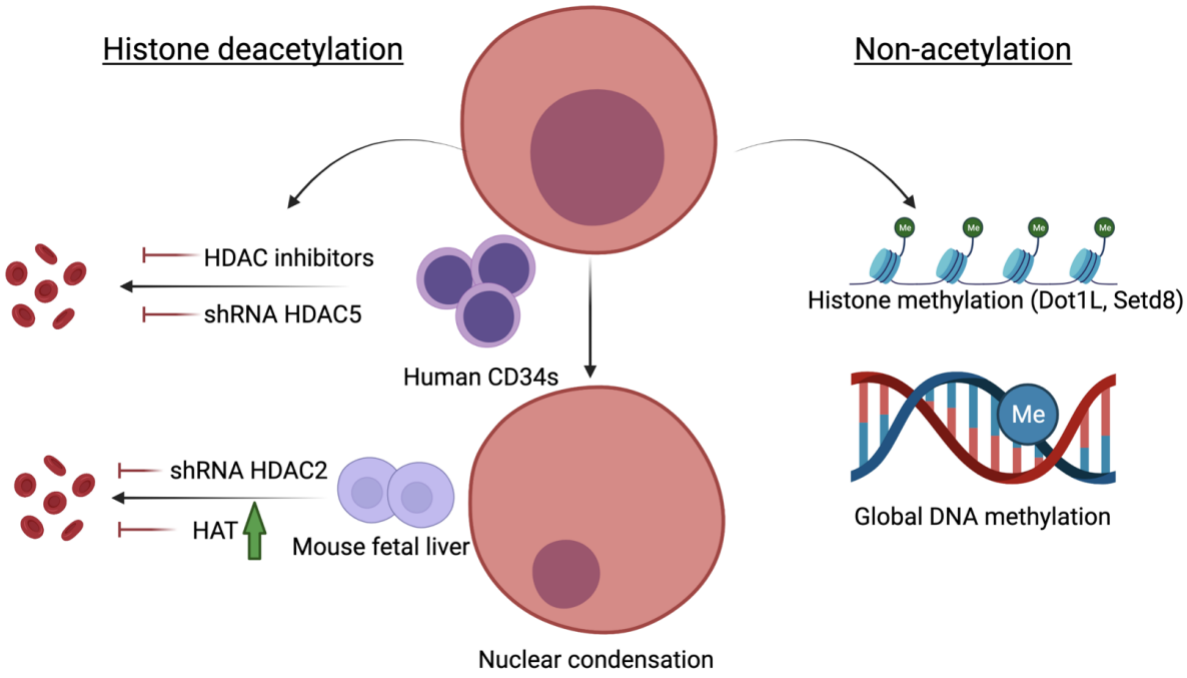

Figure 4. Emerging mechanisms of nuclear condensation in erythroblasts. Epigenetic changes are thought to be widely responsible for nuclear condensation, these can be broadly sub-divided into histone deacetylation and non-acetylation mechanisms. Non-acetylation mechanisms include a requirement for histone methylation demonstrated by erythropoietic defects in Dot1L (Feng et al., 2010). and Setd8 insufficiencies (Mallik, Getman, and Steiner 2015) and global DNA methylation (Shearstone et al., 2011). Global histone deacetylation is an appreciated requirement for erythroid nuclear condensation. This has been demonstrated using *in vitro* human CD34 and mouse fetal liver cultures. The addition of HDAC inhibitors (Yamamura et al., 2006) and HDAC5 shRNA/siRNA (Wang et al, 2021) prevents nuclear condensation and enucleation. It has further been shown that inhibition of HDAC2 prevents erythroid maturation (Ji et al., 2010). Furthermore, the mechanism by which Myc overexpression perturbs erythroid development was identified as overexpression of the HAT Gcn5 (Jayapal et al, 2010).

In preparation for enucleation the nucleus of erythroblasts is condensed 10-fold. The factors required for this process are gradually emerging (Figure 4). Nuclear condensation is thought to require changes in the epigenetic modifications on histones (reviewed in (Sundaravel, Steidl, and Wickrema 2021)). In particular, histone deacetylation is required for nuclear condensation in erythroblasts. *In vitro* cultures have shown that H4K12Ac is lost during erythroid differentiation (Popova et al. 2009). In the same study, histone deacetylase (HDAC) activity was blocked during *in vitro* differentiation using trichostatin-A. The resulting erythroblasts failed to condense their chromatin and enucleate (Popova et al. 2009). Thus, HDAC activity is required for erythropoiesis. A second study using mouse fetal liver culture systems identified shRNA knockdown of *Hdac2* resulted in the similar block in enucleation (Ji et al. 2010). Following Myc-overexpression in fetal liver erythroblasts the histone acetyltransferase (HAT) *Gcn5* was overexpressed (Jayapal et al. 2010). This resulted in an increase in H3K9Ac and H4K12Ac, and subsequent hyperproliferation and dyserythropoieis (Jayapal et al. 2010). More recently, H3K27Ac has been shown to globally decrease during erythroid development (Romano et al. 2020). Histone deacetylation is also required in human erythroblasts. Human CD34+ cells cultured toward erythroblast differentiation with HDAC inhibitors have an increase in apoptosis (Yamamura et al. 2006). A recent report found human *in vitro* erythroid cultures with knockdown of HDAC5 leads to increased H4K12Ac, insufficient chromatin condensation, and failure to enucleate (Y. Wang et al. 2021).

Beyond histone deacetylation, histone methylation is also important for nuclear condensation and enucleation. Setd8 is the protein responsible for mono-methylating

H4K20 generating H4K20me1. Deletion of Setd8 results in an embryonic lethal anemia due to a failure in nuclear condensation and erythroblast apoptosis (Malik et al. 2017). Mutation of *Dot1l*, which methylates H3K79, also results in an embryonically fatal anemia (Feng et al. 2010). Epo mediated signaling may directly influence histone modification to facilitate nuclear condensation in preparation for enucleation. In fact, direct Stat5 targets following Epo-Receptor signaling include *Suv420h2* (H4K20 trimethylase) and *Kat2b* (HAT) (Gillinder et al. 2017). These works demonstrate that histone modification is a crucial component to erythroid nuclear condensation. However, the factors guiding the many non-specific histone modification enzymes to their genomic targets in erythroblasts remains unknown.

Nuclear polarity and extrusion require a cascade of structural proteins. These cellular proteins establish polarity between the nascent reticulocyte and the to-be extruded nucleus, resulting in distinct cellular membrane compositions. The cytoskeletal membrane of the reticulocyte contains Band 3, spectrins, ankyrin, protein 4.1, and glycophorin A/C (Koury, Koury, and Bondurant 1989). While the adhesion molecule EMP, Bβ1-integrin, and α4 integrin, and CD71 are sequestered onto the membrane of the extruded nucleus (Mei, Liu, and Ji 2021). Proper membrane protein segregation is critical for RBC maturation. This is demonstrated by the elliptocytic erythrocytes found in hereditary spherocytosis and elliptocytosis patients who have mutations in the protein 4.1R (Salomao et al. 2010).

Formation of an actin contractile ring, much like during cytokinesis, is required for division between the reticulocyte and enucleated nucleus (Mei, Liu, and Ji 2021). This was first studied using mouse *in vitro* splenic erythroblasts treated with Friend virus

(Koury, Koury, and Bondurant 1989). The authors induced *in vitro* enucleation and studied partitioning of cytoskeletal proteins (Koury, Koury, and Bondurant 1989). Upon treatment with the F-actin inhibitor cytochalasin D, the authors found complete ablation of enucleation (Koury, Koury, and Bondurant 1989), confirming actin is required for enucleation. Subsequent work has shown contractile ring formation in erythroblasts is dependent on Rac GTPases (Ji, Jayapal, and Lodish 2008; Konstantinidis et al. 2012), mDia2 (Ji, Jayapal, and Lodish 2008) , myosin IIB (Ubukawa et al. 2012), and Tropomodulin3 (Sui et al. 2014).

Red cell failure

Continuous RBC generation is an enormous biological challenge. Given both the large quantity of cells required and the cellular complexity of RBC generation, it is not surprising that RBC dysfunction is a common pathogenesis of disease (Figure 5). Anemia, a deficiency in RBCs, is a particularly salient example, affecting up to a third of the world population (Chaparro and Parminder 2019). While many anemias can be explained by environmental deficiencies, those that cannot are often caused by mutations. Hereditary anemias most commonly arise from mutations in genes encoding RBC membrane proteins or the globin genes (Crispino and Weiss 2017). An example of mutations in the globin genes translating to disease is sickle-cell disease. This devastating and common disease is a collective term for mutations in the hemoglobin genes leading to the deformation of RBCs into crescent shapes (Booth, Inusa, and Obaro 2010). In the emblematic mutation, a single change in the β-globin gene results in the replacement of a glutamic acid with a valine causing a distortion of the RBC

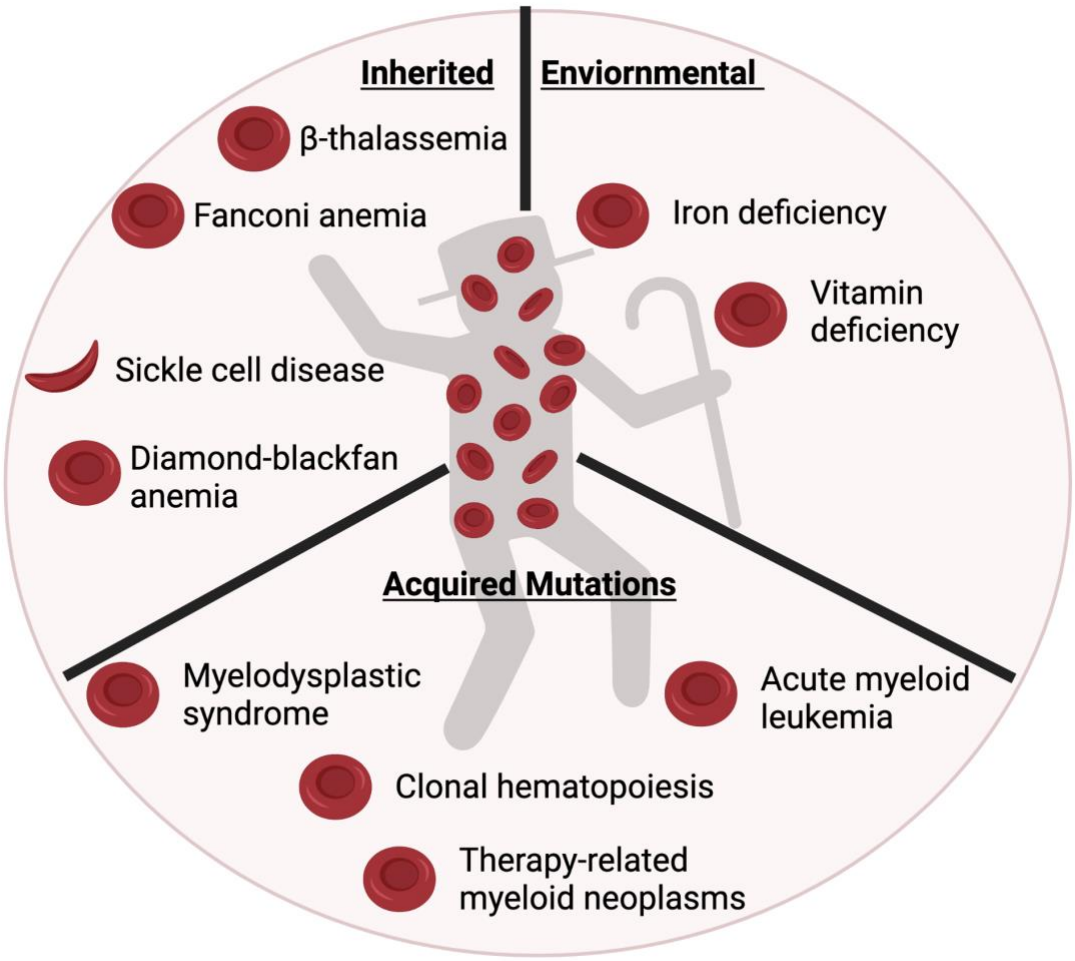

Figure 5. Overview of anemia. The causes of anemia can be broadly divided into environmental factors, inherited mutations, and acquired mutations. Many anemias can be attributed to environmental causes such as iron or vitamin deficiencies. Those that cannot are often caused by mutations in hematopoietic stem and progenitor cells (HSPCs). Hereditary anemias are caused by inherited germline mutations in genes required for red cell development or function. Anemia can also develop as a result of acquired mutations within HSPCs.

shape into a sickle which can no longer transverse through narrow capillaries (Booth, Inusa, and Obaro 2010). Congenital dyserythropoietic anemias are diseases characterized by insufficient erythroblast differentiation (Crispino and Weiss 2017) caused by mutations in *CDAN1*, *CC15ORF41*, *SEC23B*, and *KIF23* (Babbs et al. 2013; Iolascon et al. 2013). Another example, Diamond-blackfan anemia, is a hereditary anemia characterized by insufficient RBC production, which commonly occurs with mutations in the ribosomal proteins (Crispino and Weiss 2017). Fanconi anemia is also associated with mutations in *FANC*- genes, many of which are involved in DNA-repair or replication (Castella et al. 2011). Germline mutations in transcription factors can also confer a hereditary anemia. Mutations in *GATA1* (K.E. et al. 2000), *GFI1B* (Monteferrario et al. 2014), and *KLF1* (Arnaud et al. 2010; Singleton et al. 2008; Viprakasit et al. 2014) have been associated with the development of anemia in patients (Crispino and Weiss 2017). Mutations in erythroid transcription factor binding sites can also result in anemia, as demonstrated by a subset β-thalassemia patients with mutations in the β-globin promoter or locus of control (Thein 2013). Even anemias thought to be driven by iron insufficiency may in fact have a genetic component, evidenced by *TMPRSS6* mutations (Finberg et al. 2008).

Distinct from the inherited hereditary anemias described above, are anemias stemming from acquired somatic mutations in hematopoietic stem and progenitor cells (HSPCs). As discussed below mutations in HSPCs are often acquired with age or cellular stress and allow for leukemic transformation, and subsequent development of anemia.

7q, myeloid neoplasms, and anemia

Hematopoietic cells were the first tissue to be described to carry chromosomal translocations associated with the pathogenesis of cancer (Rowley 1973). One particularly common mutation in HSPCs that gives rise to anemia is the deletion of chromosome 7 or the deletion of the long arm of chromosome 7 [-7/del(7q)]. Loss of all or part of chromosome 7 is the most common high-risk cytogenetic abnormality (Greenberg et al. 1997). 42% of pediatric and 14% of adult myeloid dysplastic syndrome (MDS) patients have -7/del(7q) (Luna-Fineman et al. 1999). -7/del(7q) is significant beyond MDS, and is prevalent across myeloid diseases including juvenile myelomonocytic leukemias (Luna-Fineman *et al.*, 1999, 33%), chronic myelomonocytic leukemia (14%, Luna-Fineman *et al.*,1999) and *de novo* acute myeloid leukemia (AML) (10-15%, Baudard *et al.*, 1994). Up to 78% of aplastic anemia patients acquire -7/del(7q) at time of disease progression to AML or MDS (Luna-Fineman *et al.,* 1995). Additionally, -7/del(7q) is found in 50% of therapy-related myeloid neoplasms, a secondary myeloid malignancy resulting from chemotherapy and/or radiation used to treat a primary cancer (Armitage *et al.*, 2003; Linehan *et al.*, 2018). Regardless of the disease type, patients with -7/del(7q) have a poor prognosis and do not respond to conventional therapy.

While -7/del(7q) has been identified as a common cytogenetic alteration for nearly 50 years (Schneider and Delwel 2018) a major knowledge gap is the mechanism of how -7/del(7q) disrupts normal erythropoiesis. Originally, it was believed that loss of both copies of a tumor suppressor was required for cancer transformation (Knudson 1971). However, modern models predict many tumor suppressors are instead

haploinsufficient, meaning that loss of a single copy of a gene is sufficient for disease development (Davoli et al. 2013; White et al. 2013). Among potential tumor suppressor genes on chromosome 7, the only gene with recurring loss of both alleles is EZH2 (Ernst et al. 2010; Q. Zhang et al. 2019), suggesting that the other tumor suppressor gene(s) on 7q are haploinsufficient. Disease perpetuated by -7/del(7q) may also be representative of a contiguous gene syndrome wherein the loss of several neighboring genes has a cooperative or synergistic effect on pathogenesis.

Three commonly deleted regions on 7q have been identified: 7q35-36, 7q34, and 7q22 (Le Beau et al. 1996; Döhner et al. 1998; Jerez et al. 2012; McNerney et al. 2013). These regions each contain several possible candidates for the tumor suppressor(s) on 7q including KMT2C, EZH2, and CUL1. *KMT2C* (*MLL3*), an H3K4 methyltransferase is encoded on the 7q35-36 locus. KMT2C is a haploinsufficient tumor suppressor, but is not sufficient to accelerate myeloid disease (Chen et al. 2014). On 7q36.1 is the H3K27 methyltransferase component of the Polycomb Repressive Complex 2 (PCR2) *EZH2*. EZH2 is often mutated in myeloid neoplasms (Ernst et al. 2010), however *Ezh2* loss is insufficient for its development (Shimizu et al. 2016). 7q36.1 also contains CUL1, which is mutated in myeloid malignances (Hosono et al. 2014). LUC7L2, a splicing factor, is contained on the 7q34 locus, and splicing factors mutations are commonly found in myeloid dysplastic syndromes (Yoshida et al. 2011). 7q22 contains the homeobox-containing transcription factor CUX1, which will be discussed in the next section.

There are candidate tumor suppressors on chromosome 7 beyond the commonly deleted regions of 7q. These include *SAMD9L*, *KTM2E*, and *DOCK4*. Samd9l knockout leads to MDS, bone marrow failure, and anemia (Nagamachi et al. 2013). Loss of

Kmt2e has a mild erythroid phenotype in mice (Heuser et al. 2009). The guanine exchange factor DOCK4 is both critical for red cell development (Sundaravel et al. 2015, 2019) and recurrently disrupted in myeloid neoplasms (Hosono et al. 2014; Kjeldsen and Veigaard 2013; Yajnik et al. 2003). Thus, the pathogenesis -7/del(7q) in myeloid neoplasms and subsequent anemia involves many potential factors, though the relative contribution of each individual gene remains to be determined.

CUX1 is a tumor suppressor on 7q

As briefly described above, CUX1 is a non-clustered HOX family transcription factor (Figure 6). Full length CUX1 (also known as CULT1 or CDP) is an analog transcription factor with four DNA-binding domains: three CUT repeats and a C-terminal homeodomain (Mailly et al. 1996). CUX1 is highly conserved from *Drosophila* to humans and is essential for development (Ellis et al. 2001; Luong et al. 2002; Sinclair et al. 2001; Tufarelli et al. 1998). *CUX1* is one of the largest genes in the mammalian genome and has multiple isoforms, two of which are ubiquitously expressed (Ramdzan and Nepveu 2014).

In a breakthrough for the field, our lab identified *CUX1* to be a tumor suppressor gene encoded in the commonly deleted segment of chromosome band 7q22 (Mcnerney et al. 2013). The evidence for *CUX1* as a tumor suppressor gene is strong (Figure 6). Through transcriptome sequencing and SNP array analysis on *de novo* and therapy-related myeloid neoplasms with and without -7/del(7q), our lab identified *CUX1* as the tumor suppressor gene on the commonly deleted region of 7q22 (Mcnerney et al. 2013). *CUX1* was the most significant differentially expressed gene within the deleted

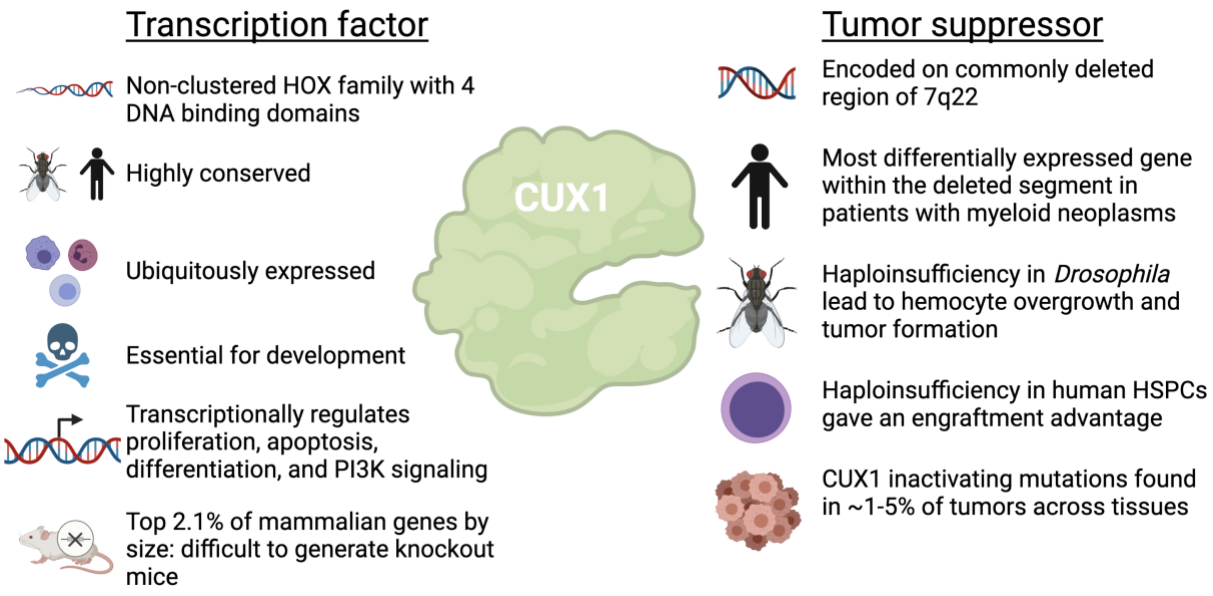

Figure 6. CUX1 is a tumor suppressor and transcription factor. The evidence supporting the conclusion that CUX1 is a tumor suppressor gene is strong. It is encoded on the commonly deleted region of 7q22, it is the most differentially expressed gene in the commonly deleted segment in patients with myeloid neoplasms (McNerney et al., 2013), CUX1 haploinsufficiency lead to hemocyte overgrowth and tumor formation in *Drosophila Melanogaster* and gave an engraftment advantage for human HPSCs in mouse xenotransplantation studies (McNerney et al., 2013), and CUX1 is commonly inactivated across a variety of different tumor types (Wong et al., 2013). CUX1 is a non-clustered HOX family transcription factor with 4 DNA binding domains (described in greater detail in Figure 7B). CUX1 is ubiquitously expressed, highly conserved, and essential for survival (Ellis et al. 2001; Luong et al. 2002; Sinclair et al. 2001; Tufarelli et al. 1998). It has been previously demonstrated that CUX1 transcriptionally regulates proliferation, apoptosis, and PI3K signaling (An et al. 2018; Arthur et al. 2017; Blochlinger, Jan, and Jan 1991; Mcnerney et al. 2013; Nepveu 2001). Being both essential and such a large gene, attempts to generate CUX1 knockout mice have largely failed (Ellis et al. 2001; Luong et al. 2002; Sinclair et al. 2001; Tufarelli et al. 1998).

segment, and was expressed at haploinsufficient levels in patients. Haploinsufficiency of the highly conserved ortholog, *cut*, led to hemocyte overgrowth and tumor formation in *Drosophila*. Additionally, *CUX1* haploinsufficiency gave an engraftment advantage to human HSPCs in mouse xenotransplants. Further supporting its role as a tumor suppressor, *CUX1* inactivating mutations occur independently of -7/del(7q) and carry a poor prognosis (Lindsley et al. 2017; Wong et al. 2013). Wong et al. reported *CUX1* inactivating mutations in ~1-5% of a diverse array of tumor types, demonstrating *CUX1*s importance in cancer in general (Wong et al. 2013).

CUX1 in hematopoiesis: CUX1 loss leads to anemia

The breakthrough discovery of CUX1 as a tumor suppressor gene on 7q generated interest in the molecular function of CUX1 during hematopoiesis. Previous work characterized CUX1 as a transcriptional regulator, with different isoforms acting as activators or repressors. (S. R. Snyder et al. 2001). RNA-seq following CUX1-knockdown in K562 cells confirms this role (Arthur et al. 2017). However, in human CD34+ cells RNA-seq after CUX1 knockdown leads to a decrease in transcription for 81% of differentially expressed genes, suggesting CUX1 acts as an activator (An et al. 2018). Previous reports indicate that the transcriptional targets of CUX1 include regulators of the cell cycle, proliferation, apoptosis, and differentiation (An et al. 2018; Arthur et al. 2017; Blochlinger, Jan, and Jan 1991; Mcnerney et al. 2013; Nepveu 2001). In particular, PI3K signaling is a well-established pathway directly regulated by CUX1. CUX1 controls transcription of the PI3K inhibitor *PIK3IP1*, and with CUX1 knockdown there is enhanced PI3K signaling and tumor growth (Wong et al. 2013). It is likely that

CUX1 plays a unique role in gene expression across divergent cell types, and more work is needed to comprehensively characterize the role of CUX1 in transcription.

How CUX1 itself is transcriptionally regulated is not well understood. CUX1 protein levels are increased after TGF-β treatment in lung fibroblasts (Ikeda et al. 2016). PI3K signaling may represent a transcriptional feedback loop wherein PI3K-AKT signaling promotes CUX1 expression (Ripka et al. 2010) which then upregulates PIK3IP1 expression (Wong et al. 2013) thereby downregulating PI3K signaling. However, beyond this hypothetical feedback loop, it is unknown how transcription of CUX1 is controlled. As CUX1 is a dosage dependent analog transcription factor, uncovering the mechanisms by which CUX1 transcription is regulated remains an important avenue for future work.

CUX1 is ranked in the top 2.1% of all mammalian genes by size. In fact, *Cux1* shares exons with an entirely different gene *Casp* which encodes a Golgi-associated protein (Gillingham, Pfeifer, and Munro 2002). Being one of the largest and most complicated genes in the mammalian genome, the generation of traditional *Cux1* knockout mice has proven quite challenging. Previous attempts to generate *Cux1* knockout mice have spanned a wide range of results from embryonic lethality to no evident phenotype, likely due to hypomorphic protein expression (Ellis et al. 2001; Luong et al. 2002; Sinclair et al. 2001; Tufarelli et al. 1998). Our lab developed *CUX1* shRNA knockdown mice as an innovate way to circumvent these problems (An et al. 2018). We generated two shRNA strains, $Cux1^{low}$ and $Cux1^{mid}$, with 12% and 54% residual CUX1 protein as measured in thymocytes, respectively (Figure 7). CUX1 knockdown in these mice led to MDS and MDS / myeloid proliferative neoplasm with a

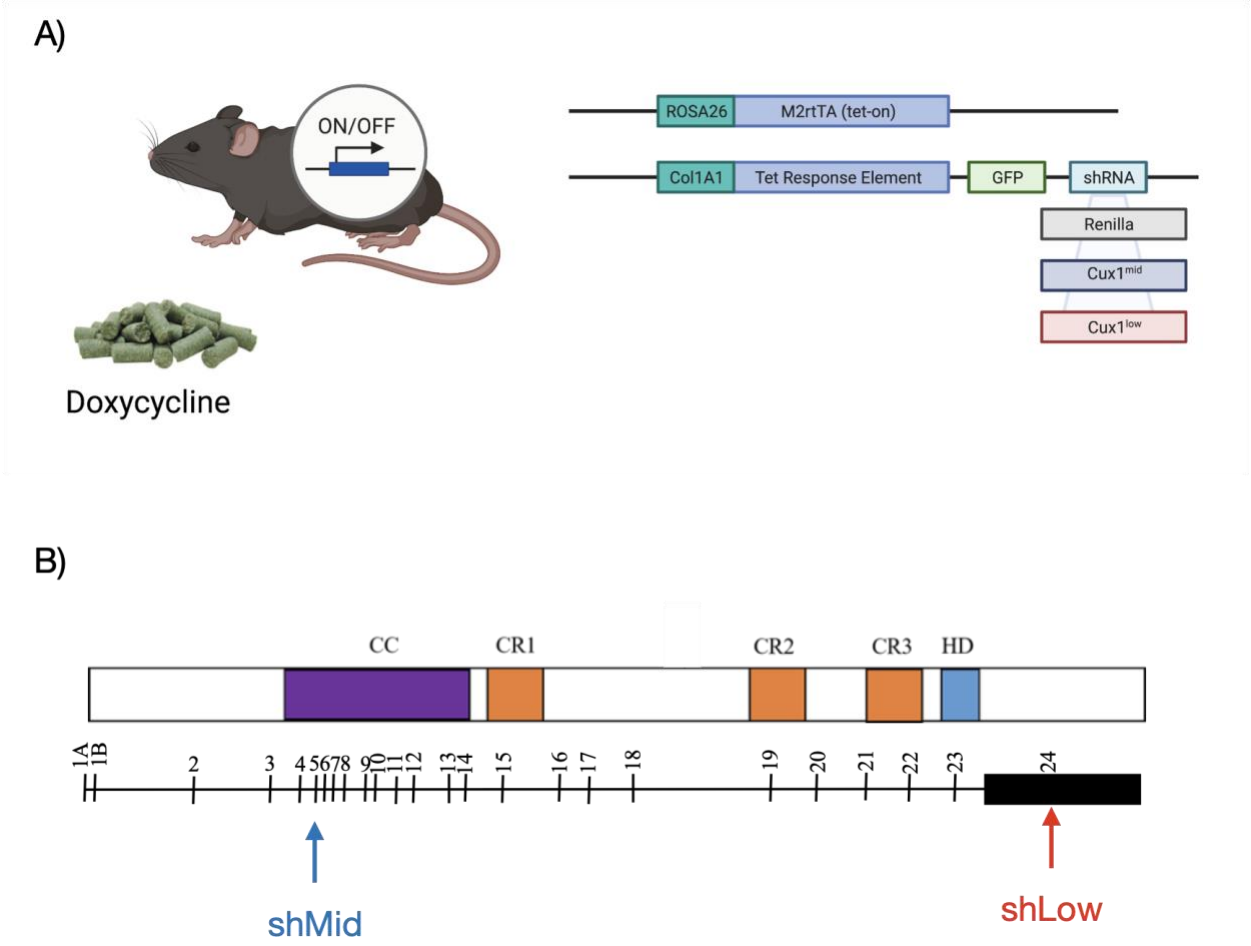

Figure 7. Inducible CUX1 knockdown mouse model. (A) CUX1 knockdown is induced upon administration of doxycycline infused chow. This activates the M2rtTA (tet-on) imbedded within the ROSA26 promoter. Tet binds the Tet Response Element under the Col1A1 locus to induce expression of GFP and an shRNA. The three options for shRNAs include an shRNA targeting Renilla luciferase which serve as wildtype littermate controls or one of two shRNAs targeting CUX1. The Cux1^{mid} shRNA results in an intermediate level of residual CUX1 protein and the Cux1^{low} shRNA results in a low level of residual CUX1 protein. **(B)** CUX1 contains 4 DNA binding domains: 3 cut repeats (CR) and the CUT homeodomain (HD). 24 coding exons, some of which are shared with the Golgi associated protein *Casp*. The shRNA for Cux1^{mid} mice target exon 5, which is shared with *Casp*. The Cux1^{low} shRNA targets the 3' untranslated region of exon 24 which is unique to CUX1 and not shared with *Casp*.

lethal and cell intrinsic anemia. The peripheral blood of Cux1^{low} mice demonstrated RBCs with anisocytosis, poikilocytosis, and polychromasia, all suggesting a severe dysplasia. RNA-seq analysis confirmed that CUX1 knockdown hematopoietic cells have increased proliferation and PI3K signaling *in vivo*. Taken together, these studies provide strong evidence that CUX1 is required for protection from the development of anemia, and therefore a critical erythroid transcription factor.

Aims of the thesis: critical gaps in knowledge that will be addressed

As introduced above critical gaps in knowledge remain in how CUX1 regulates red cell development. The data are clear that CUX1 is essential for functional RBC development as evidenced by the anemia endured by patients with CUX1 insufficiency, and through mouse modeling which indicates that knockdown of CUX1 alone is sufficient for the development of a lethal anemia. However, it remains unclear why CUX1 is required for RBC development. This work aims to identify the molecular mechanisms by which CUX1 regulates erythropoiesis through three central aims: aim 1) identify the cellular role of CUX1 in erythropoiesis, aim 2) characterize the molecular mechanisms by which CUX1 regulates erythropoiesis, and aim 3) understand the role of CUX1 in nuclear condensation (Figure 8). Understanding this process will both increase the foundational knowledge of RBC biology and create opportunities for 7q targeted molecular therapeutics.

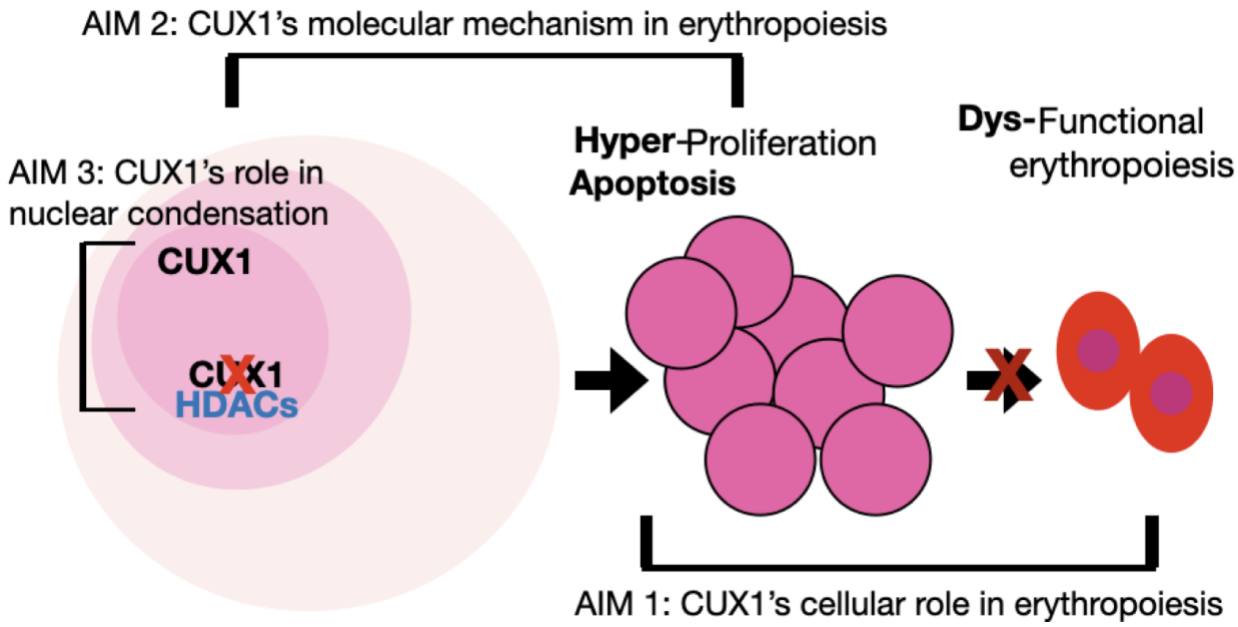

Figure 8. Central model and aims to be investigated. The central model proposed within this thesis is that CUX1 interacts with HDACs to facilitate nuclear condensation though histone deacetylation. This permits normal erythroid differentiation and functional erythropoiesis. However, in a CUX1 insufficient setting the interaction with HDACs is lost, leading to hyper-acetylation of histones and a failure to condense the chromatin in preparation for enucleation. This in turn leads to increased erythroblast proliferation and apoptosis and ultimately dysfunctional erythropoiesis and anemia. Investigation of this model is segmented into 3 components: 1) The cellular role of CUX1 2) the molecular role of CUX1 and 3) the role of CUX1 in nuclear condensation.

CHAPTER 2: MATERIALS AND METHODS

Methods for chapter 3

Mouse models

Animal studies were approved by The University of Chicago Institutional Animal Care and Use Committee. Mice were housed in the Association for Assessment and Accreditation of Laboratory Animal Care-accredited, specific pathogen-free animal care facilitates at The University of Chicago Both sexes of mice were used. Mice of different sex were housed separately, with 5 mice per cage. Tail clips were used for genotyping. Renilla, shCux1.581 ($Cux1^{mid}$), and shCux1.2812 ($Cux1^{low}$) mice were generated as described in (An et al. 2018). Briefly, a second generation reverse tet-transactivator (M2rtTA) is expressed from the endogenous *ROSA26* promoter, and an shRNA targeting Renilla luciferase of *Cux1* is expressed downstream of Col1a1. The resulting mice were genetically rtTA-$M2^{tg/tg}$;$Col1a1^{Cux1/wt}$ ($Cux1^{low}$ or $Cux1^{mid}$) or rtTA-$M2^{tg/tg}$;$Col1a1^{Ren/wt}$ (Renilla) littermate controls. Mice are on a mixed C57BL/6 x 129/Sv background. Transgene expression was induced by maintaining mice on a continuous doxycycline-containing chow diet (TD.12006, 1 mg/kg, Envigo). For all experiments, adult mice (aged 8-16 weeks) were used.

Phenylhydrazine injections

Mice were weighed the day of each injection to prepare accurate dosages of 40 mg/kg or 60 mg/kg of phenylhydrazine (Sigma-Aldrich, product ID: P26252) diluted in PBS. Final volumes were brought to 200 µL for intraperitoneal injections.

Flow cytometry

Mice were euthanized and spleen samples were collected with gentle crushing in PBS with 1% BSA to generate a single cell-suspension. Bone marrow tissue was accessed by removing the femur and tibia and processing in a mortar and pedestal to generate a single cell suspension in PBS and 1% BSA. All samples were FcR blocked (1:10,000 dilution, Fischer Scientifics, catalog number: 5012440) for 10 minutes on ice and primary antibodies were stained for 30 minutes at room temperature and rinsed in PBS with 1% BSA before analysis. When using a secondary antibody set, cells were rinsed once in PBS with 1% BSA before addition of secondary antibodies for staining 30 minutes at room temperature.

For characterization of erythroblast differentiation following phenylhydrazine injection and in the mixed bone marrow chimera the following antibodies were used: Ter119 – BUV396 (1:400 dilution, BD Biosciences, catalog number: 563827), CD71 – BV421 (1:400 dilution, BD Biosciences, catalog number: 747755). For sorting erythroblasts for RNA-sequencing, ATAC-sequencing, DAPI imaging, and FLIM the following antibodies were used: Ter119 – APC (1:400 dilution, BD Biosciences, catalog number 557909) CD71 - PE (1:400 dilution, BD Biosciences, catalog number: 553267).

Sorting MEPs for RNA-sequencing and ATAC-sequencing was conducted with the following antibodies: primary antibodies for lineage staining all biotin CD3e (1:1,000 dilution, BD Bioscience, catalog number: 553060), CD5 (1:1,000 dilution, BD Biosciences, catalog number: 553018), CD19 (1:1,000 dilution, BD Biosciences, catalog number: 553784), CD11b (1:1,000 dilution, BD Biosciences, catalog number: 553309), Ter119 (1:1,000 dilution, BD Biosciences, catalog number: 553309), B220 (1:1,000 dilution, BD Biosciences, catalog number: 553086); streptavidin-BUV395 (1:400 dilution, BD Biosciences, catalog number: 564176), Sca1-PE (1:200 dilution, BD Biosciences, catalog number: 553336), cKit-APC-Cy7 (1:200 dilution, BD Biosciences, catalog number: 560185), CD34 APC(1:100 dilution, Invitrogen, catalog number: 50-0341-82), CD16/32-PE-Cy7 (1:1,000 dilution, BD Biosciences, catalog number: 560829). Human erythroblasts were characterized using Human Fc block (1:1,000 dilution, BioLedgend, catalog number: 422301) stained for 10 minutes on ice followed by CD71-BUV395 (1:200 dilution, CATALOG) or CD71-APC (1:200 dilution, BioLegend, catalog number: 334107) and Gly-A-FITC (1:200 dilution, BioLedgend, catalog number: 349103). Human samples were stained for 30 minutes at room temperate and rinsed before analysis.

All flow cytometry was performed on an LSR Fortessa X-20 (BD Biosciences) and data analyzed with FlowJo software (Tree Star, Inc., Ashland, OR). All sorting experiments were performed on a FACSAria II (BD Biosciences).

Reticulocyte counts

Peripheral blood was collected from the tail vein and mixed at a 1:1 ratio with new methylene blue (Sigma-Aldrich, catalog number: R4132), incubated at room temperature for 5 minutes and smeared onto glass slides and allowed to air dry. 3 images per slide were taken at 100X magnification in fields with non-overlapping cells. Reticulocytes were counted for the entire field of view. RBCs were counted for $1/9^{th}$ of the field of view and multiplied by 9 to get the full RBC count. Percent reticulocytes was calculated by taking total reticulocytes divided by the full RBC count.

Complete Blood Counts

Peripheral blood was collected from the submandibular vein for complete blood counts. Complete blood counts were performed using Hemavet 950 counter (CDC Technologies, Oxford, CT).

EPO ELISA

Peripheral blood samples were taken from the submandibular vein. Samples were centrifuged at 4°C, 2000g, for 20 minutes to fractionate plasma. Manufacturer's instructions were followed for Mouse Erythropoietin/EPO Quantikine ELISA Kit (R&D systems catalog number: MEP00B).

Bone marrow transplants

Competitive transplants were generated with a total of $2x10^6$ RBC-lysed donor cells. Donor cells were comprised of 50% Renilla, $Cux1^{mid}$, or $Cux1^{low}$ (CD45.2) cells and 50% wild-type competitor (CD45.1). Donor cells were retro-orbitally transplanted into lethally irradiated (γ-irradiation, 8.5 Gy) C57BL/6 (CD45.1) recipient mice. Mice were allowed 4 weeks to recover before doxycycline was given to induce knockdown.

Apoptosis analysis

Bone marrow cells were collected from mixed bone marrow-chimera mice after one week of CUX1 knockdown, counted, and stained. Cells, single stain controls, and FMOs were rinsed 1x PBS and resuspended in 1x Annexin V binding buffer (Invitrogen, catalog number: BMS500BB). Cells were stained with Annexin V-APC (Fischer Scientific Annexin V Apoptosis Detection Kit, catalog number: 88-8007-72) as per the manufacturer's directions. 1uL of Propidium Iodide (BD Biosciences, catalog number: 556463) was added at time of data collection.

Cell cycle assays

Cell cycle was characterized as described in (An et al. 2018). Briefly, bone marrow samples were resuspended in 200 µL of BD Cytofix/Cytoperm buffer and incubated at 4°C for 20 minutes. Cells were then washed once with 1X BD Perm/Wash buffer and stained with anti-Ki67-PE/Cy7 (BioLegend, catalog number: 652401) pre-diluted in 1X

BD Perm/Wash buffer (1:20) at room temperature for 20 minutes. Cells were then washed and stained with 10 ug/mL DAPI (Thermo Fisher, catalog number: 66248) for 15 minutes on ice.

RNA-sequencing

Adult Renilla, Cux1^{mid} and Cux1^{low} mice were treated with doxycycline (TD.12006, 1000 mg/kg, Envigo) for 3 days to induce CUX1 knockdown. Bone marrow cells were collected. For MEP samples cells were lysed with ACK lysis buffer, and lineage depleted (Mouse Direct Lineage Cell Depletion kit, Miltenyi Biotech) and stained as described above for sorting. RII basophilic-erythroblast samples were stained as described above without lysis. All samples were sorted on a FACSAria II (BD Biosciences) directly into Trizol. RNA was purified by RNeasy Kit (Qiagen), and > 100 ng of RNA was used for library preparation. Two biological replicates of each genotype was performed. Barcoded RNA-seq libraries were generated with TruSeq v2 kit (Illumina) and >23 million, single end 50 bp read were generated by Illumina HiSeq.

RNA-sequencing analysis

Reads were aligned using STAR (Dobin et al. 2013), and alignments with a mapping quality <30 were removed. Differential gene expression was performed with DESeq2 (Love, Huber, and Anders 2014). In differential expression analysis, batch effects between replicates were corrected by including batch co-variates in the DESeq2 design matrix. Normalized CPM read count tables were generated following batch correction

using LIMMA (Smyth 2004). Analysis was restricted to genes with counts per million >2 in 3 or more samples. Sequencing data are available in the GEO Database GSE181626.

CFU-E and BFU-E cultures

Adult mice were sacrificed in a dissection hood and bone marrow was collected in sterile collection media. Bone marrow was collected, counted, and lysed of red blood cells. $2x10^5$ cells were prepared in 1 mL for BFU-E assay, $2x10^6$ for CFU-E assay. 300 µL of cellular stock was pipetted into 3mL of BFU-E culture medium (Stemcell Technologies, catalog number: 03436) or CFU-E culture medium (Stemcell Technologies, catalog number: 03334). Colonies were assessed visually after 48 hours for CFU-E colonies and 10-12 days for BFU-E colonies.

Liquid *in vitro* cultures

Adult mice were sacrificed in sterile conditions for tissue culture. Bone marrow was lysed and lineage depleted using a magnetic column following the manufacturer's instructions (Mouse Direct Lineage Cell Depletion kit, Miltenyi Biotech). $2x10^5$ cells of lineage depleted bone marrow was then plated in erythropoietic medium (IMDM, EPO 10 U/mL, SCF10 ng/mL, Dexamethasone 10 uM, FBS 15%, detoxified BSA 1%, holotransferin 200 µg/mL, insulin 10 µg/mL, β-mercaptoethanol 10^{-4}M, Pen/Strep 1x) and onto fibronectin coated plates for 48 hours. Cells were then transferred to erythroid

maintenance medium (IMDM, FBS 20%, L-glutamine 1x, β-mercaptoethanol 100μM) for 52 hours. Cells were collected at the end of each timepoint for flow cytometry.

Methods for chapter 4

Human erythroid cultures

Human mobilized peripheral blood CD34+ HSPCs were purchased from the Fred Hutchinson Co-operative Center for Excellence in Hematology (Seattle, WA, USA), and obtained from multiple healthy donors. CD34+ HSPCs were expanded in StemSpan SFEMII base media supplemented with CC110 culture supplement for 3 days prior to erythroid differentiation (Stemcell Technologies, Vancouver, Canada). Human cytokines SCF, IL3, IL6, and EPO were purchased from Peprotech Inc (Princeton, NJ, USA). 125,000 CD34+ cells were placed in erythroid differentiation media (SFEMII plus 25nM SCF, 10nM IL3, 10nM IL6 and 6U/mL EPO) (Sankaran et al. 2008). Cultures were grown for 7 days before collection and validated by flow cytometry for CD71 expression.

CRISPR/Cas9 editing

Guide RNAs and Cas9 were designed using Synthego bioinformatics tools and purchased from Synthego. Guides targeting safe-harbor genes targeted *AAVS1* (gAAVS1) or *HPRT* (gHPRT).

Electroporation transfection was performed using the Neon Transfection System (Thermofisher Scientific, Waltham MA, USA). RNPs were formed by mixing 0.71 µL Cas9 (20uM), 2.39 µL gRNA (30uM), and 0.9 µL Buffer T and incubating them for 15 minutes at room temperature. 200,000 CD34+ cells were resuspended in 8 µL of Buffer T, added to RNPs, and electroporated at 1600 volts, 10 ms pulse length, for 3 pulses. DNA was collected for validation of editing 1-3 days after transfection using QIAamp 96 DNA Blood Kit (Qiagen, Hilden, Germany). Amplicons containing the edited gene were PCR amplified with primers (IDT, Coralville, IA, USA) flanking the gRNA target site and Sanger sequenced by the University of Chicago DNA Sequencing and Genotyping Core Facility. Edited and control sequences were then analyzed using the ICE analysis tool (Synthego, Redwood City, CA, USA) to determine percentage of DNA edited.

CRISPR guide sequences:
gCUX1 – 5’- UGCACUGAGUAAAAGAAGCA-3’
gHPRT – 5’- GCAUUUCUCAGUCCUAAACA-3’
g AAVS1 – 5’-GGGGCCACTAGGGACAGGAT-3’

PCR Primer sequences:
CUX1 – F: 5’-CCCTCCTAGACCCTGAGCTT-3’
CUX1 - R: 5’-TTCATGTGTCCTGCACTCCC-3'
HPRT - F: 5’-AAACATCAGCAGCTGTTCTGAGTA-3’
HPRT - R: 5’-TGCATAGCCAGTGCTTGAGAA-3'
AAVS1 – F: 5’- GCTCTGGGCGGAGGAATATG-3’
AAVS1 – R: 5’- GGATTCGGGTCACCTCTCAC-3’

ATAC-sequencing

50,000 cells were washed in PBS, resuspended in lysis buffer and spun at 4°C, 500 g, for 10 minutes to fractionate cytoplasm and nuclei. Nuclei were transposed using the Nextera DNA Library Prep Kit, following the manufacturer's instructions. Following transposition DNA was purified using the MinElute Reaction Cleanup Kit (Qiagen). Libraries were generated using the NEBNext High-fidelity NGS kit. Libraries were purified with AMPure XP size selection beads. 50 bp paired-end reads were generated by Illumina HiSeq.

Sequencing reads were aligned to the mouse mm10 genome using BWA (version 0.7.12) (H. Li and Durbin 2009) and low quality reads were removed using the SAMtools q30 filter (H. Li et al. 2009). Peaks were called with MACS2 (Y. Zhang et al. 2008) with a q value of 0.05 or 0.25 as indicated. For differential accessibility, DiffBind software (Stark and Brown 2011) was applied using an FDR cutoff of <0.05.

ChIP-sequencing

ChIP-sequencing was conducted as described in (Imgruet *et al.*, 2021). Briefly, chromatin was fixed with 1% formaldehyde for 10 minutes at room temperature. The reaction was stopped with the addition of 0.125 M glycine. Fixed chromatin was harvested from $100x10^6$ K562 cells and sonicated (Bioruptor) for 10 minutes. Immunoprecipitation was conducted with Dynabead protein G magnetic beads (Thermo Fischer) and 10uG of anti-CUX1 antibody. CUX1 specific antibody is a rabbit polyclonal antibody that recognizes a C-terminal peptide (amino acids 1223-1242,

CEPPSSVGTEYSQGASPQPQH) of human CUX1 generated by the Pocono Rabbit Farm and Laboratory (Canadensis, PA) and affinity purified. Following elution, samples were treated with RNAseA and proteinase K prior to crosslink reversal. DNA was purified using Qiagen PCR purification kit. Libraries were prepared with the Ovation Ultralow Library Kit (NuGEN) and size selected with SPRIselect beads (Beckman Coulter). Illumina HiSeq was used to generated 50 bp single-end sequencing reads. Two biological replicates were performed. Sequencing data are available at GEO accession GSE181626.

CUT&RUN

CUT&RUN was conducted as described (Meers et al. 2019). 500,000 cells on day 7 after induction toward the erythroid lineage were pelleted and washed twice with Wash Buffer (20 mM Hepes, 150 mM NaCl, 0.5 M Spermidine and Roche Complete Protease Inhibitor EDTA free). Washed cells were incubated with activated Concanavalin A-coated magnetic beads (BP531) with Dig-Wash buffer (20 mM HEPES, pH7.5, 150 mM NaCl, 0.5 mM spermidine, 0.05% Digitonin and Roche complete Protease Inhibitor tablet EDTA free) for 5-10 minutes on a rotator. 10 µl bead slurry was used per sample.

The cell bound beads were incubated with anti-CUX1 antibody (1:50) in 150µl antibody buffer (Dig wash Buffer plus EDTA) overnight at 4°C on a nutator. The next day, beads were washed 3 times with 1 mL Dig Wash buffer. After final wash, 150 uL of the Protein A-MNAse (Henikoff Lab) was added at 700 ng/mL and incubated for 1 hour at 4°C. Beads were washed 3 times with 1 mL Dig Wash buffer and after last wash 24 µl

ice cold 1XpA-MNAse reaction mix (Dig Wash Buffer with 2mM $CaCl_2$). Tubes were placed in a cold block and incubated at 0°C for 30 minutes.

Tubes were placed on magnet and clear liquid was removed, followed by addition of 8 µL 4X STOP Buffer (80 mM EGTA, 0.05% Digitonin, 100 ug/ml RNAseA, 100 pg/mL of heterologous spike-in DNA (Henikoff Lab) and incubation at 37°C to release CUT & RUN fragments. Tubes were placed on a magnetic stand and 30 µL of clear liquid containing digested chromatin was transferred to new tubes and immediately proceeded with library prep using NuGen Ovation Ultralow Library system (Tecan genomics 0344NB-32). Amplified libraries were cleaned up using Qiagen MinElute PCR Purification Kit (28004). Illumina HiSeq was used to generate 50 bp paired-end sequencing reads. Two biological replicates were performed. Sequencing data are available at GEO accession number GSE181626.

ChIP-sequencing and CUT&RUN analysis

Sequencing reads were aligned to the human genome hg19 using BWA (version 0.7.12) (H. Li and Durbin 2009). Low quality reads were removed using SAMtools q30 filter (H. Li et al. 2009). Peaks were called using MACS2 (Y. Zhang et al. 2008) with a p-value threshold of 0.1 for each replicate. To identify high confidence reproducible peaks, the peaks identified in MACS2 were subsequently analyzed by the irreproducible discovery rate (IDR) (Q. Li et al. 2011) on the top 250,000 peaks from each replicate. Peaks with an IDR value of <0.05 were kept for analysis.

Confocal microscopy

For all imagining, we used #1.5 cover glass pre-treated treated with Poly-L-Lysine for 1-2 hours. 0.5E6 sorted RII-erythroblasts were resuspended in 150 µL PBS and settled onto coverslips for one hour. TSA treated control cells were treated with 20 µM TSA (Abcam, catalog number: ab146598) diluted in PBS for 1 hour at room temperature. Cells were then fixed with 4% PFA for ten minutes at room temperature and then permeabilized in 0.2% Triton X-100 diluted in PBS for 20 minutes at room temperature. Cells were then stained with 1 mg/mL DAPI for 5 minutes and rinsed in PBS. VECTASHIELD (Vector Laboratories, catalog number: H-1000-10) was used as a mounting medium and slides were stored in light protected slide boxes at 4°C prior to imaging.

Fluorescence Lifetime Image Microscopy

Fluorescence images were collected on a Leica Stellaris8 Falcon confocal microscope using a 63X NA 1.4 objective in the FLIM module of LASX software (Leica Microsystems GmbH). Excitation by means of an extended-range white light laser was sequentially captured per fluorescent probe in by-frame mode, pulse picker 40 MHz, at intensities producing at most one photon per pulse. DAPI was excited at 405 nm to produce intensity images and at 440 nm for lifetime data. Images were accumulated to obtain sufficient counts. DAPI was recorded on HyDX-SMD detector and other probes on HyDS or -SMD class detectors. Three to five fields of view were taken of each preparation, and “blind” as to treatment prediction. Arrival times were exported into BIN

format, and the image lifetimes per pixel were fit using FLIMfit5.1.1 software (S. C. Warren et al. 2013) using a 3-exponential term model. Lifetime maps were exported as tif and measured in FIJI. Stacks of images were assembled per field of view for each fluorescence probe and the lifetime map. Cells were segmented by means of the 405-DAPI outlines, watershed applied, and then areas, signal mean values, and standard deviation of mean values were measured per cell in each image using custom macro script in FIJI.

Cell culture and transfections

K562 cells were cultured and gCUX1 and gHPRT cell lines were generated as previously described (Imgruet *et al.*, 2021). Briefly, gCUX1 and gHPRT cells lines were generated using the RNP-based CRISPR/Cas9 delivery system (Gundry et al. 2016). Our guide targeting *CUX1* was designed using the BROAD shRNA Genetic Perturbation Platform (GPP) sgRNA Designer (Doench et al. 2016). sgRNA and Cas9 were mixed at a ratio of 9:1 and incubated at room temperature for 10 minutes to generate RNPs. Cells were resuspended with RNPs and electorporated with 3 pulses at 1450 V of 10 ms using the Neon Transfection System (ThermoFisher). Single-clones were generated then validated by sanger sequencing and western blot.

Western blots

Equal numbers of sorted RII-basophilic erythroblasts were lysed in 2X SDS sample buffer and processed for immunoblotting as previously reported (An et al., 2018). For

protein detection, antibodies targeting H3 (Abcam, 1:3,000 dilution, catalog number: ab176842), and H3K18Ac (Abcam, 1:20,000 dilution, catalog number: ab40888), H3K23Ac (Abcam, 1:1,000 dilution, catalog number: ab177275), H3K27Ac (Abcam, 1:3,000 dilution, catalog number: 177178), H4K12Ac (Abcam, 1:10,000 dilution, catalog number: ab177793), Acetyl-lysine (PTM Biolabs, 1:80,000 dilution, catalog number: PTM-101) were used. For visualization goat anti-rabbit secondary (Abcam, 1:5,000 dilution, catalog number: ab97051) was used on a BioRad Imager.

Methods for chapter 6

Generation of CUX1-MCherry reporter mouse

CUX1-MCherry reporter mice were generated via CRISPR/Cas9-mediated insertion. The guide sequence [sequence 1] 5'-CCATCGAATGGGAGTTCTGA-3' was designed using the Broad Institute design tools to target the final coding exon of CUX1. To facilitate insertion, regions flanking the cut site were amplified to generate 2-kb and 3-kb homology arms. The homology arms were PCR amplified from B6C3F1 mouse genomic DNA using [sequences 2 and 3], resulting in a 5097 bp product topo cloned into the pCR-XL_2 vector. The MCherry tag was PCR amplified from the pMcherry-N1 plasmid and then Gibson cloned using [sequences 4 and 5] in the middle of the 5097bp genomic sequence. The plasmid was then transformed into NEB 5-α Competent *E. coli* and plated on ampicillin plates (100 ug/mL) for selection. Successfully grown colonies were selected and expanded overnight in 100 mL LB broth with ampicillin (100 ug/mL). The

donor plasmid was purified using FosmidMax kit (epicenter #FMAX046). The donor sequence and orientation were confirmed by sanger sequencing using [sequences 6-8] which span both homology arms and the MCherry insert. CRISPR-Cas9 crRNA, tracrRNA, and Cas9 nuclease were purchased from Synthego. Ribonucleoprotein was assembled for microinjection as described in manufacturer's instructions with a final concentration of 20 ng/uL guide, 50 ng/uL Cas9 nuclease, and 12.6 ng/uL donor plasmid. Mixes were then injected into the nuclei of C57BL/6J embryos. PCR spanning the insert was used to identify successful insertions which were validated by Sanger Sequencing using primer sets [sequences 9-14] (Table 1).

Table 1: CUX1-MCherry primers

Reference Number	Sequence
1	CCATCGAATGGGAGTTCTGA
2	CATGGTGGTTCTCAGCCATA
3	ACACTGAGGGGCAATAGTGG
4	ATCGAATGGGAGTTCGGCGGCGGCGGCAGCGTACCGGTCGCCACC ATGGTGAGCAAGGGC
5	GGCCCGGCGCCCTCACTTGTACAGCTCGTCCATGCCGCCG
6	TAATACGACTCACTATAGGG
7	ACCTGGTGCGGAAGAAGAAG
8	CGTTAAGTGCGCAACACG
9	GCCCATCGAATGGGAGTT, GATTGGGCTTAATGCTCCTTTG
10	GCGAACTTGAACAGCATCATC, GCGTTAAGTGCGCAACAC
11	ATCCACCGCCTGGAGAA, CCTTGGCCTATGGCGATTT
12	GACGGCGAGTTCATCTACAA, GGAGGTGATGTCCAACTTGAT
13	GGCCATCATCAAGGAGTTCA, GGGAAGGACAGCTTCAAGTAG
14	GACTACTTGAAGCTGTCCTTCC, GATGGTGTAGTCCTCGTTGTG

Sequences used in the generation of the CUX1-MCherry mouse. Sequence 1 is the guide sequence used for CRISPR/Cas9 editing. Sequences 2 and 3 were used to generate the homology arms. Sequences 4 and 5 were used to insert MCherry into the homology arms. Sequences 6-8 were used to confirm the identity of the donor plasmid. Sequencing pairs 9-14 were used to identify successfully edited mice.

CFU-assay

Adult homozygous CUX1-MCherry reporter mice were sacrificed under sterile conditions. Bone marrow was isolated and lysed of red blood cells and cKit+ cells were sorted based on MCherry expression. 3,000 cKit+ bone marrow cells were plated in CFU media M3434 (Stemcell Technologies, catalog number:03434). 11 days after plating in CFU media colonies were counted.

Single-cell RNA-sequencing

Renilla, $Cux1^{mid}$, and $Cux1^{low}$ bone marrow was retro-orbitally transplanted into lethally irradiated wild-type recipient CD45.1+ mice. Recipient mice were given 4 weeks to recover before doxycycline treatment for 5 days to induce CUX1 knockdown. Mice were then sacrificed and their bone marrow was lysed of red blood cells and lineage depleted (Mouse Direct Lineage Cell Depletion kit, Miltenyi Biotech). Cells were sorted for cKit+, GFP+, lineage- cells. The resulting cell population of 1 mL of cells at a concentration of $1x10^6$ cells / mL was processed for single cell RNA-sequencing following the 10X genomics manufacturer protocol, aiming for a recovery of 10,000 cells per population. Reads were 100 bp in length and paired end.

Single-cell RNA-sequencing analysis

Reads were aligned using CellRanger with a customized reference genome GRCm38 mm10 where Cux1 and Casp transcripts are differentiated. Quality control was performed using Seurat v4.0 where cells with fewer than 400 UMIs and more than 8% mitochondrial transcripts were discarded. Clustering was performed using KNN by

Seurat FindClusters(), and clusters were annotated using canonical lineage specific genes and orthogonally validated using SingleR package with Novershtern Hematopoietic Data (Novershtern et al. 2011).

Statistical analysis and plotting

Statistical analysis was performed as indicated in the figure legends. Unless otherwise indicated, all replicates represent biological replicates. Tests were carried out using GraphPad Prism version 9.1.0 (216). For all plots values were indicated as follows: non-significant $p>0.05$; * $p<0.05$; ** $p<0.01$; *** $p<0.001$; **** $p<0.0001$.

Data availability

The data discussed in this thesis have been deposited in NCBI's Gene Expression Omnibus (Edgar, Domrachev, and Lash 2002) and are accessible through GSE181626.

CHAPTER 3: CUX1 REGULATES ERYTHROBLAST SURVIVAL AND PROLIFERATION

Introduction

The average human adult produces 200 billion red blood cells (RBCs) every day (Neildez-Nguyen et al. 2002). This massive production of red cells is generated through an intricate process beginning with commitment of hematopoietic stem cells to the erythroid lineage. Highly synchronized erythroid progenitor expansion and differentiation culminates in the nearly exclusive transcriptional production of hemoglobin. Mammalian RBCs are unique in that they undergo nuclear extrusion, a process which may enhance oxygen transport. However, the process of nuclear condensation preceding enucleation remains poorly understood (reviewed in (Mei, Liu, and Ji 2021)). Given the complexity and volume of RBC production, it is unsurprising that defects in erythropoiesis, manifesting as anemia, is a prevalent public health problem affecting up to a third of the world's population (Chaparro and Parminder 2019). In one study of American individuals over 65 years of age, 24% were anemic, and the incidence was significantly higher in Black Americans (Denny, Kuchibhatla, and Cohen 2006). Across ages and populations, anemia is associated with increased morbidity and mortality.

Anemia can often be explained by cell extrinsic causes, such as iron or B12 deficiency. For anemias that are otherwise unexplainable, it has recently become clear that a substantial proportion of patients harbor somatic mutations in malignancy-related genes within their hematopoietic stem and progenitors cells (HSPCs) in the form of clonal hematopoiesis (Bolton et al. 2020). These patients with clonal hematopoiesis and

a cytopenia do not have an overt malignancy, although they have an increased risk of transformation. Loss of *CUX1*, either through *CUX1* inactivating mutations or loss of all or part of chromosome 7 [-7/del(7q)] are recurrent genetic phenomenon in clonal hematopoiesis (Dimitriou et al. 2016; Jacobs et al. 2012; Takahashi et al. 2017). -7/del(7q) and CUX1 mutations are also recurrent in fulminant myeloid malignancies (Armitage et al. 2003; Baudard et al. 1994; Luna-Fineman et al. 1999; McNerney, Godley, and Le Beau 2017). Myeloid neoplasms are often accompanied by cytopenia and dysplasia; dysplastic features in the erythroid lineage include enlarged size, nuclear multilobation, nuclear budding, and nuclear-cytoplasmic asynchrony, wherein the chromatin matures more slowly than the cytoplasm (Goasguen et al. 2018).

Given the critical role for CUX1 in erythropoiesis, we sought to determine the mechanism by which CUX1 regulates RBC development. Herein, we report that CUX1-knockdown mice have an impaired response to acute anemia leading to decreased survival. We identify multiple cellular defects in the course of erythropoiesis due to CUX1-deficiency, including increased proliferation and apoptosis.

Results

CUX1 is required for erythropoiesis

We previously reported that, with age, CUX1-knockdown mice develop anemia with erythroid dysplasia (An et al., 2018). Bone marrow transplant recipients also develop macrocytic anemia, indicating the requirement for CUX1 in steady-state erythropoiesis is hematopoietic intrinsic. To confirm this result, we turned to our CUX1-knockdown

mouse models which express two independent, doxycycline-inducible shRNA transgenes targeting *Cux1*, Cux1^{mid} and Cux1^{low} (Figure 7) (An et al., 2018). Mice expressing an shRNA targeting renilla luciferase are included as controls (Ren). We transplanted Ren or Cux1^{low} CD45.2(+) bone marrow into lethally irradiated wild-type CD45.1(+) recipients, allowed them 4 weeks to recover, induced CUX1 knockdown for 7 weeks before profiling erythropoiesis (Figure 9A). We find that, as reported (An et al. 2018), CUX1 loss leads to the development of anemia, indicated by the reduced RBC values (Figure 9B). Further indicating anemia, Cux1^{low} mice have enlarged spleens, dominated by erythroblasts indicative of extramedullary erythropoiesis (Figure 9C).

To identify the stage of erythroblast differentiation disrupted by CUX1 deficiency we performed flow cytometry on the bone marrow of these mice. CD71 (TRFC, transferrin receptor) and Ter119 (LY76) are used to mark erythroblasts throughout terminal erythroid differentiation (Figure 1B). These markers delineate four populations of erythroblasts: RI pro-erythroblasts, RII basophilic-erythroblasts, RIII polychromatic-erythroblasts, and RIV orthochromatic-erythroblasts. Orthochromatic-erythroblasts enucleate and emigrate from the bone marrow into the peripheral blood becoming reticulocytes. We find Cux1^{low} erythroblasts have a reduction in RII basophilic-erythroblasts and increase in RIV orthochromatic-erythroblasts (Figure 9D). Taken together these results confirm our previous work that CUX1 knockdown leads to anemia and disrupts erythropoiesis.

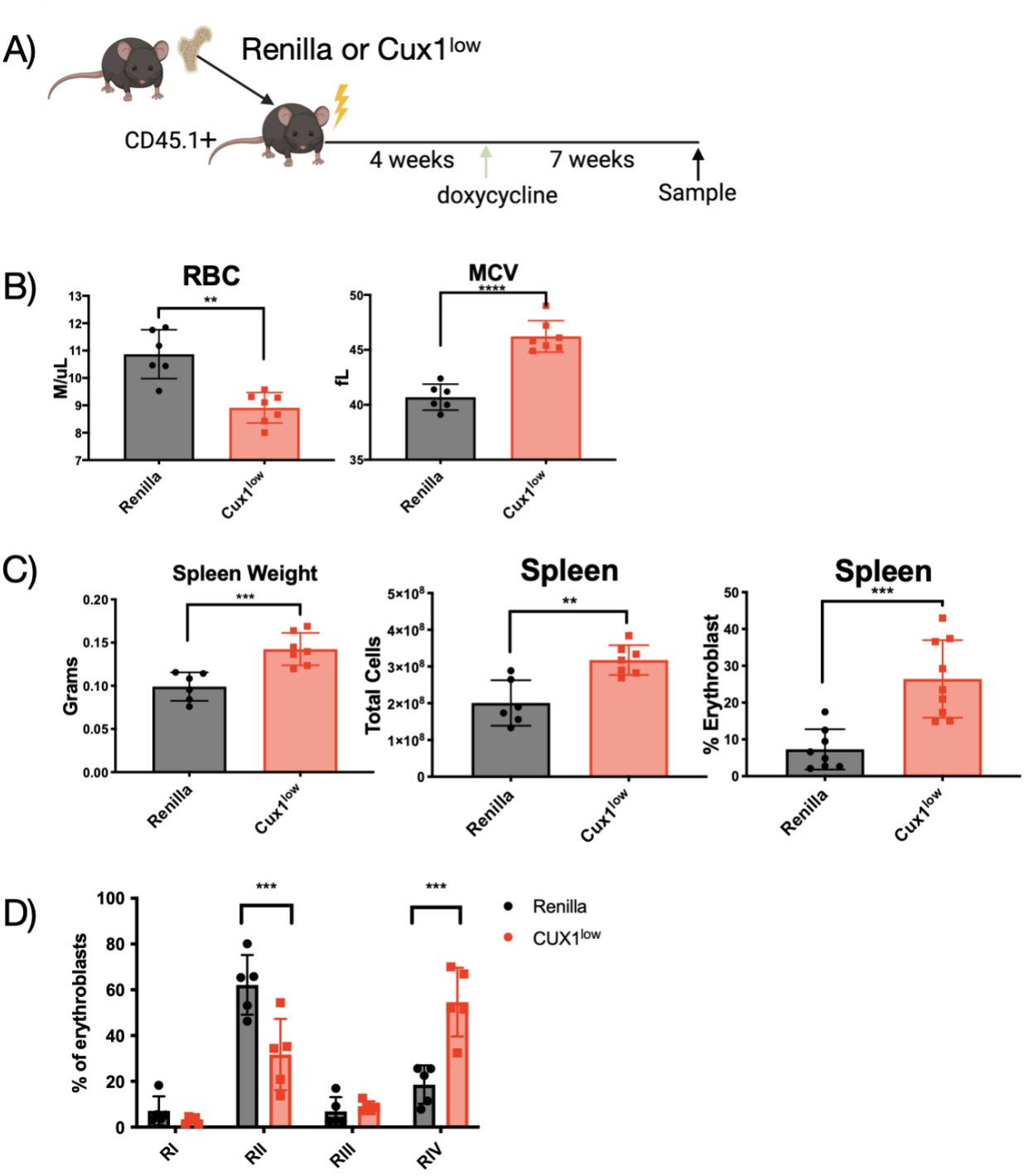

Figure 9. CUX1 is required for erythropoiesis. (A) Experimental model for (A-D). Ren or Cux1^{low} bone marrow was transplanted into lethally irradiated CD45.1+ wild-type recipients. Recipient mice were given 4 weeks to removed and then treated with doxycycline to induce knockdown for 7 weeks before profiling. **(B)** Complete blood counts on the peripheral blood (Ren n=6, Cux1^{low} n=7). **(C)** Spleen weight and composition following CUX1 knockdown (Ren n=6, Cux1^{low} n=7) **(D)** Erythroblast

Figure 9, continued

differentiation stage in recipient knockdown mice (Ren n=6, Cux1^{low} n=7). For all data each point represents an individual mouse. The mean ± SD is shown. Student *t* test **P* ≤ .05, ***P* ≤ .01, ****P* ≤ .001.

CUX1 during in vitro erythropoiesis

As *Cux1* is expressed throughout hematopoietic lineages, it is unclear at what stage(s) CUX1 is required for erythropoiesis. For instance, phenotypic hematopoietic stem cell (HSC) numbers also decrease with time in CUX1-knockdown mice, evincing the possibility that anemia may result from HSC exhaustion (An et al., 2018). To create a system to characterize CUX1's cell intrinsic role in erythropoiesis we aimed to generate *in vitro* liquid cultures. These cultures began with HSCs which are induced to differentiate into erythroblasts through a cytokine cocktail. After culturing, $Cux1^{low}$ cells may have dysfunctional differentiation into erythroid cells (Figure 10A). However, cultures were comprised primarily of cell debris making the results inconclusive.

As an alternative approach to profile the *in vitro* erythroid potential of $Cux1^{low}$ HSPCs, we plated lineage depleted progenitors in BFU-E and CFU-E methylcellulose cultures. Before terminal erythroid differentiation, erythroid progenitors progress through differentiation as BFU-Es and CFU-Es identified by colony formation in methylcellulose. The result of these cultures indicates CUX1 may regulate splenic erythroblasts during the proliferative CFU-E and BFU-E stages, perhaps as an early response to anemia, but does not regulate bone marrow erythroblasts (Figure 10B). Therefore, we moved to an alternative model to assess the role of CUX1 in erythroblasts.

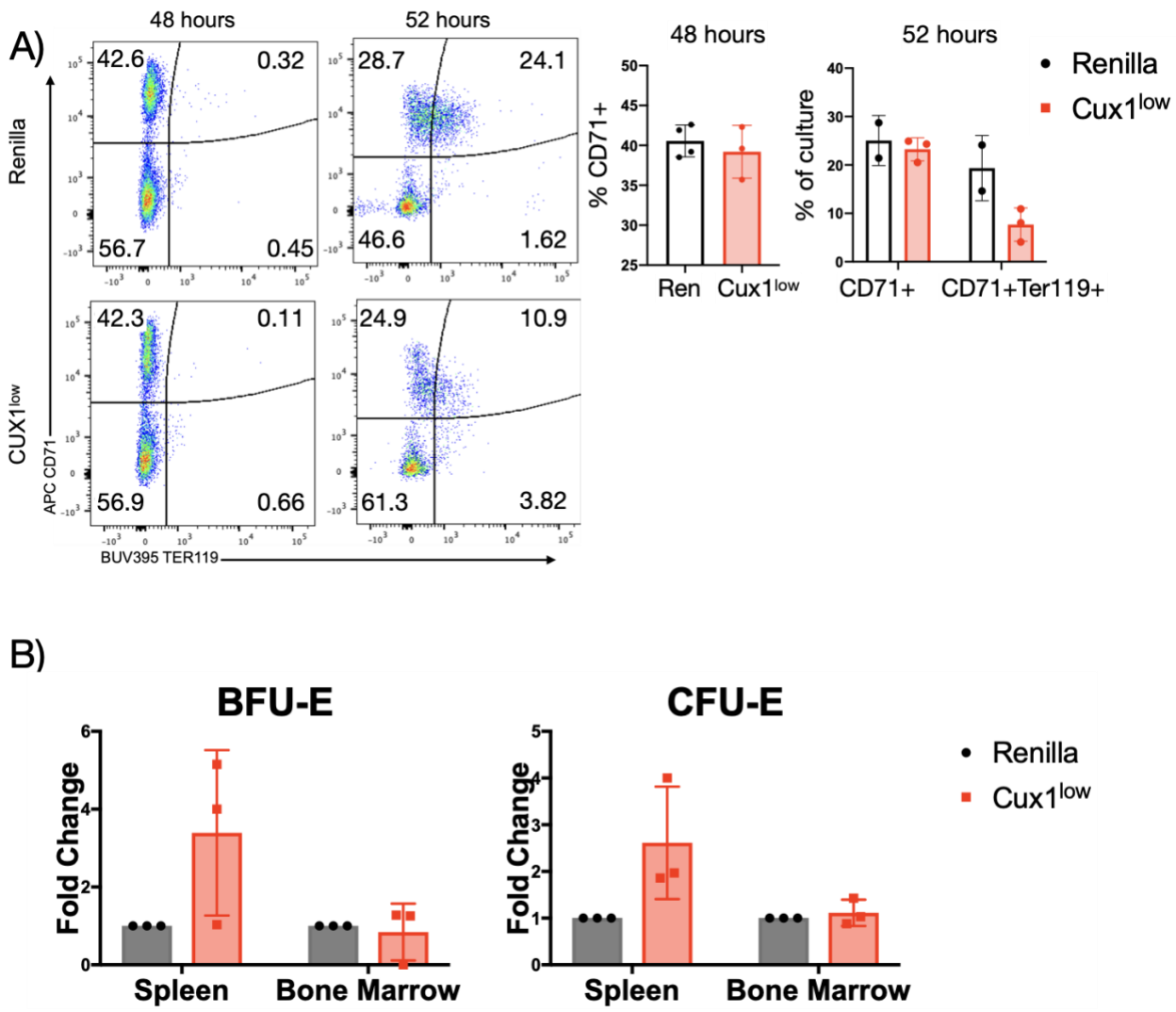

Figure 10. CUX1 does not discernibly regulate erythropoiesis *in vitro*. (A-B) Ren and Cux1^{low} bone marrow and spleen cells **(B)** were isolated lineage depleted following one week of knockdown. **(A)** Hematopoietic progenitors were plated in liquid *in vitro* cultures and sampled at 48 and 52 hours after culture induction. **(B)** Spleen and bone marrow progenitors were plated in BFU-E and CFU-E cultures, total colonies formed were counted.

CUX1 is required for stress-induced erythropoiesis

As liquid *in vitro* cultures were inconclusive, we tested the requirement for CUX1 in phenylhydrazine-induced stress erythropoiesis. This enabled us to identify the role of CUX1 in erythroid progenitors, as phenylhydrazine only affects the erythroid lineage and recovery is dependent on erythroid progenitors (Harandi et al. 2010). After one week of doxycycline, we treated mice with two doses of 60 mg/kg of phenylhydrazine to induce a hemolytic anemia from which 90% of Ren control mice recover from (Figure 11A). In stark contrast, only 36% of $Cux1^{mid}$ and 11% of $Cux1^{low}$ mice survive this acute anemic stress (Figure 11A). This result shows that in addition to a role in steady-state erythropoiesis, CUX1 is also required in stress-erythropoiesis. Furthermore, defects in CUX1-deficient HSCs notwithstanding, CUX1 is required in erythroid progenitors to sustain recovery from acute anemic stress.

We sought to characterize the stages of erythroid development disrupted by CUX1 deficiency. We were unable to assess erythropoiesis after exposure to two doses of phenylhydrazine due to the moribund state of CUX1-knockdown mice. As such, we assessed mice after a single dosage of 60 mg/kg phenylhydrazine. Following this treatment, all biological groups had a similar RBC nadir (Figure 11B), and all responded with increased reticulocytes, i.e. immature RBCs indicative of a normal response to anemia. However, reticulocytes comprise almost half of RBCs in $Cux1^{low}$ mice, a sign of aberrant red cell production (Figure 11C). Even at a single dosage of 60 mg/kg phenylhydrazine some mice (10% of Ren, 26% of $Cux1^{mid}$ and 28% of $Cux1^{low}$) were unable to recover (Figure 12). Therefore, we lowered the dosage to 40 mg/kg to assess erythroid differentiation without morbidity. Following acute anemic stress, there is

normally an expansion of early erythroblasts as evidenced by the increase proportion of RI and RII erythroblasts in phenylhydrazine-treated Ren mice compared to untreated mice (Figure 11D). In contrast, CUX1 insufficient mice fail to mount this response and appear more similar to untreated mice in their erythroblast distribution (Figure 11D). The spleen is a critical source of stress erythropoiesis in mice, and a similar reduction in RII was observed in the spleen 4 days following acute anemic stress (Figure 12B). Overall, these results indicate that CUX1 deficiency in erythroblasts lead to an ineffective and ultimately fatal response to acute anemia characterized by attenuated erythroblast expansion and the generation of immature RBCs.

CUX1-deficiency leads to increased erythroblast proliferation and apoptosis

Our next aim was to uncover the cellular role of CUX1 in erythroblasts. In our previous work, we reported that $Cux1^{low}$ erythroblasts do not have increased apoptosis at steady-state (An et al., 2018). However, that analysis did not consider that kidney fibroblasts produce erythropoietin in response to anemia-induced hypoxia (Watowich 2011). Erythropoietin increases RBC production by promoting early erythroblast survival through reduction of apoptosis (Watowich 2011). To determine if erythropoietin signaling may be masking the true phenotype of $Cux1^{low}$ erythroblasts, we examined serum erythropoietin in $Cux1^{low}$ mice at steady-state. Indeed, as soon as one month after CUX1-knockdown, $Cux1^{low}$ mice have significantly elevated serum erythropoietin

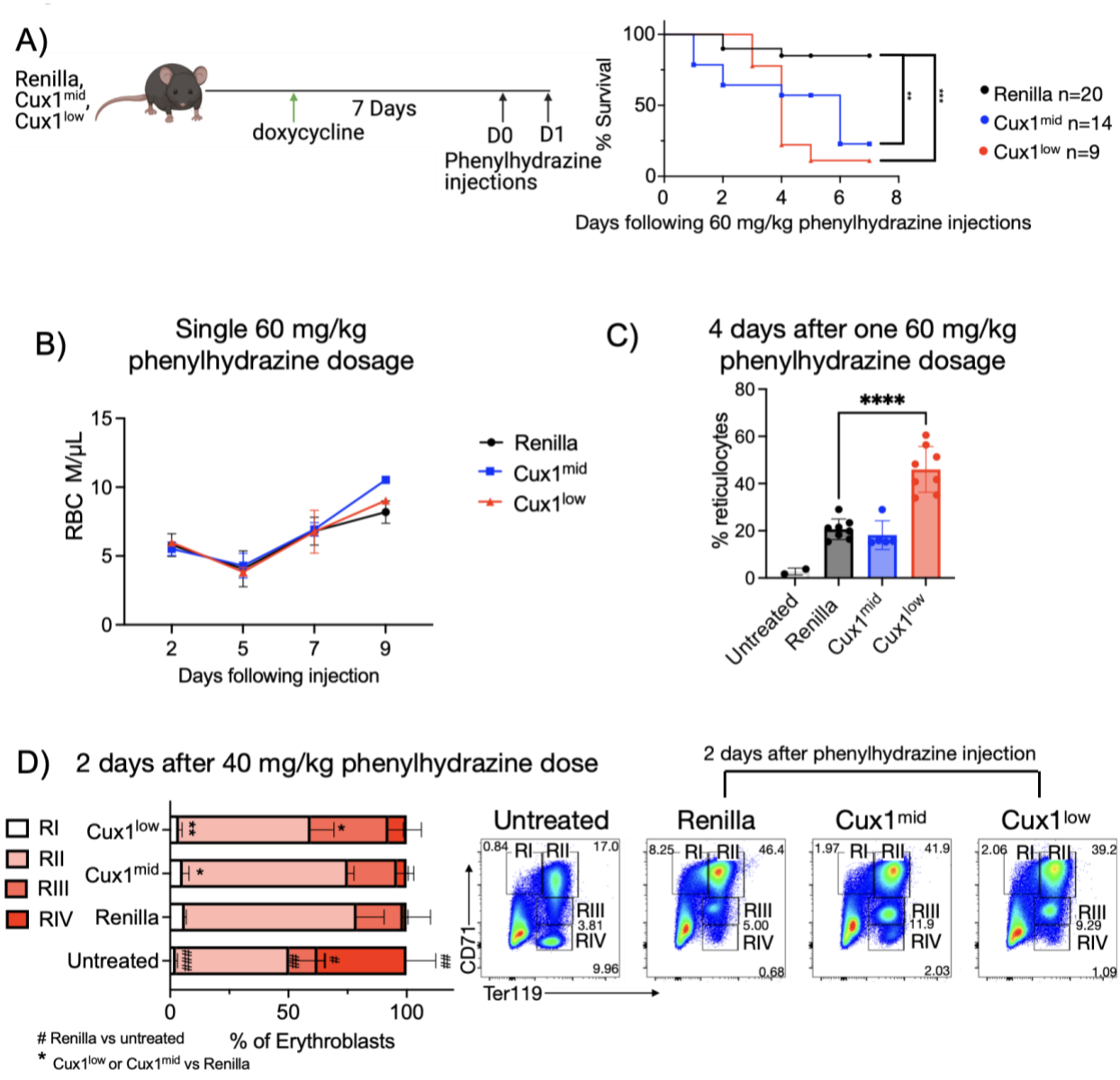

Figure 11. CUX1 is required for stress erythropoiesis. (A-D) Adult Cux1^{low}, Cux1^{mid} and littermate Ren mice were doxycycline treated to induce CUX1 knockdown for one week before phenylhydrazine injection. **(A)** Kaplan-Meier survival plot of Cux1^{low} (n=9), Cux1^{mid} (n=14), and Ren (n=20) mice following acute anemic stress induced by two injections of 60 mg/kg phenylhydrazine (log-rank test). **(B)** RBC from complete blood counts following one injection of 60 mg/kg phenylhydrazine (n=3-4 per condition). **(C)** Peripheral blood reticulocytes 4 days after one injection of 60 mg/kg phenylhydrazine (n=2 no phenylhydrazine, n=5-8 Ren, Cux1^{mid}, and Cux1^{low}). **(D)** Flow cytometric analysis of bone marrow erythroblasts 2 days after one injection of 40 mg/kg phenylhydrazine (n=3-4 mice per condition). For all data each point represents an individual mouse. The mean ± SD is shown. Student *t* test *$P \leq 0.05$, **$P \leq 0.01$, ***$P \leq 0.001$.

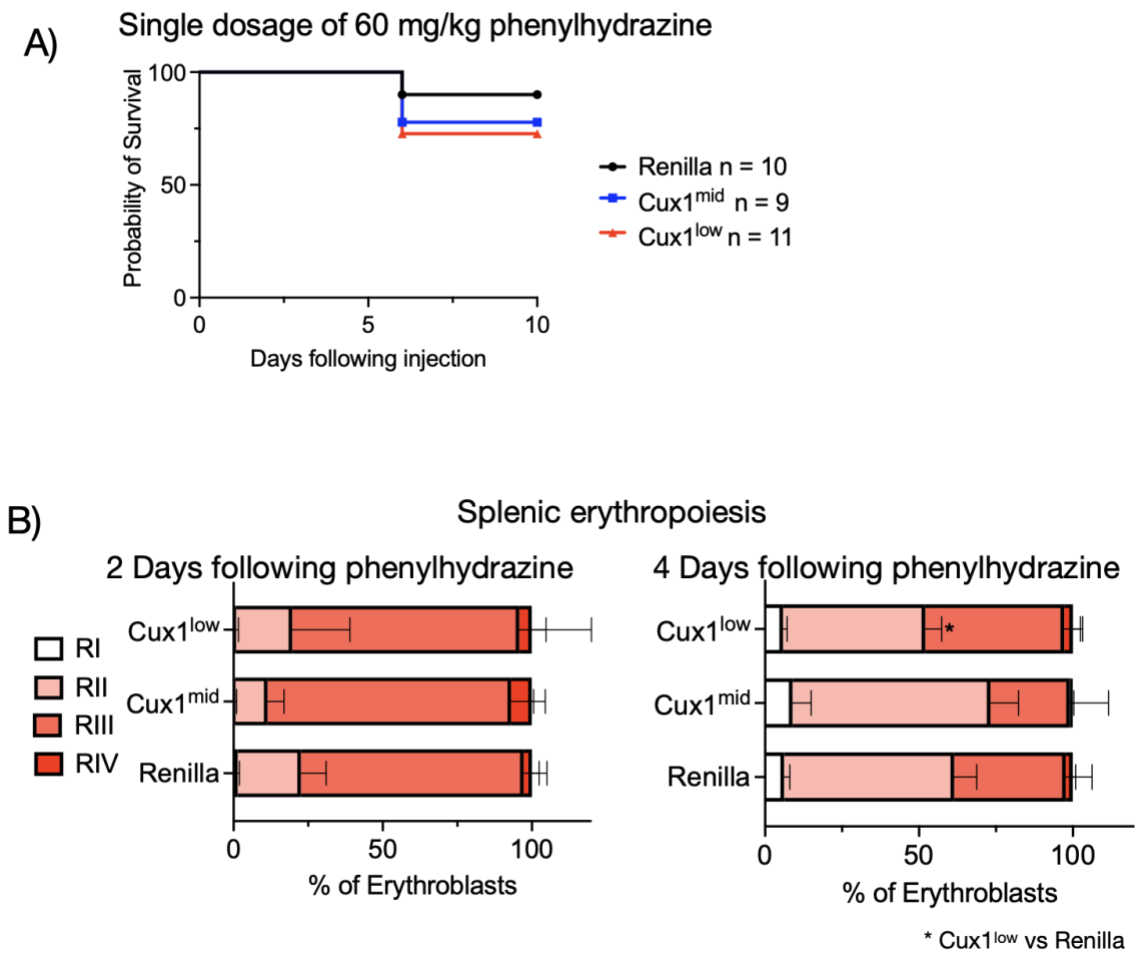

Figure 12. Splenic erythropoiesis and CBC values following acute anemic stress and CUX1 knockdown (A-B) Adult Cux1^{low}, Cux1^{mid} and littermate Ren mice were doxycycline treated to induce CUX1 knockdown for one week before phenylhydrazine injection. **(A)** Kaplan-Meier survival plot of Cux1^{low} (n=11), Cux1^{mid} (n=9), and Ren (n=10) mice following acute anemic stress induced by one dosage of 60 mg/kg phenylhydrazine (n.s. log-rank test). **(B)** Flow cytometric analysis of splenic erythroblasts 2 or 4 days after one injection of 40 mg/kg phenylhydrazine (n=3-4 mice per condition). Student *t* test **P* ≤ .05, ***P* ≤ .01, ****P* ≤ .001.

and reticulocytosis, indicative of an early anemia and erythropoietin-induced response (Figure 13A). This result indicated the need for an experimental design that circumvents the influence of erythropoietin induction. To this end, we generated mixed bone marrow chimeras with wild-type support marrow to maintain erythropoiesis and prevent anemia (Figure 13B). We transplanted CD45.2+ Ren, Cux1^{mid}, or Cux1^{low} bone marrow at a 1:1 ratio with CD45.1+ competitor bone marrow into lethally irradiated CD45.1+ wild type recipients. Traditionally CD45 isogenic markers are used to distinguish donors in a mixed bone marrow chimera, however not all erythroblasts express CD45 (Fajtova et al. 2013). As an alternative, we leveraged the design of our transgenic mice, in which the shRNAs are embedded within the 3' UTR of *GFP* in the *Col1A1* locus (Figure 7) (An et al., 2018). With this approach, nearly all experimental erythroblasts are GFP+ (Figure 14). Following transplantation, we allowed engrafted mice to recover for 4 weeks and then treated them for one week with doxycycline to induce shRNA expression (Figure 13B).

We profiled GFP+ bone marrow erythroblast differentiation stage, apoptosis, and proliferation to determine the role of CUX1 in erythroblasts at a cellular level. Compared to Ren, Cux1^{low} bone marrow erythroblasts have a reduction in early RI and RII erythroblasts and an increase in late stage RIII and RIV erythroblasts in the mixed bone marrow chimera, recapitulating findings following acute anemic stress (Figure 11D). Spleen erythroblasts followed a similar trend but did not reach statistical significance (Figure 13C). These results contrast with the characterization of Cux1^{low} erythropoiesis without support marrow whereby Cux1^{low} mice had an increase in early RI and RII

erythroblasts (An et al., 2018). This difference is likely explained by heightened erythropoietin signaling in the anemic Cux1^{low} mice at steady-state (Figure 13A) leading to increased early erythroblast survival in our prior work. Thus, in the absence of elevated erythropoietin, Cux1^{low} mice have fewer immature erythroblasts compared to controls.

We reassessed apoptosis, now in the mixed bone marrow chimera setting, and found that Cux1^{low} bone marrow erythroblasts have significantly increased apoptosis indicating that CUX1 is required for erythroblast survival (Figure 13D). Cell cycle analysis revealed that Cux1^{low} bone marrow erythroblasts have a lower percentage of cells in G1 and a shift of cells into G2/M, suggesting CUX1 normally inhibits cell cycling (Figure 13E). Taken together, these results indicate that CUX1 promotes erythroblast survival and constrains proliferation to enable optimal red cell production. In addition, these experiments highlight the importance of including support bone marrow cells to deconvolute the cell intrinsic roles of erythroid factors from the extrinsic effects of often collateral anemia.

CUX1 regulates proliferation and differentiation gene signatures

Upon finding that CUX1 regulates erythroblast survival and proliferation, we aimed to characterize the molecular mechanism by which CUX1 controls these pathways. As a HOX-family transcription factor, we predicted CUX1 would play a transcriptional role in erythroblasts and/or megakaryocyte-erythroid progenitors (MEPs), the final hematopoietic progenitor before complete commitment to the erythroid lineage.

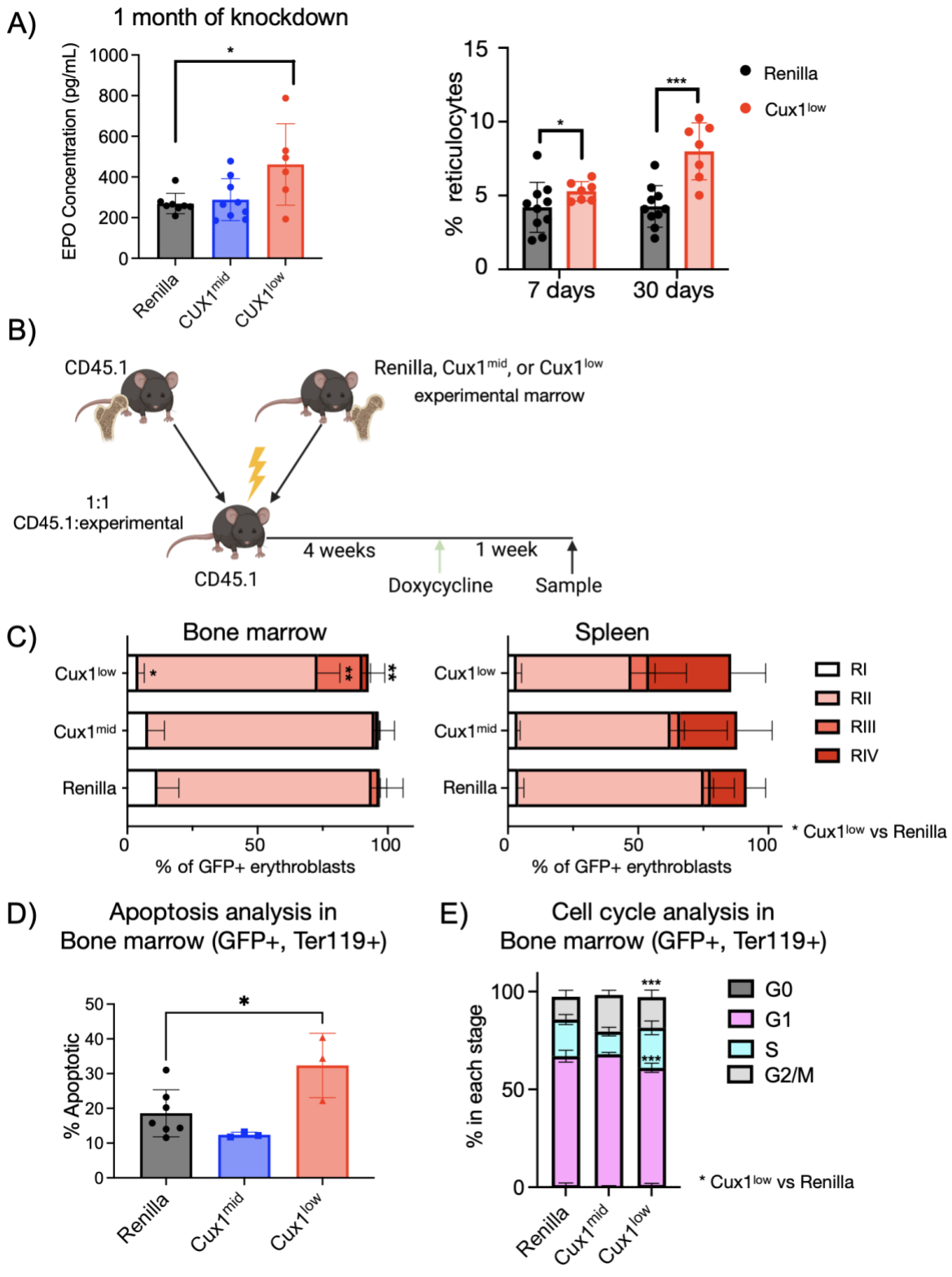

Figure 13. CUX1 regulates erythroblast differentiation, survival, and proliferation.

Figure 13, continued

(A) Erythropoietin ELISA on peripheral blood of mice treated with doxycycline for one month (n=5-9) Peripheral blood reticulocytes after 7 or 30 days of knockdown (n=7-10 mice per condition). **(B)** Experimental setup for (C-E) experimental CD45.2+ bone marrow was mixed at a 1:1 ratio with CD45.1+ wild-type support marrow and transplanted into CD45.1+ recipients. Transplant recipients were allowed 4 weeks to recover and treated for one week to induce shRNA expression before erythroblast characterization. **(C)** Differentiation stage of GFP+ erythroblasts (n=6-9). **(D)** Apoptosis of GFP+ Ter119(+) erythroblasts as measured by Annexin V and PI (n=3-7). **(E)** Cell cycle analysis of GFP+ erythroblasts (n=6-9). For all figures each point represents an individual mouse. The mean ± SD is shown. Student *t* test $*P \leq 0.05$, $**P \leq 0.01$, $***P \leq 0.001$.

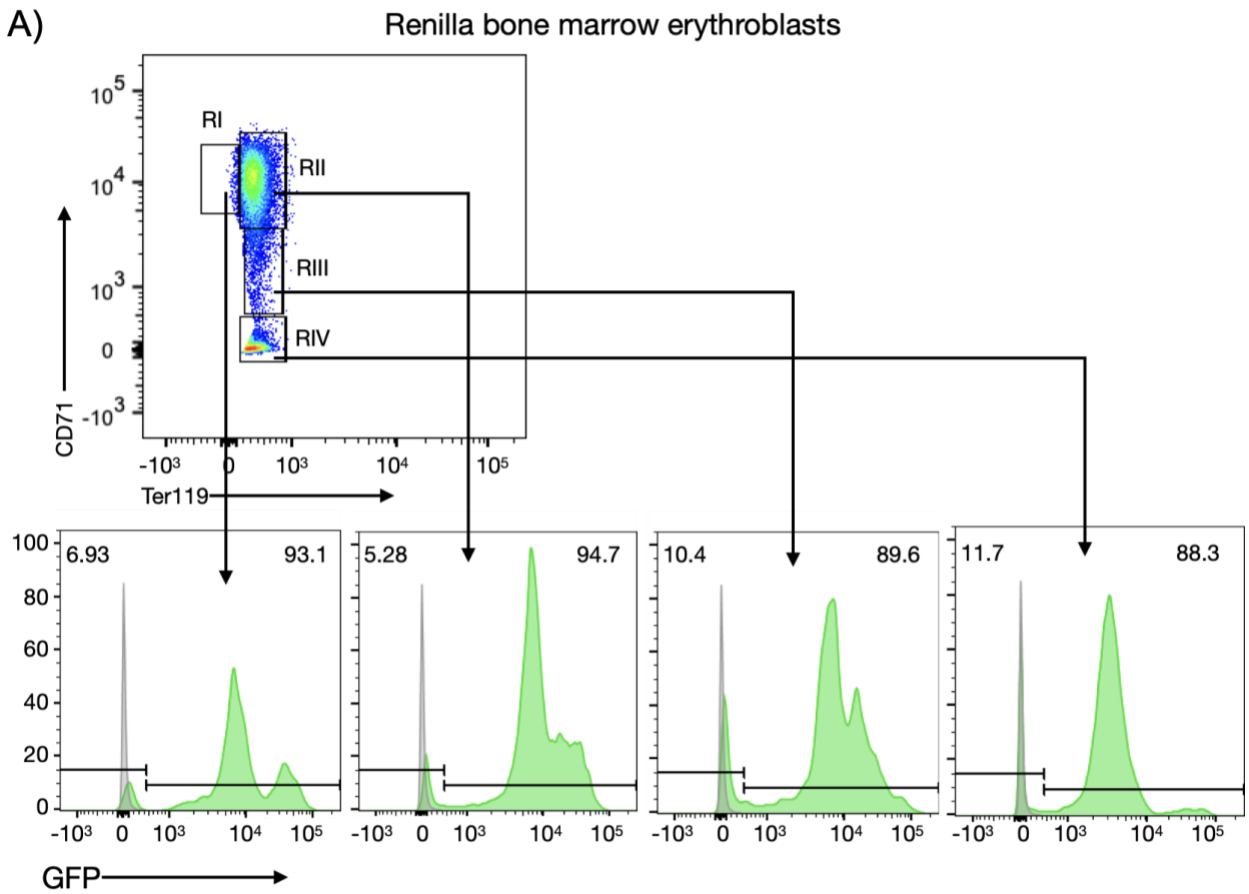

Figure 14. Gating schema for experimental erythroblasts.
GFP+ cells were gated on prior to classical CD71 vs. Ter119 erythroid gating, allowing for a mixed bone marrow chimera assessing erythroblasts. Percentages represent % GFP+ of each erythroid differentiation stage.

We profiled the transcriptome of MEPs and RII basophilic erythroblasts from Ren, Cux1^{mid}, and Cux1^{low} mice at steady-state 3 days following CUX1-knockdown. This early time frame was chosen as the mice are not yet anemic (An et al., 2018) keeping the transcriptional profile of MEPs and erythroblasts unaffected by increased erythropoietin signaling. RNA-seq analysis revealed only 35 genes with transcriptional differences in Cux1^{low} vs Ren MEPs (FDR < 0.05) (Figure 15A, circles, Figure 16A). We note that in our previous characterization, MEP numbers were unchanged following CUX1-knockdown (An et al., 2018). In contrast, principle component analysis (PCA) suggests Cux1^{low} erythroblasts are transcriptionally unique from Ren and Cux1^{mid} samples (Figure 15A, triangles). That Cux1^{mid} MEPs and RIIs clustered with their Ren counterparts is likely explained by the poor *CUX1* knockdown in these cell types (Figure 16C), and may also explain why few cellular changes were observed in Cux1^{mid} erythroblasts (Figure 10). Based on these data we further evaluated differences between Ren and Cux1^{low} RII basophilic erythroblasts.

Cux1^{low} RII erythroblasts had 374 differentially expressed genes (FDR < 0.05) (Figure 15B). Gene set enrichment analysis (Subramanian et al. 2005) determined increased cell cycle genes (“Hallmark G2M Checkpoint” gene set) in erythroblasts following CUX1 loss (Figure 15C), consistent with the increased proliferation of Cux1^{low} cells *in vivo* (Figure 13E). Cux1^{low} erythroblasts have increased expression of PI3K signaling pathway genes (“Hallmark PI3K AKT MTOR Signaling”) (Figure 15C), a pathway critical in regulating erythroblast survival and proliferation (Ghaffari et al. 2006; Kharas et al. 2010; Jiwang Zhang et al. 2006). Conversely, Cux1^{low} erythroblasts have

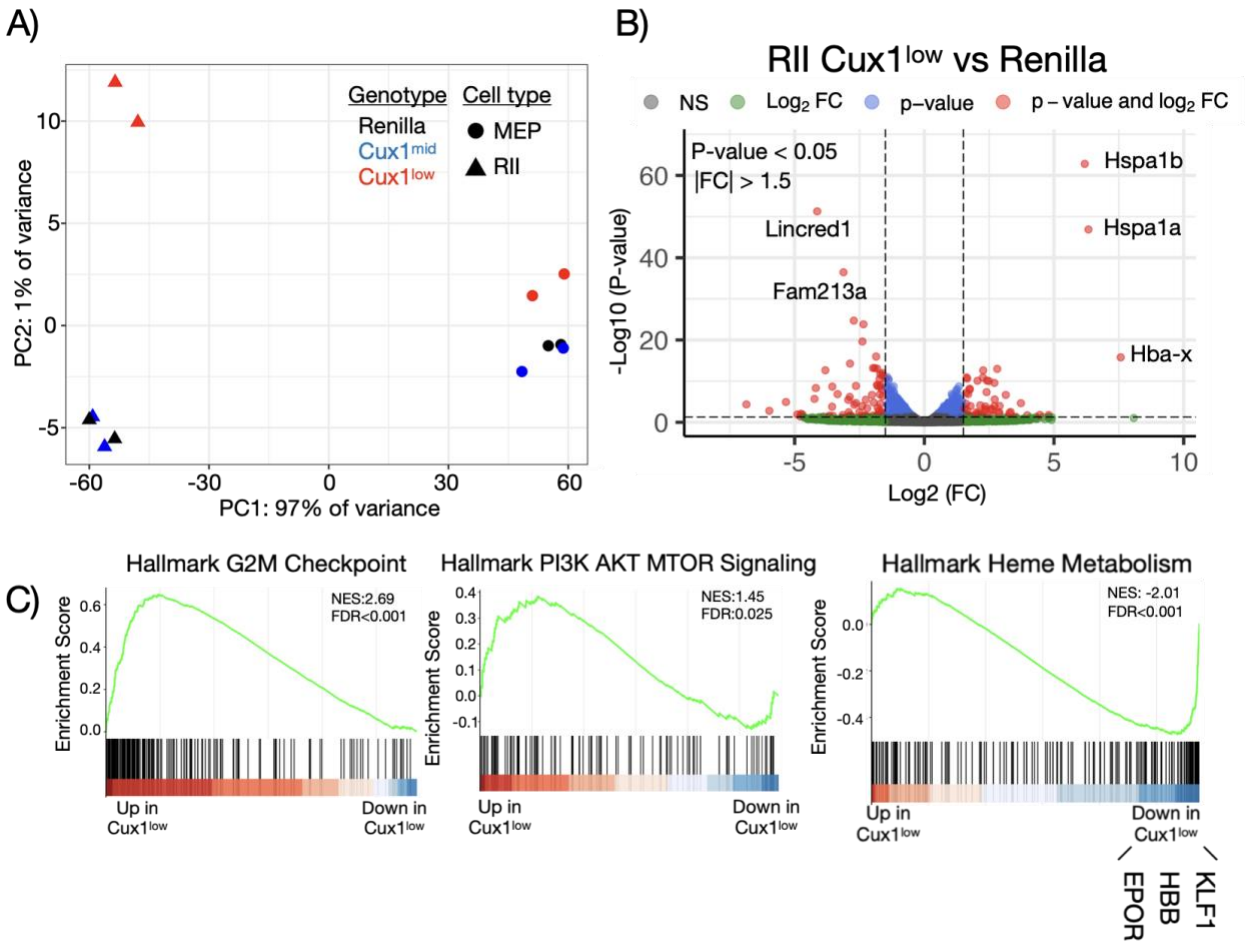

Figure 15. CUX1 knockdown transcriptionally alters erythroblast differentiation and proliferation (A-C). RNA-sequencing of RII-basophilic erythroblasts (CD71+Ter119+) and megakaryocyte-erythrocyte progenitors (Lin-cKit+CD34-CD16/32-) from Ren, Cux1^{mid}, and Cux1^{low} mice treated for 3 days with doxycycline (n=3). **(A)** PCA plot of all RNA-sequencing samples. **(B)** Volcano plot showing gene expression changes between Ren and Cux1^{low} RII-basophilic erythroblasts. Green indicates log_2(FC) > |1.5|. Blue represents p-value < 0.05. Red represents both log_2(FC) > |1.5| and p-value < 0.05. **(C)** GSEA of RNA-sequencing comparing RII-basophilic erythroblasts from Ren and Cux1^{low} mice

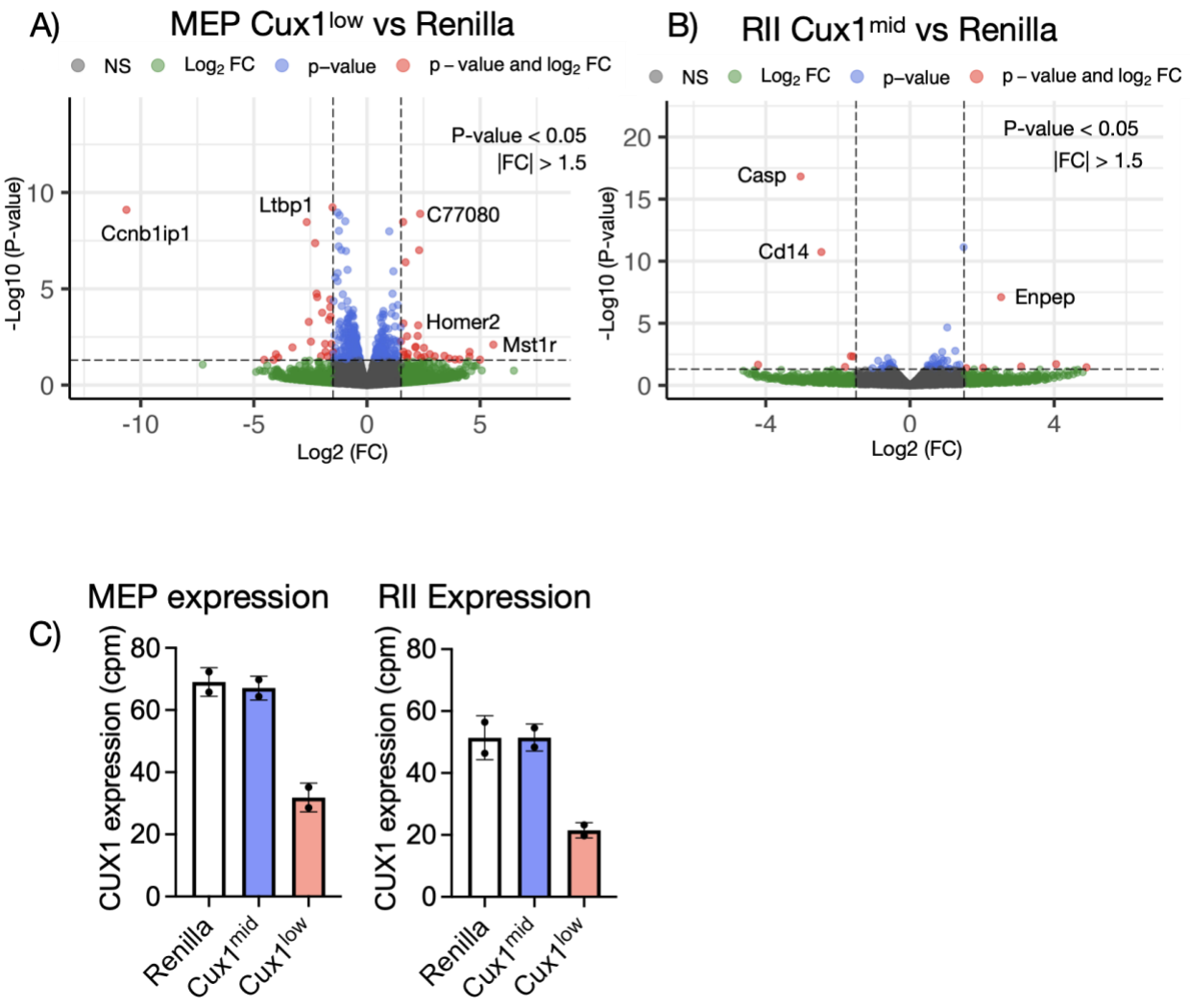

Figure 16. Few transcriptional differences are found among MEPs and between Ren and Cux1^{mid} samples. (A-B) Volcano plot showing gene expression changes between indicated genotypes and cell types. Green indicates log_2(FC) > |1.5|. Blue represents p-value < 0.05. Red represents both log_2(FC) > |1.5| and p-value < 0.05. **(C)** Relative CUX1 expression across cell types and genotypes generated from RNA-seq data.

decreased expression of key genes required for red cell differentiation (“Hallmark Heme Metabolism”) including *EPOR*, *HBB*, and *KLF1*, further supporting the observation that CUX1 is critical for erythropoiesis (Figure 15C). In conclusion, CUX1 has a modest transcriptional impact in MEPs and RIIs, and low levels of CUX1 are associated with increased proliferative and PI3K signaling signatures and decreased differentiation signatures in RIIs.

Conclusions

We previously reported that CUX1 knockdown in mice leads to myeloid malignancies characterized by anemia with age (An et al., 2018). We recapitulate these findings (Figure 9) and focus on the cellular role of CUX1 in erythropoiesis. We were unable to employ an *in vitro* system to conclusively study CUX1 during red cell development (Figure 10). Therefore, we utilized phenylhydrazine as a system of acute anemic stress to study the role of CUX1 in erythroblasts (Figure 11). We established that CUX1 is vital for recovery from acute anemic stress, indicating that while CUX1 likely has important roles in HSCs and progenitors, it also has a critical role in erythroblasts.

To uncover the unbiased cellular role of CUX in erythropoiesis we utilized mixed bone marrow-chimeras (Figure 13), and find that CUX1 is required for survival and regulates proliferation. It’s unclear how CUX1 knockdown promotes erythroblast proliferation and apoptosis. However, one possibility that will be discussed more in

future sections is evinced by the transcriptional evidence of enhanced PI3K signaling in Cux1^{low} RII-basophilic erythroblasts (Figure 15C). RNA-seq analysis of RIIs following CUX1 knockdown confirmed our results that CUX1 regulates erythroblast proliferation and differentiation (Figure 15).

CHAPTER 4: CUX1 IS REQUIRED FOR NUCLEAR CONDENSATION IN ERYTHROBLASTS

Introduction

No obvious transcriptional target CUX1 was revealed by RNA-sequencing of MEP and RIIs. Therefore, to identify the molecular mechanisms by which CUX1 regulates erythropoiesis we performed ATAC-sequencing following CUX1 knockdown. The chromatin of erythroblasts is distinct. Throughout erythroid differentiation the nucleus is condensed 10-fold in preparation for enucleation (Mei, Liu, and Ji 2021). Furthermore, the transcriptional activity, and therefore the chromatin architecture, of erythroblasts is almost exclusively involved in the production of hemoglobin and iron transport factors. The unique chromatin condition of erythroblasts provides an interesting landscape to study the activity of CUX1. Therefore, we profiled chromatin accessibly following CUX1 loss and the direct DNA targets of CUX1 in erythroblasts.

Results

CUX1 knockdown leads to extensive opening of erythroblast chromatin

We next attempted to identify direct genomic targets of CUX1 in murine RII basophilic-erythroblasts. Both ChIP-sequencing (Schmidt et al. 2014) and CUT&RUN (Meers et al. 2019) failed to map CUX1 binding sites in murine erythroblasts, perhaps due to the low expression of CUX1 in these cells. As an alternative model system, we

turned to primary human CD34+ HSPCs. We cultured the CD34+ cells in erythroid promoting conditions for 7 days to induce erythroid differentiation (Sankaran et al. 2008). At this time point, cultured cells are ~80% CD71+ and a small fraction (~3%) are also GlyA+, making these equivalent to pro- and basophilic mouse erythroblasts (Figure 17). Of note, *CUX1* CRISPR editing in human CD34+ cells also disrupts erythropoiesis under these conditions (Baeten *et al*., under revision). We performed CUT&RUN for CUX1 to identify CUX1's genomic occupancy on day 7 of erythroid differentiation. Analysis revealed 4,716 binding sites for CUX1 (IDR < 0.05). In contrast to our prior report that CUX1 preferentially binds distal enhancers (Arthur et al. 2017), the majority of CUX1 binding sites in erythroid cells are near transcriptional start sites (Figure 18A). This result may reflect enhancer decommissioning observed during erythropoiesis (Schulz et al. 2019). GREAT analysis (McLean et al. 2010) shows CUX1 targets are significantly enriched for genes in categories of "Human Phenotype: Anemia of inadequate production (ID: HP:0010972)" (binomial FDR = 0.00604) and "Mouse Phenotype Single KO: abnormal erythropoiesis (ID: MP:0000245)" (binomial FDR = 0. 00001). Motif analysis revealed an enrichment for STAT, AP1, and GATA motifs in CUX1 binding sites, all of which are quintessential transcriptional regulators in erythropoiesis (Ferreira et al. 2005; Jacobs-Helber and Sawyer 2004; Won et al. 2009) (Figure 18B). These results indicate CUX1 binds widely in developing erythroid cells, with an enrichment at critical erythroid genes, and at sites likely co-occupied by other key erythroid regulators.

To determine if CUX1 regulates chromatin accessibility in murine MEPs and RII erythroblasts, we performed ATAC-seq (Buenrostro et al. 2015) in these populations.

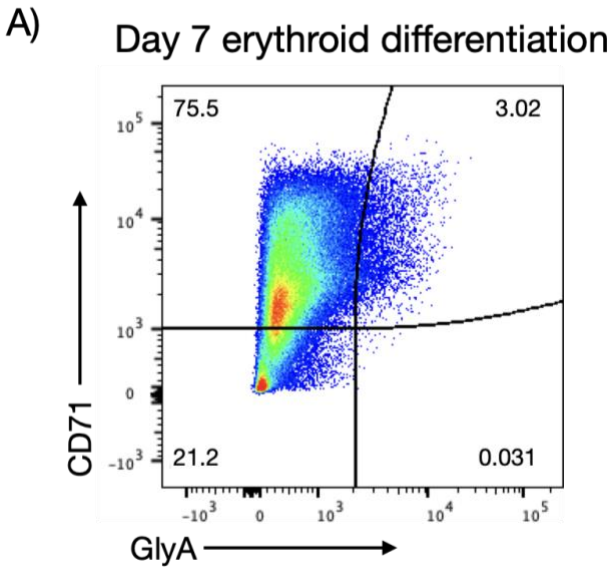

Figure 17. Differentiation of human erythroblasts using *in vitro* culture. Flow cytometry analysis of human CD34 erythroid cultures 7 days after erythroid induction.

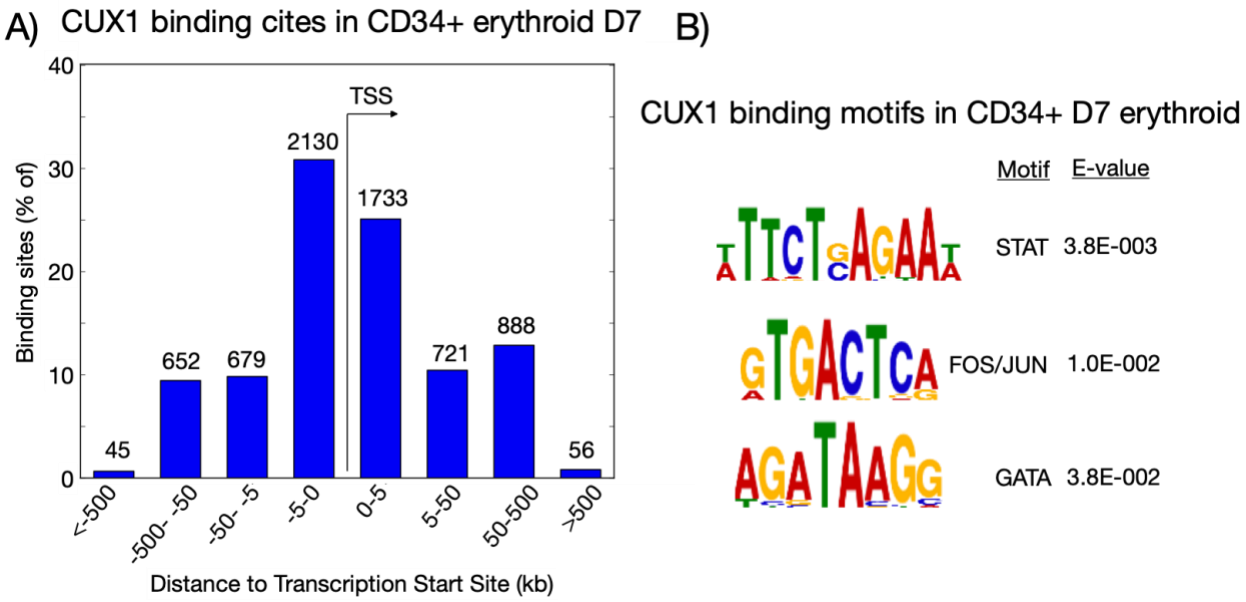

Figure 18. CUX1 binds promoters and CUX1 binding sites contain motifs of quintessential erythroid factors
(A) Profile of regions CUX1 occupies in human CD34+ cells on D7 of erythroid differentiation **(B)** Meme suite (Bailey and Elkan 1994) analysis of motifs CUX1 occupies in CD34+ D7 cells.

Similar to the transcriptional profiles, there were few changes in chromatin accessibility between Ren and Cux1^{low} MEPs (Figure 19A), and Cux1^{mid} samples largely resembled Ren counterparts (Figure 19C). In contrast, Cux1^{low} erythroblasts gained 3,821 peaks compared to Ren erythroblasts (FDR < 0.05), indicating more regions of accessible chromatin following CUX1 loss (Figure 20A). To test this finding more rigorously, we performed DiffBind analysis (Ross-Innes et al. 2012) which revealed 6,191 sites (57% of peaks) had increased accessibility in Cux1^{low} cells (FDR < 0.05) (Figure 20B). As can be appreciated in the MA-plot in Figure 20B, the vast majority of sites gained accessibility, even if they did not meet the 5% FDR threshold. These data indicate that CUX1 has a profound impact on chromatin accessibility in erythroblasts and little effect on MEPs.

During terminal erythroid differentiation erythroblasts condense their chromatin ten-fold in preparation for enucleation (Reviewed in (Mei, Liu, and Ji 2021)). Our previous data indicate that CUX1 deficiency disrupts differentiation. Thus, perhaps increased chromatin accessibility in CUX1-knockdown cells reflects a block in differentiation. To test this hypothesis, we compared the chromatin accessibility profiles of Cux1^{low} erythroblasts to Ren MEPs, reasoning that if Cux1^{low} erythroblasts have stalled chromatin condensation, they would be more akin to control MEPs than control RIIs. However, PCA analysis does not support this conclusion. Principle component 1 (64% of variance) distinctly delineates samples by cell type, including clustering Cux1^{low} erythroblasts with Ren erythroblasts (Figure 20C). Nonetheless, Cux1^{low} RIIs clearly segregate away from Ren RIIs. Thus, Cux1^{low} erythroblasts are not in a progenitor-like

chromatin state and are instead, in a distinct and aberrant state not represented in the normal erythroid trajectory.

We then asked if the distinct chromatin state of Cux1^{low} RIIs was due to increased accessibility at normally accessible sites or were *de novo* accessible sites not normally present. To distinguish these possibilities, we lowered the peak calling cut-off of Ren samples to identify putative sub-threshold peaks in control cells. These low-threshold peaks in Ren RIIs are perhaps representative of areas transitioning between open and closed states. We chose a cut-off of FDR < 0.25 as the resulting Ren (FDR < 0.25) and Cux1^{low} (FDR <0.05) thresholds resulted in comparable number of peaks (Figure 20D). This analysis revealed that 74.9% of the peaks called in Cux1^{low} RIIs (FDR < 0.05) were present in Ren RIIs (FDR < 0.25, Figure 20D). This result demonstrates that the majority of ATAC-seq peaks in Cux1^{low} erythroblasts are present in control samples, albeit at lower levels. In other words, sites of pre-existing accessibility become more open in the absence of CUX1 in RII cells. This phenomenon can also be appreciated by visual inspection of IGV browser tracks (Figure 20E) (Thorvaldsdóttir, Robinson, and Mesirov 2013).

To determine if CUX1 directly binds the genomic regions that gained ATAC-seq accessibility, we used UCSC LiftOver (Kuhn, Haussler, and James Kent 2013) to convert the human CUX1 CUT&RUN peaks to mouse genomic coordinates. Following LiftOver, we retained 3,516 CUX1 binding sites (84%). We found 78% of CUX1 binding sites were accessible in the Cux1^{low} erythroblasts suggesting CUX1 may be responsible for the changes in chromatin accessibility. An exemplary region of the genome shows increased accessibility in Cux1^{low} erythroblasts, with CUX1 directly binding the

accessible regions (Figure 20E). Thus, regions with low levels of accessibility become significantly more open following CUX1, and many of these sites are direct CUX1 targets.

Erythroblast chromatin condensation is dependent on CUX1

Given the breadth and magnitude of changes in chromatin accessibility upon CUX1 loss, we anticipated a corresponding impact on overall nuclear condensation. As a proxy for nuclear condensation, we first measured nuclear size in Ren and Cux1^{low} RII erythroblasts by DAPI immunofluorescence staining. As controls, we included Ren RI and RIV erythroblasts, which have larger and smaller nuclear areas respectively (Figure 21A). Compared to Ren RIIs, Cux1^{low} RIIs had significantly larger nuclear size (Figure 21A). While this result is consistent with defective nuclear condensation in Cux1^{low} cells, we aimed to measure chromatin compaction more directly. To this end, we employed Fluorescence Lifetime Imaging Microscopy (FLIM) which measures chromatin compaction by DAPI fluorescence lifetime (Estandarte et al. 2016; Spagnol and Dahl 2016). Longer DAPI lifetime is associated with decondensed chromatin while a shorter lifetime is indicative of condensed chromatin (Estandarte et al. 2016; Spagnol and Dahl 2016). Compared to Ren RII erythroblasts, Cux1^{low} RII's have longer DAPI fluorescence lifetimes consistent with less condensed chromatin (Figure 21B). Indeed, the mean DAPI lifetime of Cux1^{low} RII cells was akin to Ren RIIs treated with the histone deacetylase (HDAC) type I and II inhibitor, trichostatin-A (Figure 21B). These results confirm that CUX1 is required for chromatin condensation during terminal erythroid differentiation.

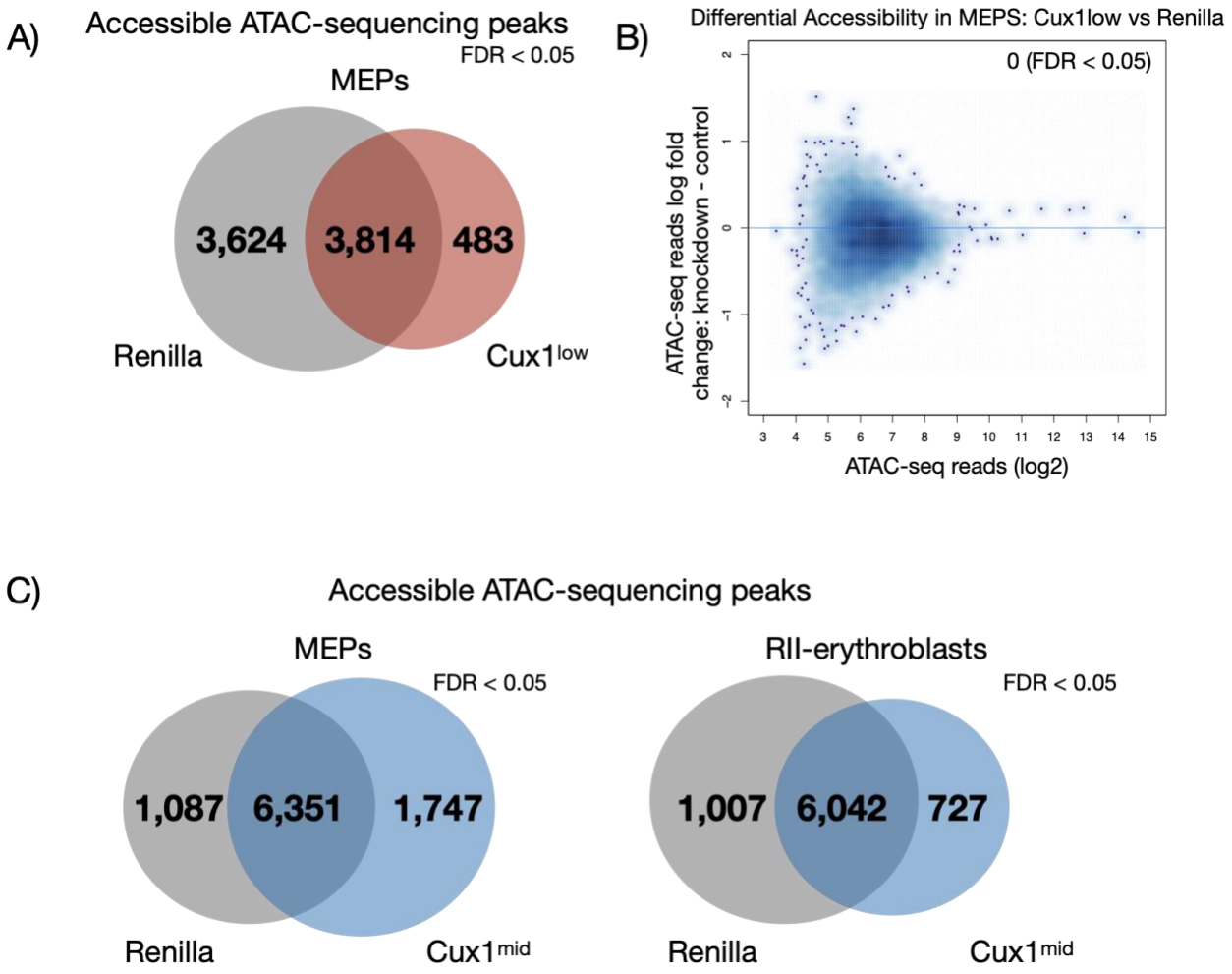

Figure 19. Chromatin accessibility in MEPs and Cux1^{mid} samples
(A-C). ATAC-sequencing of RII-basophilic erythroblasts and Megakaryocyte-erythrocyte progenitors from Ren, Cux1^{mid}, and Cux1^{low} mice treated for 3 days with doxycycline. Venn diagrams show absolute peak number.

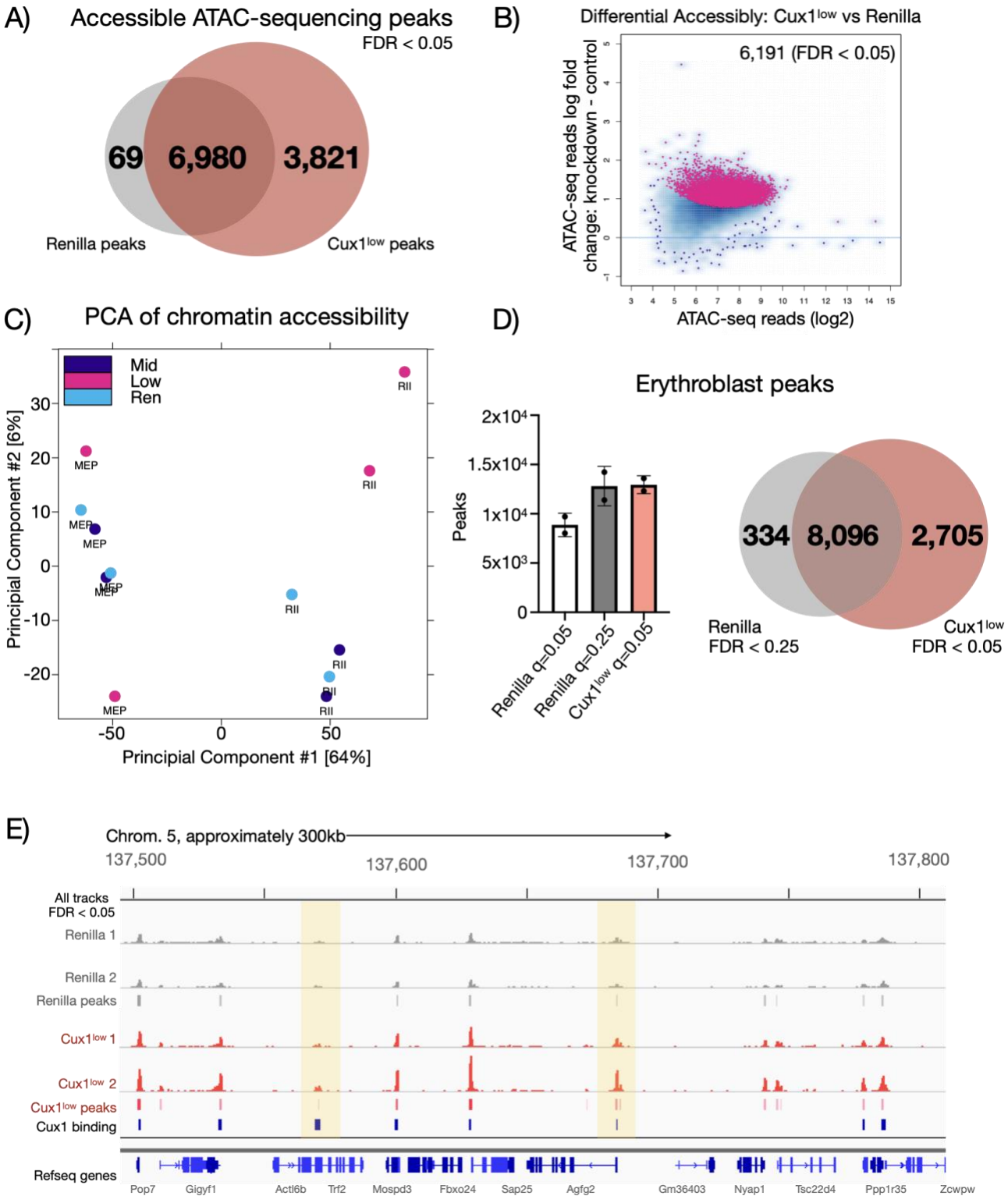

Figure 20. Cux1^{low} erythroblasts have increased global chromatin accessibility (A-E). ATAC-sequencing of RII-basophilic erythroblasts (CD71+Ter119+) and megakaryocyte-erythrocyte progenitors (Lin-cKit+CD34-CD16/32-) from Ren and

Figure 20, continued

Cux1^{low} mice treated for 3 days with doxycycline (n=2 biological replicates). **(A)** Venn diagram of absolute peak number (FDR < 0.05) from Ren and Cux1^{low} RII-erythroblasts. **(B)** MA plot from DiffBind (Brown, 2011) analysis of Ren and Cux1^{low} peaks. Pink dots indicate FDR < 0.05. **(C)** PCA plot of chromatin accessibility of MEP and RII cells across genotypes. **(D)** Absolute peak number from Ren samples (MACs q<0.25 or q<0.05) and Cux1^{low} samples (q<0.05). Venn diagram of overlap between ATAC-seq peaks from Cux1^{low} RIIs (q<0.05) and Ren RIIs at a less stringent cut-off (q<0.25). **(E)** Example genomic region comparing ATAC-seq data from Ren and Cux1^{low} RII erythroblasts. CUX1 CUT&RUN data is derived from human CD34+ cells on day 7 of erythroid differentiation conditions. Human data was converted to murine genomic coordinates by liftOver (Kuhn, Haussler, and James Kent 2013).

To determine if the role of CUX1 in nuclear condensation is conserved in human cells, we measured the size of human erythroblasts following CUX1 knockdown. We used CRIPSR/Cas9 to target *CUX1* (gCUX1) in primary human CD34+ cells or safe-harbor control genes with 38.3-65.6% editing efficiency and placed them in erythroid promoting conditions for 7-14 days (Imgruet et al. 2021) (Baeten *et al*., under revision). At the end of the culture period, gCUX1 erythroid cells were larger than control cells by FSC-A (Figure 21C). To test if the increased size was a reflection of the nuclear size, we measured DAPI fluorescence area of the human cells throughout differentiation. At day 7 in the culture gCUX1 cells also had a significantly larger nuclear area than the control counterparts (Figure 21D). Taken together, these results indicate that CUX1 regulates nuclear condensation in both human and mouse erythroblasts.

CUX1 is required for histone deacetylation in erythroblasts

During erythropoiesis the chromatin undergoes dynamic changes in preparation for condensation and enucleation (reviewed in (Sundaravel, Steidl, and Wickrema 2021)) The mechanisms governing nuclear condensation preceding enucleation in erythroblasts is an active area of research. However, it is known that histone deacetylation is required during erythropoiesis in both human and mouse cells (Popova et al. 2009; Yamamura et al. 2006). To identify the molecular mechanism by which CUX1 regulates chromatin condensation we first investigated if CUX1 transcriptionally regulates HATs (histone acetyl transferases) or HDACs. By RNA-seq, we find no significant differences in the expression level of HATs or HDACs between Ren and

Cux1^{low} MEPs or RII erythroblasts (Figure 22A). This observation connotes CUX1 does not transcriptionally regulate writers or erasers of histone acetylation.

CUX1 has been reported to directly interact with histone deacetylases (Kühnemuth et al. 2015a; S. De Li et al. 1999; Sharma et al. 2009). To investigate whether CUX1 co-occupies genomic sites with HDACs, we performed ChIP-seq in the Tier-1 ENCODE human erythroid leukemia cell line K562 (Gauwerky, Lusis, and Golde 1982). This enabled us to identify potential partners of CUX1 by intersecting CUX1 binding sites with publicly available HDAC occupancy datasets. Analysis revealed 26,497 CUX1 ChIP-seq peaks in K562 cells (IDR < 0.05). We observed 65%, 44%, and 23.8% of CUX1 binding sites overlap with peaks of HDAC1, HDAC2, and HDAC3, respectively (Figure 23A). The high percentage of co-occupancy of CUX1 and HDAC1 is consistent with prior reports that HDAC1 is a known binding partner of CUX1 (Kühnemuth et al. 2015a; S. De Li et al. 1999; Sharma et al. 2009). These results led us to consider that CUX1 interacts with HDACs in erythroblasts to promote histone deacetylation. To test this model, we examined global histone acetylation levels following CUX1 loss in K562 cells. We evaluated previously reported mass spectrometry-based measurements of histone post-translational modifications of CRIPSR-edited *CUX1* (gCUX1) and *HPRT* (gHPRT) K562 cells (Yuan et al. 2018) (Imgruet et al., 2021). H3K23Ac, H3K18Ac, and H3K20Ac were significantly increased in gCUX1 cells, consistent with a role for CUX1 in regulating histone deacetylation (Figure 23B).

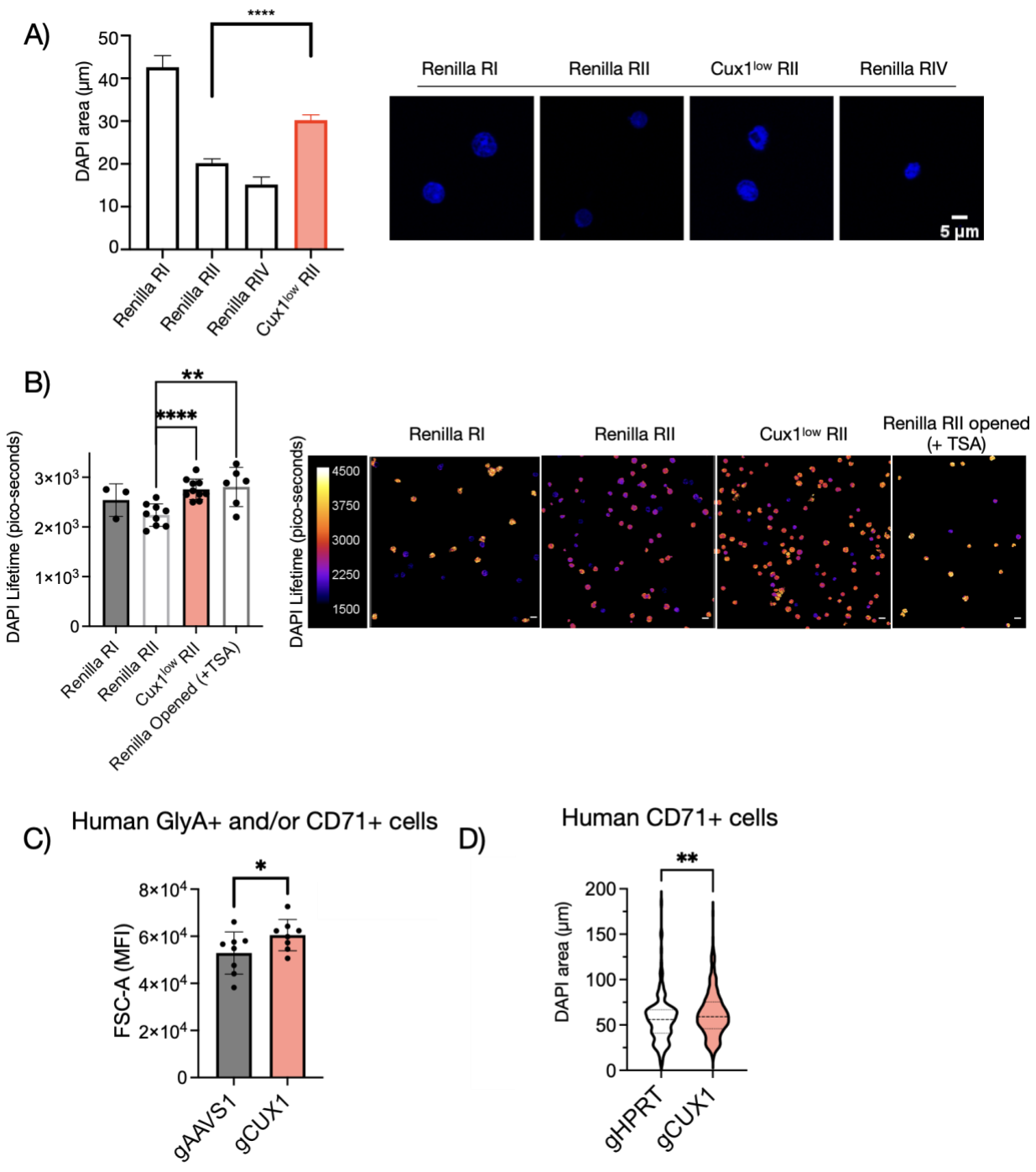

Figure 21. CUX1 is required for chromatin condensation during terminal erythroid differentiation. (A-B). Immunofluorescence microscopy on sorted erythroblasts from Cux1^{low} or Ren mice after one week of knockdown. **(A)** Nuclear size as measured by total DAPI area, mean and SEM is plotted next to representative image (n=5). **(B)** Fluorescence Lifetime Imaging Microscopy (FLIM) of DAPI in murine erythroblasts. Each point is the mean fluorescence lifetime of an individual slide (n=3-10). White scale bar represents 10 µm. Representative image showing DAPI lifetime of nuclear area of

Figure 21, continued

nucleated erythroblasts is shown. Color indicates DAPI lifetime from shortest 1500 picoseconds to longest 4500 picoseconds. **(C)** FSC-A from human CD34s after culturing in erythroid promoting conditions for 14 days with CUX1 knockdown (gCUX1) or a guide targeting editing safe-harbor gene AAVS1 (gAAVS1) (n=8). **(D)** Nuclear size measured by total DAPI area in human CD34 cells cultured in erythroid promoting conditions for 7 days with CUX1 knockdown (gCUX1) or guide targeting safe-harbor gene HPRT (gHPRT) (n=2). Student *t* test *$P \leq .05$, **$P \leq .01$, ***$P \leq .001$.

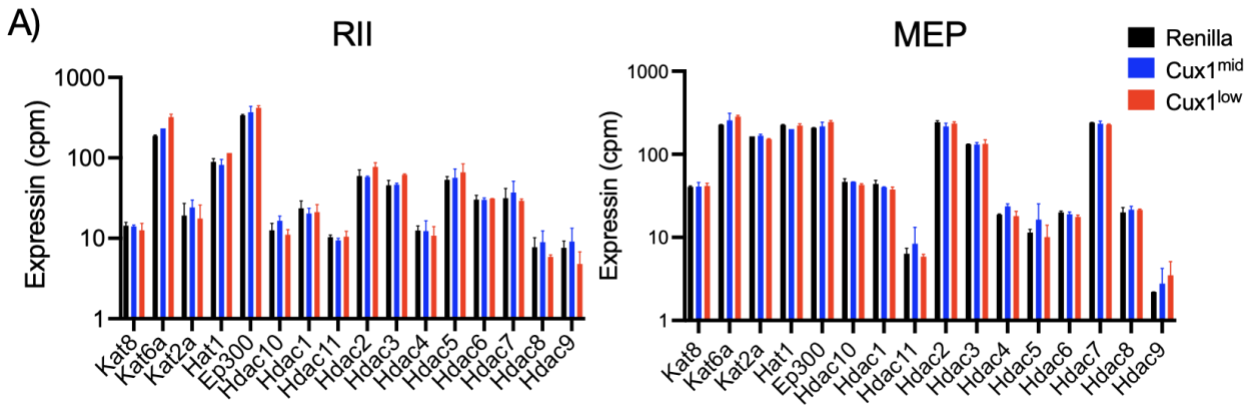

Figure 22. Expression of histone acetyl transferases and histone deacetylases. Relative expression of histone acetyl transferases and histone deacetylases following CUX1 knockdown cell types and genotypes generated from RNA-seq data.

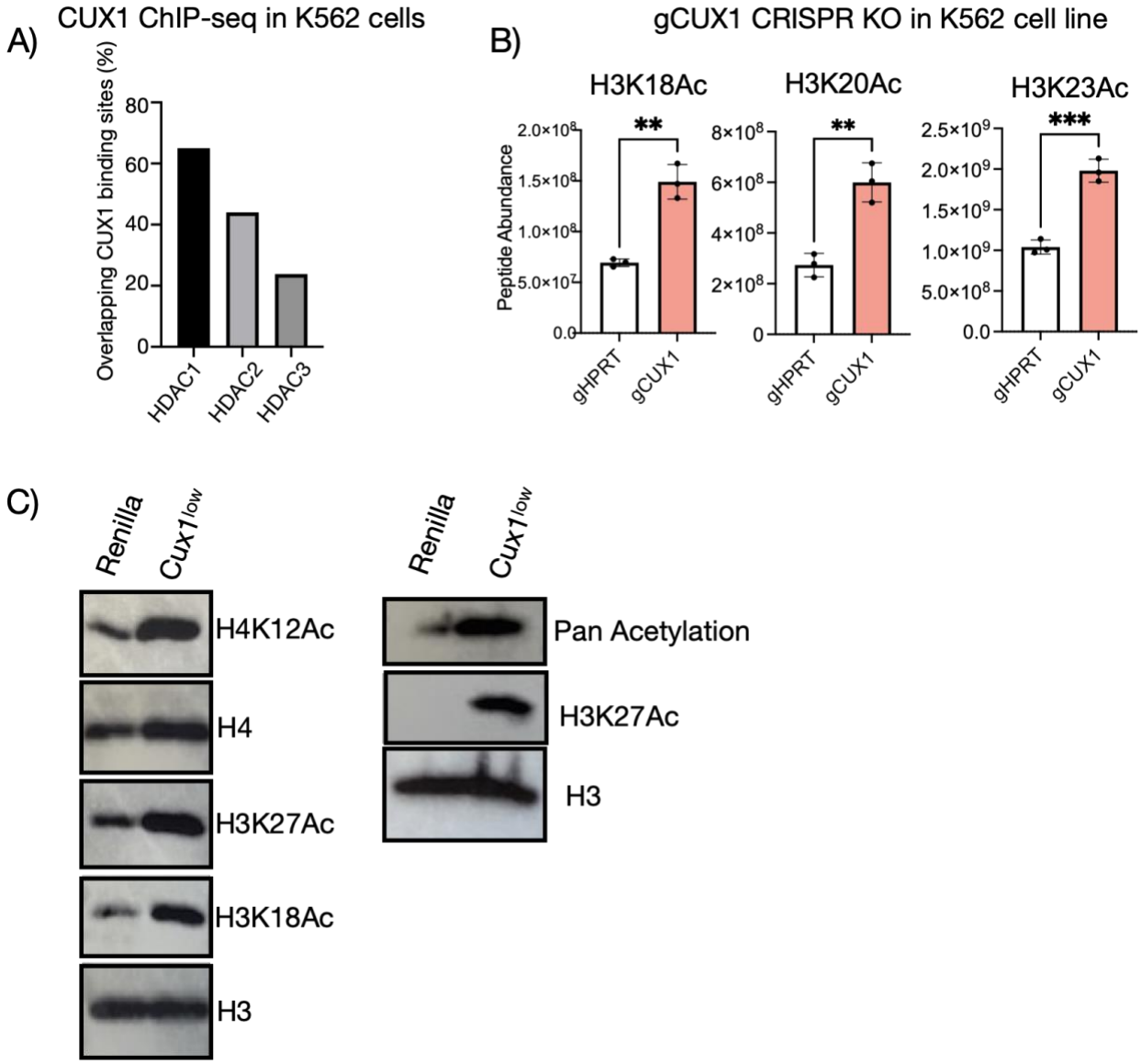

Figure 23. CUX1 is required for histone deacetylation in erythroblasts
(A) Intersection of CUX1 and HDAC ChIP-seq binding sites in K562 cells. :GSE91720 (Lou et al. 2020), GSE12712 and GSE127356 (Jing Zhang et al. 2020). **(B)** Acetylated peptide abundance from LC-MS/MS in K562 cells with CUX1 knockdown (gCUX1) or control (gHPRT) (Imgruet et al. 2021) **(C)** Sorted RII-basophilic erythroblasts from Ren and Cux1^{low} mice with CUX1-knockdown for one week. Representative western blot shown (n=3, total histone acetylation n=2) Student *t* test *$P \leq .05$, **$P \leq .01$, ***$P \leq .001$.

To ascertain if CUX1 is required for histone deacetylation in primary erythroblasts, we sorted RII erythroblasts from Ren and Cux1^{low} mice one week after shRNA induction and performed western blots for total histone acetylation. As shown in Figure 6C, total histone acetylation is elevated in Cux1^{low} RII cells. We then probed for acetylation marks reported to decrease during erythropoiesis including H4K12Ac (Jayapal et al., 2010; Popova et al., 2009; Y. Wang et al., 2021) and H3K27Ac (Romano et al. 2020). We find increased deposition of both of these marks, as well as H3K18Ac and H3K23Ac, following CUX1 knockdown (Figure 23C). These data confirm that CUX1 is essential for histone deacetylation in erythroblasts.

Conclusions

Using primary human stem cells differentiated into erythroblasts (Figure 17) we find CUX1 binds promoters in erythroblasts and occupies binding sites shared by quintessential erythroid transcription factors (Figure 18). ATAC-sequencing on murine RIIs and MEPs reveals a novel role for CUX1 in chromatin condensation. CUX1 does not regulate the accessibility of MEP chromatin (Figure 19). However, there is a global and dramatic increase in chromatin accessibility in erythroblasts following CUX1 knockdown (Figure 20). We confirm CUX1 regulates erythroblast nuclear size through confocal microscopy of DAPI nuclear area (Figure 21A). We then go on to show CUX1 knockdown is directly linked with nuclear condensation using Fluorescence Lifetime Imaging Microscopy (Figure 21B), and that human erythroblasts experience similar increases in nuclear size with CUX1 loss (Figure 21C, D). Finally, we identify the

molecular mechanism responsible for the failure of chromatin condensation to be impaired histone deacetylation (Figure 23).

CHAPTER 5: DISCUSSION

Conclusions

In this dissertation we examined the mechanisms of tumor suppressor gene CUX1 in red blood cell development. We first confirmed CUX1 is vital for recovery from acute anemic stress (Figure 11), thereby indicating that CUX1 is essential in erythroblasts. We then identified the cellular role of CUX1 as a regulator of erythroblast survival and proliferation (Figure 13). RNA-sequencing of erythroblasts confirmed that CUX1 indeed regulates the proliferation and development of red cell progenitors (Figure 15). We go on to identify through ATAC-sequencing that knockdown of CUX1 leads to a dramatic increase in erythroblast chromatin accessibility (Figure 20). These data led us to hypothesize that CUX1 regulates nuclear condensation during red cell development. Both confocal microscopy on nuclear size and Fluorescence Lifetime Imaging Microscopy to validate that indeed, CUX1 loss leads to a defect in erythroblast chromatin condensation (Figure 21). Finally, we find the mechanism by which CUX1 regulates nuclear condensation to be through histone deacetylation. Thus, we put forth a model wherein CUX1 interacts with histone deacetylases to nuclear condensation during terminal erythroid development (Figure 24). Taken together, these results are critical for the understanding of the pathogenesis of CUX1 loss in anemia and red cell biology as a whole.

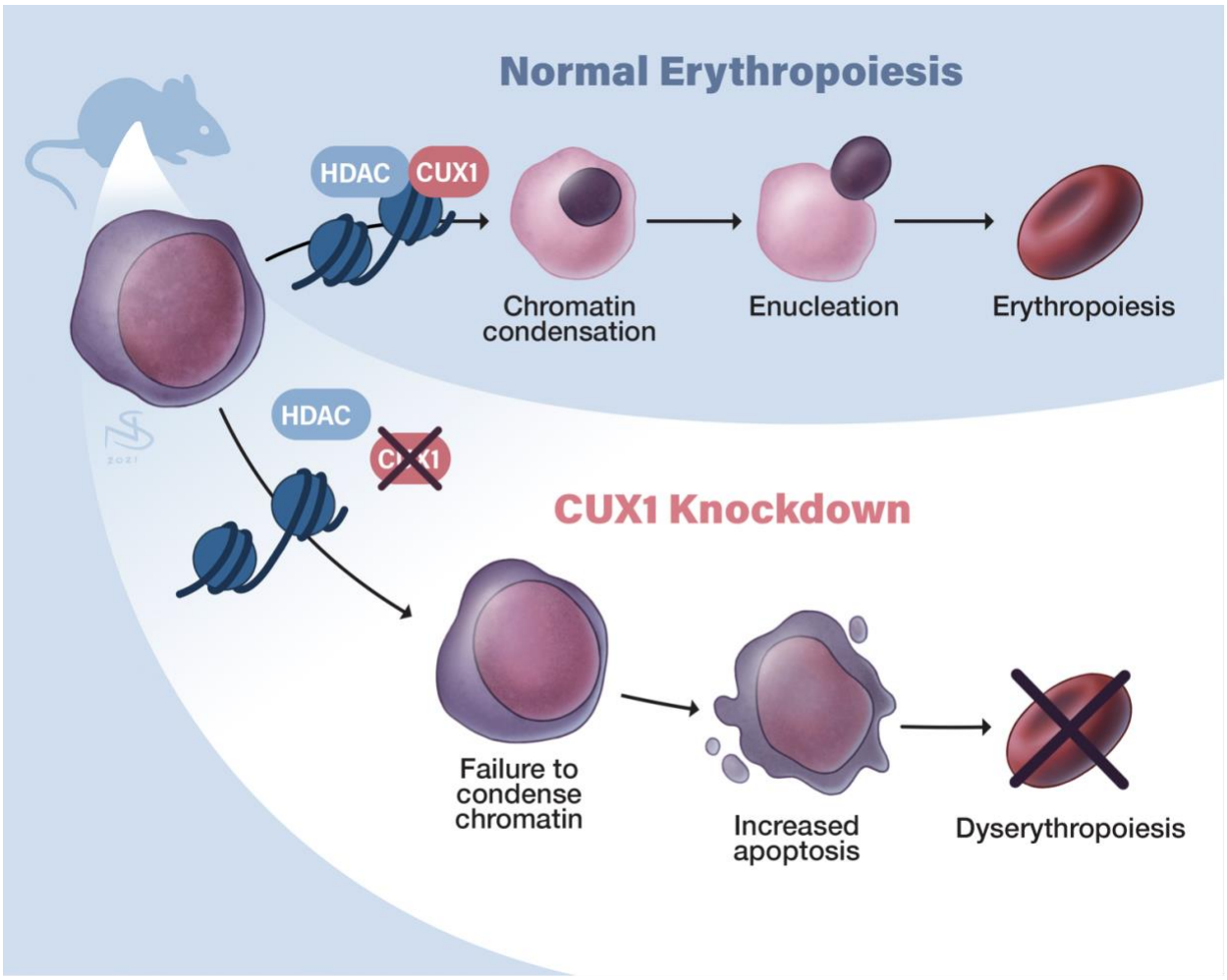

Figure 24. Model of CUX1 interacting with HDACs to facilitate histone deacetylation in erythroblasts. Our model of the role of CUX1 in erythropoiesis. In cases of CUX1 sufficiency, CUX1 interacts with HDACs to facilitate histone deacetylation. This allows for nuclear condensation and functional erythropoiesis. In the setting of CUX1 knockdown there is a failure to deacetylate and condense the chromatin, leading to increased erythroblast apoptosis and dyserythropoiesis.

Discussion

We previously reported that CUX1 knockdown in mice leads to myeloid malignancies characterized by anemia with age (An et al., 2018). This result established that loss of this single chromosome 7 encoded gene recapitulates fundamental features of myeloid malignancies in patients. In this thesis, we focused on the mechanistic role of CUX1 in erythropoiesis. We established that CUX1 is vital for recovery from acute anemic stress, indicating that while CUX1 likely has important roles in HSCs and progenitors, it also has a critical role in erythroblasts.

To uncover the unbiased cellular role of CUX in erythropoiesis we utilized mixed bone marrow-chimeras, and find that CUX1 is required for survival and regulates proliferation. It's unclear how CUX1 knockdown promotes erythroblast proliferation and apoptosis. One possibility is evinced by the transcriptional data indicating enhanced PI3K signaling in $Cux1^{low}$ RII-basophilic erythroblasts (Figure 15C). PI3K signaling is a delicate balance in erythroblasts; too little (Haseyama et al. 1999; Von Lindern et al. 2001; Sivertsen et al. 2006) prevents erythroblast proliferation, leading to apoptosis and stalled development. While too much PI3K activity (Ghaffari et al. 2006; Kharas et al. 2010; Jiwang Zhang et al. 2006) also results in increased apoptosis, hyper-proliferation, and dysregulated differentiation. CUX1 is known to directly regulate PI3K signaling through transcriptional control of the PI3K inhibitor, PIK3IP1 (Wong et al. 2013). Indeed, *CUX1* knockdown cells have decreased *Pik3ip1* by RNA-seq. Thus, although not directly tested herein, lowered levels of negative regulators of PI3K may translate to increased PI3K activity, resulting in increased proliferation and apoptosis. In this case,

PI3K inhibitors could potentially resolve these defects to promote RBC differentiation and abating the anemia experienced with CUX1 loss.

Centrally, in the course of identifying presumed transcriptional targets of CUX1, we uncovered a new role for CUX1 in the epigenetic regulation of erythroblast nuclear condensation. Based on our findings, we propose a model wherein CUX1 binds to sites of accessible DNA in maturing erythroblasts where it recruits HDACs to actively deacetylate and close chromatin (Figure 24). While the role of HDACs in erythropoiesis has been appreciated (Jayapal et al., 2010; Ji, Yeh, Ramirez, Murata-Hori, & Lodish, 2010; Y. Wang et al., 2021; Yamamura et al., 2006), how HDACs are recruited to DNA during nuclear condensation has remained unclear, as HDACs do not have intrinsic DNA binding activity. Our data implicate CUX1 as this missing link and reveal CUX1 to be a novel epigenetic regulator of erythropoiesis.

Normally, chromatin is condensed throughout human erythropoiesis as evinced by ATAC-seq data of HSCs, MEPs, and erythroblasts (Schulz et al. 2019). CUX1 knockdown cells do not exist on this pathway, however (Figure 20) suggesting they are a deviation without a normal counterpart. This may reflect the finding that HATs and HDACs normally co-exist at active genes and dynamically regulate histone acetylation (Wang, Z. et al., 2009). The absence of CUX1 disrupts this balance, and steers the cells to an aberrant epigenetic state. Despite this wide-spread chromatin opening, CUX1 knockdown caused only modest effects on gene transcription, yet had a marked impact on nuclear size and condensation. It is unclear why gene expression is not more impacted, although our results are reminiscent of those observed after knockout of the H4K20 methyltransferase and transcriptional repressor *Setd8* (*Kmt5a*) (Malik et al.

2017). RNA-seq of *Setd8*-/- CD71+/Ter119+ fetal erythroblasts yielded gene expression changes and nuclear decompaction on par with that seen in Cux1^{low} cells. Perhaps gene expression effects may be deferred to later stages of development, as seen in HDAC5 knockdown erythroblasts (Wang, Y. et al., 2021). Alternatively, histone deacetylation in erythroblasts may be functionally more important for achieving the unique genome architecture required for nuclear extrusion rather than regulating gene expression. Indeed, HDACs do not always repress gene expression as commonly thought (Seto and Yoshida 2014).

The cellular changes in erythroblasts may also be tied to epigenetic defects; disruption of Setd8 (Malik et al. 2017), HDAC5 (Wang, Y. et al., 2021), and the histone acetyltransferase Gcn5 (Jayapal et al., 2010) all lead to increased apoptosis in erythroblasts. On the other hand, CUX1 knockdown is frequently associated with increased cellular proliferation (reviewed in (Liu et al. 2020)), thus this could be a general feature of CUX1 tumor suppressor activity in hematopoietic cells. Aberrantly increased proliferation may prematurely advance Cux1^{low} cells through developmental stages while bypassing the necessary post-mitotic differentiation required for successful RBC generation. Accelerated progression through the cell cycle without differentiation may explain the increase in reticulocytes (Figure 13C, D) and shift toward late stage erythroblasts (Figure 9D, Figure 11B, and Figure 13C) found with CUX1 knockdown.

While RBC enucleation is largely a mammalian feature, RBCs in all vertebrates undergo nuclear condensation (Ji, Murata-Hori, and Lodish 2011). Enucleation is thought to enable a higher cellular concentration of hemoglobin, and allow RBCs to nimbly traverse tight capillary spaces. Other mammalian cell types also condense and

remove their nuclei as a normal course of differentiation, namely skin keratinocytes and lens fiber cells. The process in these two cells appears distinct, however; while erythroblasts expel nuclei, keratinocytes and lens fiber cells are thought to undergo internal nuclear degradation (Rogerson, Bergamaschi, and O'shaughnessy 2018). However, CUX1 may indeed play a role in the maturation of these cell types as well as evidenced by the skin problems experienced by $Cux1^{low}$ mice (An et al. 2018). To our knowledge, the eye functioning of CUX1 insufficient mice has not been investigated. Ostensibly, mammalian RBCs appear to be an anomaly among cell types with regards to nuclear condensation and enucleation. Yet, if one considers that RBCs are estimated to comprise 70% of adult human cells (Bianconi et al. 2013), nuclear condensation is disproportionally understudied and understood.

The finding that CUX1 loss drives chromatin condensation through histone deacetylation provides an opportunity for therapeutic intervention. In patients with myeloid neoplasms, drugs such as erythropoietin or lenalidomide show transient positive results for a subset of patients. However, even in responsive patients, therapies typically fail within 2-3 years (Bejar and Steensma 2014) leaving patients dependent on RBC transfusions. Therefore, new cytogenetic specific therapies are urgently needed. Here we identify the molecular mechanism by which CUX1, a common driver of anemia pathogenesis across myeloid malignancies, regulates erythropoiesis. Our finding that CUX1 facilitates erythropoiesis via histone deacetylation may be leveraged for potential therapeutic design through HAT inhibitors. While currently not as specific as their HDAC inhibitor counterparts (Dahlin et al. 2017), both naturally occurring and synthetic HAT inhibitors exist and have shown promise in preclinical studies (Yuan Cheng et al. 2019).

Given the importance of HATs in other cancer types and that efforts to drug the epigenome are expanding (Yuan Cheng et al. 2019), we anticipate that understanding the mechanistic role of CUX1 in erythropoiesis will enable future therapeutic opportunities.

Future directions

The studies described in this thesis open the avenue for many new lines of work. While we are confident CUX1 regulates nuclear condensation through histone deacetylation, the mechanisms surrounding this remain unclear. We hypothesize that CUX1 interacts with its known binding partner, HDAC1. The first evidence showing an interaction between CUX1 and HDAC1 is from before the turn of the millennium (S. De Li et al. 1999). Here, the authors generate a C-terminal CUX1-GST fusion protein and show an interaction between HDAC1 and the fusion protein (S. De Li et al. 1999). Along with deacetylase activity in the fraction precipitated with the CUX1-fusion, which is inhibited by TSA (S. De Li et al. 1999). The interaction between HDAC1 and CUX1 was confirmed in kidney cells ten years later (Sharma et al. 2009) and then again in 2015 in macrophages (Kühnemuth et al. 2015).

However, our attempts to Co-immunoprecipitate (co-IP) HDAC1 and CUX1 in primary mouse erythroblasts and the K562 cell line have thus far been unsuccessful. Interrogating which specific HDAC interacts with CUX1 is of critical clinical relevance, as HDAC restoration may rescue erythropoiesis in CUX1 insufficient cells. To identify CUX1 binding partners in primary erythroid cells, future studies should perform CUX1-co-IP mass spectrometry on sorted RII-erythroblasts. The result of this experiment will

be noteworthy regardless of if CUX1 interacts with HDAC1 as we hypothesize. If CUX1 does not interact with HDAC1 in primary erythroblasts a new line of questioning emerges. Why is CUX1 co-occupying HDAC binding sites? What complexes is CUX1 a part of in erythroblasts? Is CUX1 perhaps part of an epigenetic complex in direct competition with HDACs? And, interestingly, what alternative transcription factor(s) must be guiding HDACs to their targets during erythropoiesis?

Supposing CUX1 is found to interact with HDAC1, as reported. Then to confirm the interaction, ChIP-sequencing should be performed for HDAC1 both with and without CUX1 knockdown. This could demonstrate that loss of CUX1 is directly responsible for changes in genomic occupancy of HDAC1. The sites of HDAC1 occupancy in erythroblasts should be intersected with CUX1 binding sites to identify the genomic targets of the CUX1-HDAC complex. Another interesting experimental avenue is to investigate if knockdown of HDAC1 results in a similar loss of genomic occupancy for CUX1. We already know that HDAC inhibition by TSA treatment with TSA results in a similar expansion of nuclear area (Figure 21A).

Following this detailed mechanistic profiling, experiments attempting to rescue nuclear condensation should be performed. First, it should be addressed if restoration of HDAC1 expression is sufficient for nuclear condensation with CUX1 loss. The result of this experiment would be informative irrespective of the result. If HDAC1 overexpression is insufficient for restoration this indicates the CUX1-HDAC1 interaction is paramount for nuclear condensation. However, if exogenous HDAC1 expression rescues nuclear condensation without CUX1 there is an alternative chaperone guiding HDAC1 to its genomic targets during erythropoiesis, and it should be investigated. All of these studies

could be easily altered to be performed on a different HDAC, as indicated by the CUX1-IP Mass spec. Furthermore, it should be determined if molecular inhibition of HATs are sufficient to normalize acetylation levels and rescue nuclear condensation. This can be done using the *in vitro* CD34 cultures as a preliminary study, and subsequently given as a treatment to $Cux1^{low}$ mice treated with phenylhydrazine in our *in vivo* mouse model. These mechanistic studies would be an excellent follow-up to the work in this thesis and would identify which molecular therapies have the potential to assist patients with CUX1 deficiencies.

Another line of interrogation opened by the work described herein is the relationship between CUX1 and the histone acetyltransferase p300. Previous work described CUX1 often occupies the binding sites of p300 (Arthur et al. 2017). While not detailed in this thesis, we have ChIP-seq evidence to suggest CUX1 occupies p300 binding sites in K562 cells. It would be interesting to investigate if CUX1 directly interacts with p300, and to what end. While it is known that CUX1 interacts with HDAC1, to our knowledge, the interaction of CUX1 and p300 has never been identified. In fact, attempts at a CUX1-p300 Co-IP were attempted in macrophages (Kühnemuth et al. 2015), but did not yield evidence of an interaction. However, this could an interaction specific to hematopoietic cells. If CUX1 does interact with p300, does CUX1 enhance or inhibits the acetylation activity of p300? Is CUX1 ever in complex with both HDAC1 and p300 simultaneously? Alternatively, CUX1 may not interact with p300, and instead actively competes with p300 for genomic binding sites in a histone acetylation tug-of-war.

The relationship between human and mouse erythropoiesis is another curiosity. It would be beneficial to confirm the requirement of CUX1 for nuclear condensation in primary human erythroblasts beyond what is outlined in this thesis. Interrogating the relative size and chromatin accessibility of erythroblasts from anemic human patients with and without CUX1 loss would be of great interest. If the above rescue experiments are successful, restoring erythroid differentiation in erythroblasts from patients with CUX1 loss using a HAT inhibitor would be particularly salient. Taken together, the work in this thesis outlines the mechanistic role of CUX1 in erythropoiesis. Future work should investigate the conservation of this mechanism and leverage its discovery to restore erythropoiesis in settings of CUX1 loss.

Furthermore, it would be interesting to see if the histone deacetylation mediated by CUX1 is critical in other cell types. Of particular interest is the role of CUX1 in megakaryocytes. Originating from the same final progenitor (MEP) as erythrocytes, megakaryocytes have an equally complex process of development. Unlike the enucleation experienced by RBCs, megakaryocytes undergo an opposite cellular maturation: endomitosis. This results in the replication of megakaryocyte nuclear content to x2N without cellular division (up to 64N), and is thought to increase the number of resulting platelets (Mazzi et al. 2018). While incompletely understood, this process relies on HDACs, as evidenced by megakaryocyte ploidy defects in *Hdac1/Hdac2* knockout mice (Wilting et al. 2010) and human CD34+ cells differentiated towards megakaryocytes with HDAC inhibitors (Ali et al. 2013). Additionally, thrombocytopenia is common side effect of clinical treatment with HDAC inhibitors (Cang, Ma, and Liu 2009). In our mouse model, CUX1 knockdown leads to

megakaryocyte dysplasia including micromegakaryocytes, hypolobation (abnormally spaced nuclear lobes), and giant platelets (An et al. 2018). How does CUX1 impact megakaryocyte ploidy and development? Is it through histone deacetylation, perhaps via HDAC1, as in erythrocytes? More broadly, how does an MEP hold the potential to become two of the most divergent and essential cell types? What factors decide the fate of an MEP, and where and how does CUX1 fit into the choice? In all cases, I sincerely look forward to the development of this work- there is so much left to discover.

CHAPTER 6: MAPPING CUX1 DURING HEMATOPOIESIS

Introduction

The advent of single-cell RNA-sequencing technologies has ushered in a new era for hematopoiesis. Historically, the dogma in the field has been that HSCs progress through a series of distinct progenitors, making a bifurcating decision regarding lineage commitment at each interval. However, the recent adoption of single-cell technology into the field of hematopoiesis has suggested this model may be too simplistic and HSC commitment is instead a continuous process (Velten et al. 2017). How HSCs transition from multipotency to lineage commitment is an active and fascinating area of research.

There is much evidence that CUX1 regulates HSC fate. In mice, CUX1 dosage impacts HSPC number and fate (An et al. 2018). The *Drosophila* ortholog *cut* plays a key role in development, both in hemopoietic tissue (Mcnerney et al. 2013) and beyond (Blochlinger, Jan, and Jan 1991). Therefore, to understand the role of CUX1 during hematopoietic development we generated a CUX1-MCherry reporter mouse and conducted single-cell RNA-sequencing on HSPCs following CUX1 knockdown.

Results

Generation of CUX1-MCherry reporter mouse

To understand the role of CUX1 in hematopoiesis we generated a CUX1-MCherry reporter mouse. We chose to introduce a C-terminal tag on the final coding exon of CUX1, as previous work suggested tagging CUX1 in this fashion does not disrupt DNA

binding. As the transcriptional regulation of CUX1 is not well understood, tagging the protein will enable us to study protein level across cell types and throughout development. MCherry was selected as the reporter color because it can be crossed with our GFP expressing knockdown mouse model (Figure 7). Successful integration of the MCherry tag was validated by western blot and sanger-sequencing, and MCherry expression was validated by flow (Figure 25A, B).

In a preliminary study to understand how CUX1 protein level correlates with stem cell function we sorted cKit+ cells based on CUX1-MCherry expression as MCherry^{high} or MCherry^{neg} and assayed the cells for colony forming potential by CFU. Strikingly, all of the colonies formed were exclusively generated from MCherry^{high} seeding cells (Figure 25C). Thus, CUX1 is correlated with stem cell potential, though further validation and interrogation of the mechanism is required.

Single-cell RNA-sequencing of CUX1 knockdown mice

To investigate how loss of CUX1 impacts hemopoietic progenitors we performed single cell RNA-sequencing on lineage negative cKit+ Ren, Cux1^{mid}, and Cux1^{low} cells. This will enable us to identify changes across all hematopoietic progenitor cells simultaneously, and by using both the Cux1^{low} and Cux1^{mid} shRNA mouse models we will be able to assess how CUX1 dosage impacts hemopoietic development. The single-cell RNA-seq sequencing experiment was successful, generating unique clusters for all genotypes (Figure 26). These preliminary results are promising and require further data analysis and interpretation.

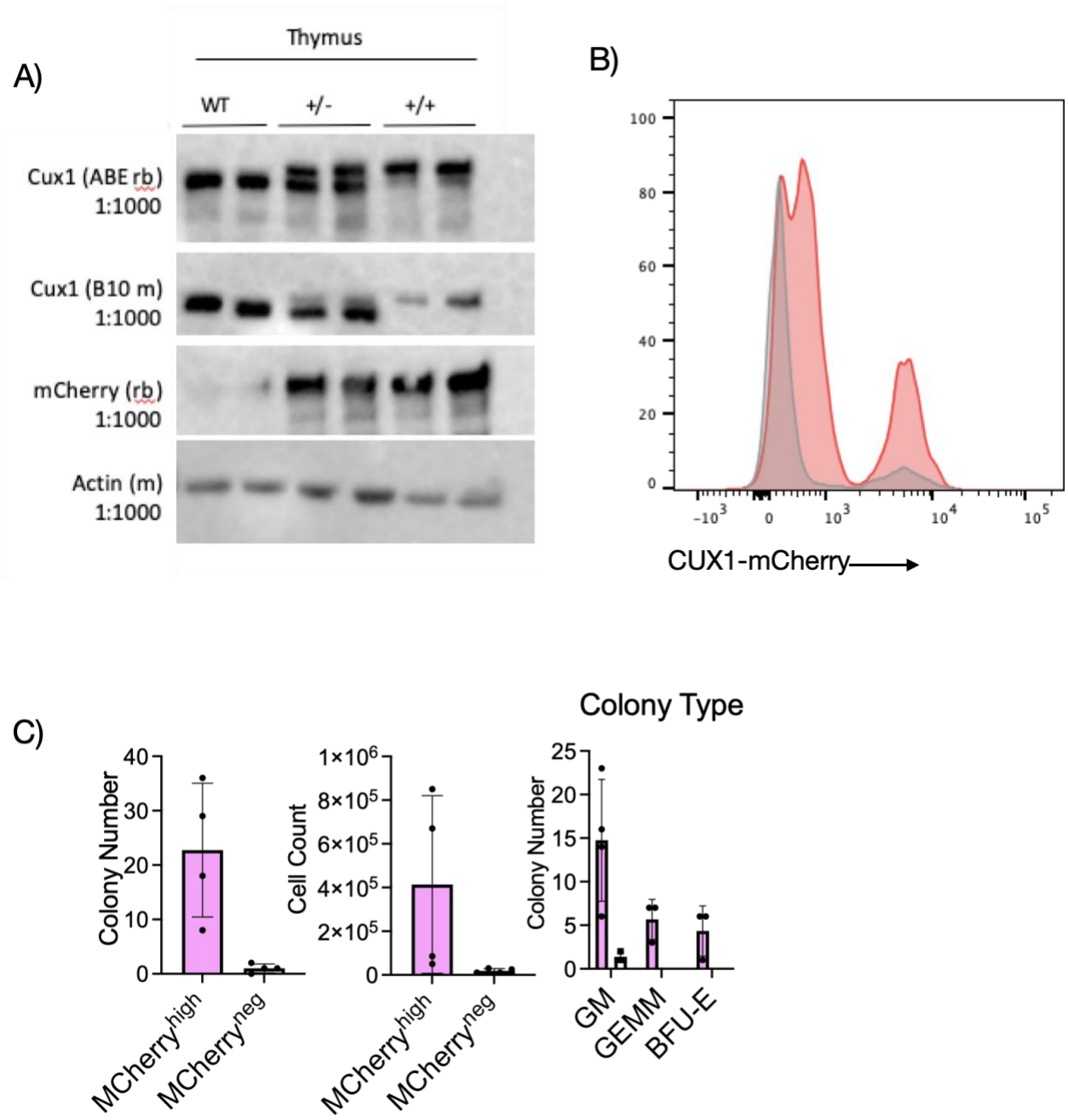

Figure 25. Successful generation of CUX1-MCherry reporter mouse. (A) Western blot on adult CUX1-MCherry thymus tissue **(B)** Flow cytometry showing MCherry protein functionality by detection of PE-Dazzle (mCherry) in bone marrow Lineage(-) Sca-1+ cKit+ cells. **(C)** CFU assays of cKit+ bone marrow progenitors sorted based on MCherry fluorescence.

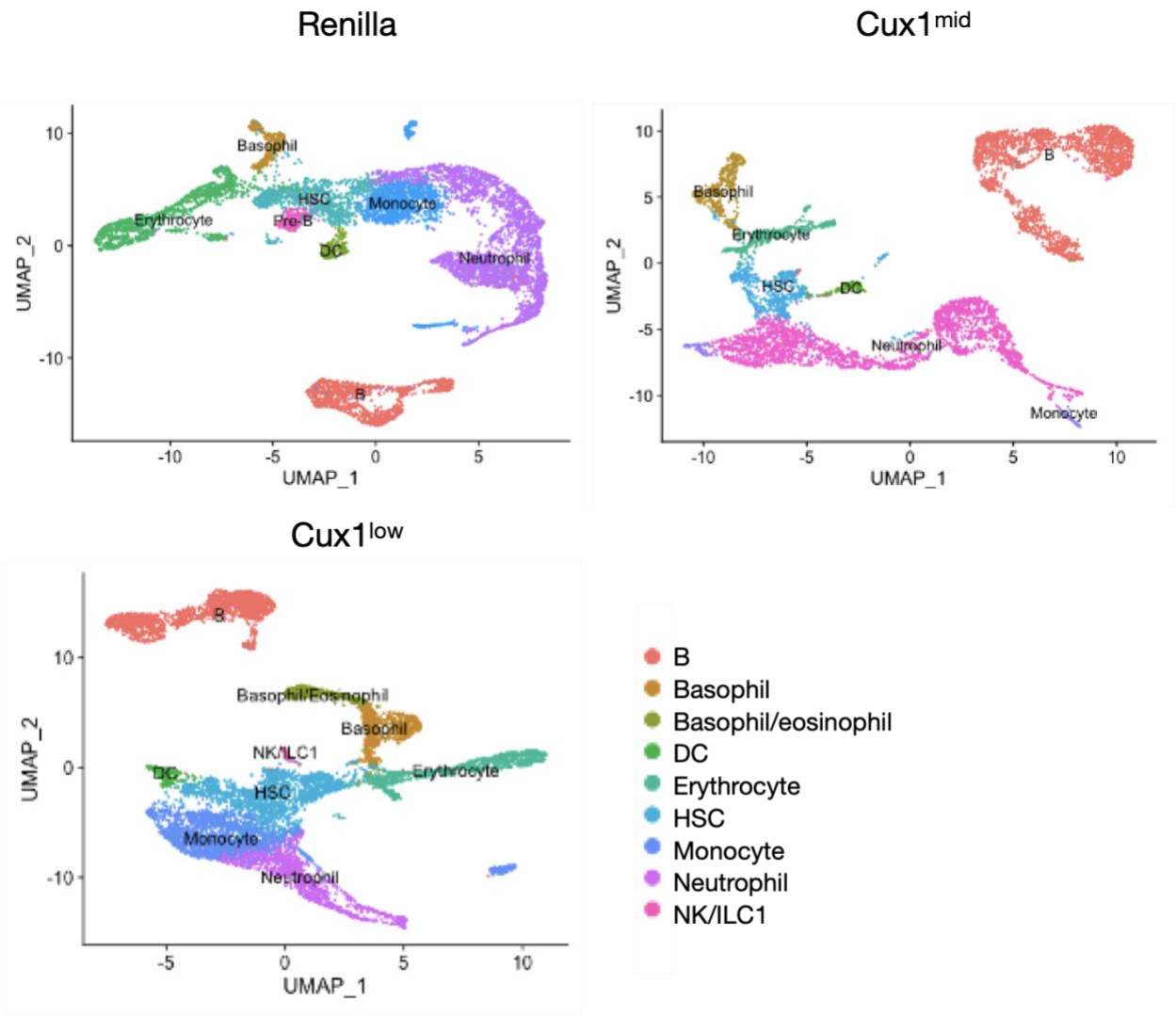

Figure 26. Successful single-cell RNA-sequencing of hemopoietic stem and progenitors. cKit(+) Lineage(-) bone marrow cells were sorted from Ren, Cux1^{mid}, and Cux1^{low} mice following knockdown. Clustering analysis reveals the expected distinct transcriptional profiles of hemopoietic stem and progenitor cells, along with unique cluster composition following CUX1 knockdown.

Conclusions

We successfully generated a CUX1-MCherry reporter mouse and conducted single-cell RNA-sequencing of hemopoietic progenitors in our shRNA CUX1 knockdown mouse model. The data resulting from the reporter mouse and single-cell sequencing will no doubt be utilized in future work interrogating the role of CUX1 in hematopoiesis and beyond.

Future Directions

Much work remains to be done to understand the function of CUX1 during hematopoiesis. The results from the CUX1-MCherry mice suggest CUX1 may be required for HSC function. However, future results confirming and extending this hypothesis is needed. To begin this process we have crossed the CUX1-MCherry reporter to a full body GFP reporter mouse (Schaefer et al. 2001). This will enable us to delineate the origin of transplanted progenitors regardless of CUX1 status. It will be noteworthy to see if the lineage potential of CUX1-MCherry^{high} hematopoietic stem cells differs from their CUX1-MCherry^{neg} counterparts *in vivo*. It will also be of interest to determine if CUX1 expression is a fixed characteristic. This will be accomplished by transplanting CUX1-MCherry^{neg} HSCs into wild-type recipients and assaying the bone more marrow following recovery for CUX1-MCherry^{high} HSCs. This can be done in a series of permutations with a variety of different progenitor cells to establish the lineage potential and CUX1 expression of HSPCs. There are many interesting possibilities of how CUX1 protein levels may correlate with different progenitor populations and change throughout development.

Furthermore, the single-cell RNA-seq results will have interesting data regarding dynamics of CUX1 RNA expression in hemopoietic development. The single-cell RNA-seq data may also reveal how different dosages of CUX1 alter the fate of HSPCs directly, and how CUX1 RNA-level is correlated with different lineage outcomes. Between the CUX1-MCherry reporter and the single-cell RNA-sequencing it is an exciting time to study CUX1 in hematopoiesis!

The CUX1-MCherry mouse will be useful for a variety of other studies. For example, crossing the CUX1-MCherry mouse to our shRNA knockdown mouse lines will give us granular information on our shRNA reporter mouse lines. By crossing these two strains we can determine which cell types and tissues have the most robust knockdown, measure the length of time required for maximum knockdown, and understand how CUX1 protein levels are restored after removing doxycycline. The CUX1-MCherry reporter mouse can be used to measure CUX1 protein stability, regulation, and turnover. Additionally, the reporter could be used to determine what factors influence CUX1 protein levels. More broadly, CUX1 is known to be essential for development. Employing the CUX1-MCherry reporter mouse, we can map CUX1 levels throughout embryogenesis to gain insight into where and when CUX1 is present during development. These discoveries could reveal how CUX1 is endogenously regulated, what therapeutics may be employed to alter its expression, and uncover novel roles for CUX1 in organogenesis.

REFERENCES

Abraham, Allistair A, and John Tisdale. 2021. “Gene Therapy for Sickle Cell Disease - Moving from the Bench to the Bedside.” *BLOOD*. http://dx.doi.org/10.1182/blood.2019003776.

Ali, A. et al. 2013. “Thrombocytopenia Induced by the Histone Deacetylase Inhibitor Abexinostat Involves P53-Dependent and-Independent Mechanisms.” *Cell Death and Disease* 4(7): 1–11.

An, Ningfei et al. 2018a. “Gene Dosage Effect of CUX1 in a Murine Model Disrupts HSC Homeostasis and Controls the Severity and Mortality of MDS.” *Blood* 131(24): 2682–97. http://www.bloodjournal.org/content/131/24/2682.abstract.

Armitage, James O. et al. 2003. “Treatment-Related Myelodysplasia and Acute Leukemia in Non-Hodgkin’s Lymphoma Patients.” *Journal of Clinical Oncology* 21(5): 897–906.

Arnaud, Lionel et al. 2010. “A Dominant Mutation in the Gene Encoding the Erythroid Transcription Factor KLF1 Causes a Congenital Dyserythropoietic Anemia.” *American Journal of Human Genetics* 87(5): 721–27. http://dx.doi.org/10.1016/j.ajhg.2010.10.010.

Arthur, Robert K., Ningfei An, Saira Khan, and Megan E. McNerney. 2017. “The Haploinsufficient Tumor Suppressor, CUX1, Acts as an Analog Transcriptional Regulator That Controls Target Genes through Distal Enhancers That Loop to Target Promoters.” *Nucleic Acids Research* 45(11): 6350–61.

Babbs, Christian et al. 2013. “Homozygous Mutations in a Predicted Endonuclease Are a Novel Cause of Congenital Dyserythropoietic Anemia Type I.” *Haematologica* 98(9): 1383–87.

Bailey, Timothy and, and Charles Elkan. 1994. “Fitting a Mixture Model by Expectation Maximization.” *AAAI Press*: 3–9.

Baudard, M. et al. 1994. “Acute Myelogenous Leukaemia in the Elderly: Retrospective Study of 235 Consecutive Patients.” *British Journal of Haematology* 86(1): 82–91.

Le Beau, Michelle M. et al. 1996. “Cytogenetic and Molecular Delineation of a Region of Chromosome 7 Commonly Deleted in Malignant Myeloid Diseases.” *Blood* 88(6): 1930–35.

Bejar, Rafael, and David P Steensma. 2014. “Recent Developments in Myelodysplastic Syndromes.” *Blood* 124(18): 2793–2804.

Bianconi, Eva et al. 2013. “An Estimation of the Number of Cells in the Human Body.” *Annals of Human Biology* 40(6): 463–71.

Blochlinger, Karen, Lily Yeh Jan, and Yuh Nung Jan. 1991. “Transformation of Sensory Organ Identity by Ectopic Expression of Cut in Drosophila.” *Genes and Development* 5(7): 1124–35.

Bolton, Kelly L. et al. 2020. “The Clinical Management of Clonal Hematopoiesis: Creation of a Clonal Hematopoiesis Clinic.” *Hematology/Oncology Clinics of North America* 34(2): 357–67.

Booth, Catherine, Baba Inusa, and Stephen K. Obaro. 2010. “Infection in Sickle Cell Disease: A Review.” *International Journal of Infectious Diseases* 14(1): 2–12.

Bouscary, Didier et al. 2003. “Critical Role for PI 3-Kinase in the Control of Erythropoietin-Induced Erythroid Progenitor Proliferation Critical Role for PI 3-Kinase in the Control of Erythropoietin-Induced Erythroid Progenitor Proliferation.” *Blood* 101(9): 3436–43.

Buenrostro, Jason D, Beijing Wu, Howard Y Chang, and William J Greenleaf. 2015. “ATAC-Seq : A Method for Assaying Chromatin Accessibility Genome-Wide.” *Current Protocols in Molecular Biology* 29(January): 1–9.

Cang, Shundong, Yuehua Ma, and Delong Liu. 2009. “New Clinical Developments in Histone Deacetylase Inhibitors for Epigenetic Therapy of Cancer.” *Journal of Hematology and Oncology* 2: 1–11.

Cantor, Alan B., and Stuart H. Orkin. 2002. “Transcriptional Regulation of Erythropoiesis: An Affair Involving Multiple Partners.” *Oncogene* 21: 3368–76.

Castella, Maria et al. 2011. “Origin, Functional Role, and Clinical Impact of Fanconi Anemia Fanca Mutations.” *Blood* 117(14): 3759–69.

Chaparro, Camila M., and S. Suchdev Parminder. 2019. “Anemia Epidemiology, Pathophysiology, and Etiology in Low- and Middle-Income Countires.” *Ann N Y Acad Sci* 1450(1): 15–31.

Chen, Chong et al. 2014. “MLL3 Is a Haploinsufficient 7q Tumor Suppressor in Acute Myeloid Leukemia.” *Cancer Cell* 25(5): 652–65. http://dx.doi.org/10.1016/j.ccr.2014.03.016.

Cheng, Yong et al. 2009. “Erythroid GATA1 Function Revealed by Genome-Wide Analysis of Transcription Factor Occupancy, Histone Modifications, and MRNA Expression.” *Genome Research* 19(12): 2172–84.

Cheng, Yuan et al. 2019. “Targeting Epigenetic Regulators for Cancer Therapy: Mechanisms and Advances in Clinical Trials.” *Signal Transduction and Targeted Therapy* 4(1). http://dx.doi.org/10.1038/s41392-019-0095-0.

Chin, Hiroshi et al. 1996. “Physical and Functional Interactions between Stat5 and the Tyrosine- Phosphorylated Receptors for Erythropoietin and Interleukin-3.” *Blood*

88(12): 4415–25. http://dx.doi.org/10.1182/blood.V88.12.4415.bloodjournal88124415.

Cohen-Kaminsky, Sylvia et al. 1998. “Chromatin Immunoselection Defines a TAL-1 Target Gene.” *EMBO Journal* 17(17): 5151–60.

Crispino, John D, and Mitchell J Weiss. 2017. “Erythro-Megakaryocytic Transcription Factors Associated with Hereditary Anemia.” *Blood* 123(20): 3080–89.

Dahlin, Jayme L. et al. 2017. “Assay Interference and Off-Target Liabilities of Reported Histone Acetyltransferase Inhibitors.” *Nature Communications* 8(1). http://dx.doi.org/10.1038/s41467-017-01657-3.

Damen, J. E. et al. 1993. “Phosphatidylinositol 3-Kinase Associates, via Its Src Homology 2 Domains, with the Activated Erythropoietin Receptor.” *Blood* 81(12): 3204–10. http://dx.doi.org/10.1182/blood.V81.12.3204.3204.

———. 1995. “Phosphorylation of Tyrosine 503 in the Erythropoietin Receptor (EpR) Is Essential for Binding the P85 Subunit of Phosphatidylinositol (PI) 3-Kinase and for EpR-Associated PI 3-Kinase Activity.” *Journal of Biological Chemistry* 270(40): 23402–8. http://dx.doi.org/10.1074/jbc.270.40.23402.

Davoli, Teresa et al. 2013. “Cumulative Haploinsufficiency and Triplosensitivity Drive Aneuploidy Patterns and Shape the Cancer Genome.” *Cell* 155(4): 948. http://dx.doi.org/10.1016/j.cell.2013.10.011.

Denny, Susan D., Maragatha N. Kuchibhatla, and Harvey Jay Cohen. 2006. “Impact of Anemia on Mortality, Cognition, and Function in Community-Dwelling Elderly.” *American Journal of Medicine* 119(4): 327–34.

Dimitriou, Marios et al. 2016. “Perturbed Hematopoietic Stem and Progenitor Cell Hierarchy in Myelodysplastic Syndromes Patients with Monosomy 7 as the Sole Cytogenetic Abnormality.” *Oncotarget* 7(45): 72685–98.

Dobin, Alexander et al. 2013. “STAR: Ultrafast Universal RNA-Seq Aligner.” *Bioinformatics* 29(1): 15–21.

Doench, John G et al. 2016. “Optimized SgRNA Design to Maximize Activity and Minimize Off-Target Effects of CRISPR-Cas9.” *Nature Biotechnology* 34(2): 184–91. http://dx.doi.org/10.1038/nbt.3437.

Döhner, Konstanze et al. 1998. “Molecular Cytogenetic Characterization of a Critical Region in Bands 7q35-Q36 Commonly Deleted in Malignant Myeloid Disorders.” *Blood* 92(11): 4031–35.

Edgar, Ron, Michael Domrachev, and Alex E. Lash. 2002. “Gene Expression Omnibus: NCBI Gene Expression and Hybridization Array Data Repository.” *Nucleic Acids Research* 30(1): 207–10.

Ellis, Tammy et al. 2001. “The Transcriptional Repressor CDP (Cutl1) Is Essential for Epithelial Cell Differentiation of the Lung and the Hair Follicle.” *Genes and Development* 15(17): 2307–19.

Ernst, Thomas et al. 2010. “Inactivating Mutations of the Histone Methyltransferase Gene EZH2 in Myeloid Disorders.” *Nature Genetics* 42(8): 722–26.

Eshghi, Shawdee et al. 2007. “A4β1 Integrin and Erythropoietin Mediate Temporally Distinct Steps in Erythropoiesis: Integrins in Red Cell Development.” *Journal of Cell Biology* 177(5): 871–80.

Estandarte, Ana Katrina et al. 2016. “The Use of DAPI Fluorescence Lifetime Imaging for Investigating Chromatin Condensation in Human Chromosomes.” *Scientific Reports* 6(July): 1–12.

Evans, T., M. Reitman, and G. Felsenfeld. 1988. “An Erythrocyte-Specific DNA-Binding Factor Recognizes a Regulatory Sequence Common to All Chicken Globin Genes.” *Proceedings of the National Academy of Sciences of the United States of America* 85(16): 5976–80.

Fajtova, Michaela et al. 2013. “Immunophenotypic Profile of Nucleated Erythroid Progenitors during Maturation in Regenerating Bone Marrow.” *Leukemia & Lymphoma* 54(11): 2523–30. http://www.tandfonline.com/doi/full/10.3109/10428194.2013.781167.

Feng, Yi et al. 2010. “Early Mammalian Erythropoiesis Requires the Dot1L Methyltransferase.” *Blood* 116(22): 4483–91.

Ferreira, Rita, Kinuko Ohneda, Masayuki Yamamoto, and Sjaak Philipsen. 2005. “GATA1 Function , a Paradigm for Transcription Factors in Hematopoiesis.” *Molecular and Cellular Biology* 25(4): file:///C:/Users/Admin/Desktop/GMFG/1064.pdf.

Finberg, Karin E. et al. 2008. “Mutations in TMPRSS6 Cause Iron-Refractory Iron Deficiency Anemia (IRIDA).” *Nature Genetics* 40(5): 569–71.

Fujiwara, Tohru et al. 2009. “Discovering Hematopoietic Mechanisms through Genome-Wide Analysis of GATA Factor Chromatin Occupancy.” *Molecular Cell* 36(4): 667–81. http://dx.doi.org/10.1016/j.molcel.2009.11.001.

Fujiwara, Y. et al. 1996. “Arrested Development of Embryonic Red Cell Precursors in Mouse Embryos Lacking Transcription Factor GATA-1.” *Proceedings of the National Academy of Sciences of the United States of America* 93(22): 12355–58.

Gauwerky, CE, AJ Lusis, and DW Golde. 1982. “Human Leukemia Cell Line K562 Responds to Erythroid-Potentiating Activity.” *Blood* 59(2): 300–305. http://dx.doi.org/10.1182/blood.V59.2.300.300.

Ghaffari, Saghi et al. 2006. “AKT Induces Erythroid-Cell Maturation of JAK2-Deficient Fetal Liver Progenitor Cells and Is Required for Epo Regulation of Erythroid-Cell Differentiation.” *Blood* 107(5): 1888–92.

Gillinder, Kevin R. et al. 2017. “Direct Targets of PStat5 Signalling in Erythropoiesis.” *PLoS ONE* 12(7): 1–20.

Gillingham, Alison, Andrea Pfeifer, and Sean Munro. 2002. “CASP, the Alternatively Spliced Product of the Gene Encoding the CCAAT-Displacement Protein Transcription Factor, Is a Golgi Membrane Protein Rellated to Giantin.” *Molecular Biology of the Cell* 13(November): 3761–2002.

Gnanapragasam, Merlin Nithya et al. 2016. “EKLF / KLF1-Regulated Cell Cycle Exit Is Essential for Erythroblast Enucleation.” *Blood* 128(12): 1631–42. www.bloodjournal.org.

Goasguen, Jean E. et al. 2018. “Dyserythropoiesis in the Diagnosis of the Myelodysplastic Syndromes and Other Myeloid Neoplasms: Problem Areas.” *British Journal of Haematology* 182(4): 526–33.

Goldman, Daniel. 2008. “Theoretical Models of Microvascular Oxygen Transport to Tissue.” *Microcirculation* 15(8): 795–811.

Greenberg, Peter et al. 1997. “International Scoring System for Evaluating Prognosis in Myelodysplastic Syndromes.” *Blood* 89(6): 2079–88. http://dx.doi.org/10.1182/blood.V89.6.2079.

Gundry, Michael C. et al. 2016. “Highly Efficient Genome Editing of Murine and Human Hematopoietic Progenitor Cells by CRISPR/Cas9.” *Cell Reports* 17(5): 1453–61.

Hajdu, Steven I. 2003. “A Note from History: The Discovery of Blood Cells.” *Annals of clinical and laboratory science* 33(2): 237–38.

Harandi, Omid F. et al. 2010. “Murine Erythroid Short-Term Radioprotection Requires a BMP4-Dependent, Self-Renewing Population of Stress Erythroid Progenitors.” *Journal of Clinical Investigation* 120(12): 4507–19.

Haseyama, Y et al. 1999. “Phosphatidylinositol 3-Kinase Is Involved in the Protection of Primary Cultured Human Erythroid Precursor Cells from Apoptosis.” *Blood* 94(5): 1568–77. http://www.ncbi.nlm.nih.gov/pubmed/10477682.

Hattangadi, Shilpa M et al. 2015. “From Stem Cell to Red Cell: Regulation of Erythropoiesis at Multiple Levels by Multiple Proteins , RNAs , and Chromatin Modifications.” *Blood* 118(24): 6258–69.

Heuser, Michael et al. 2009. “Loss of MII5 Results in Pleiotropic Hematopoietic Defects, Reduced Neutrophil Immune Function, and Extreme Sensitivity to DNA Demethylation.” *Blood* 113(7): 1432–43.

Hong, Wei et al. 2005. “FOG-1 Recruits the NuRD Repressor Complex to Mediate Transcriptional Repression by GATA-1.” *EMBO Journal* 24(13): 2367–78.

Hosono, N. et al. 2014. “Recurrent Genetic Defects on Chromosome 7q in Myeloid Neoplasms.” *Leukemia* 28(6): 1348–51.

Ikeda, Tetsurou et al. 2016. “Transforming Growth Factor-β-Induced CUX1 Isoforms Are Associated with Fibrosis in Systemic Sclerosis Lung Fibroblasts.” *Biochemistry and Biophysics Reports* 7: 246–52. http://dx.doi.org/10.1016/j.bbrep.2016.06.022.

Imgruet, Molly et al. 2021. “Loss of a 7q Gene, CUX1, Disrupts Epigenetic-Driven DNA Repair and Drives Therapy-Related Myeloid Neoplasms.” *Blood*.

Iolascon, Achille, Hermann Heimpel, Anders Wahlin, and Hannah Tamary. 2013. “Congenital Dyserythropoietic Anemias: Molecular Insights and Diagnostic Approach.” *Blood* 122(13): 2162–66.

Ishikawa, Fumihiko et al. 2005. “Development of Functional Human Blood and Immune Systems in NOD/SCID/IL2 Receptor γ Chainnull Mice.” *Blood* 106(5): 1565–73.

Jacobs-Helber, Sarah M., and Stephen T. Sawyer. 2004. “Jun N-Terminal Kinase Promotes Proliferation of Immature Erythroid Cells and Erythropoietin-Dependent Cell Lines.” *Blood* 104(3): 696–703.

Jacobs, Kevin B. et al. 2012. “Detectable Clonal Mosaicism and Its Relationship to Aging and Cancer.” *Nature Genetics* 44(6): 651–58.

Jayapal, Senthil Raja et al. 2010a. “Down-Regulation of Myc Is Essential for Terminal Erythroid Maturation.” *Journal of Biological Chemistry* 285(51): 40252–65.

———. 2010b. “Down-Regulation of Myc Is Essential for Terminal Erythroid Maturation.” *Journal of Biological Chemistry* 285(51): 40252–65.

Jerez, Andres et al. 2012. “Loss of Heterozygosity in 7q Myeloid Disorders: Clinical Associations and Genomic Pathogenesis.” *Blood* 119(25): 6109–17.

Ji, Peng et al. 2010. “Histone Deacetylase 2 Is Required for Chromatin Condensation and Subsequent Enucleation of Cultured Mouse Fetal Erythroblasts.” *Haematologica* 95(12): 2013–21.

Ji, Peng, Senthil Raja Jayapal, and Harvey F. Lodish. 2008. “Enucleation of Cultured Mouse Fetal Erythroblasts Requires Rac GTPases and MDia2.” *Nature Cell Biology* 10(3): 314–21.

Ji, Peng, Maki Murata-Hori, and Harvey F. Lodish. 2011. “Formation of Mammalian Erythrocytes: Chromatin Condensation and Enucleation.” *Trends in Cell Biology* 21(7): 409–15. http://dx.doi.org/10.1016/j.tcb.2011.04.003.

K.E., Nichols et al. 2000. “Familial Dyserythropoietic Anaemia and Thrombocytopenia Due to an Inherited Mutation in GATA1.” *Nature Genetics* 24(march): 266–70.

Kerenyi, Marc A., and Stuart H. Orkin. 2010. “Networking Erythropoiesis.” *Journal of Experimental Medicine* 207(12): 2537–41.

Kharas, Michael G et al. 2010. “Constitutively Active AKT Depletes Hematopoietic Stem Cells and Induces Leukemia in Mice Constitutively Active AKT Depletes Hematopoietic Stem Cells and Induces Leukemia in Mice.” *Blood* 115(7): 1406–15.

Kinross, Kathryn M., Allison J. Clark, Rosa M. Iazzolino, and Patrick Orson Humbert. 2006. “E2f4 Regulates Fetal Erythropoiesis through the Promotion of Cellular Proliferation.” *Blood* 108(3): 886–95.

Kjeldsen, Eigil, and Christopher Veigaard. 2013. “DOCK4 Deletion at 7q31.1 in a de Novo Acutemyeloid Leukemia with a Normal Karyotype.” *Cellular Oncology* 36(5): 395–403.

Klingmüller, Ursula, Svetlana Bergelson, Jonathan G. Hsiao, and Harvey F. Lodish. 1996. “Multiple Tyrosine Residues in the Cytosolic Domain of the Erythropoietin Receptor Promote Activation of STAT5.” *Proceedings of the National Academy of Sciences of the United States of America* 93(16): 8324–28.

Knudson, A. 1971. “Mutation and Cancer: Statistical Study of Retinoblastoma.” *Proceedings of the National Academy of Sciences* 68(4): 820–23.

Konstantinidis, Diamantis G. et al. 2012. “Signaling and Cytoskeletal Requirements in Erythroblast Enucleation.” *Blood* 119(25): 6118–27.

Koury, S. T., M. J. Koury, and M. C. Bondurant. 1989. “Cytoskeletal Distribution and Function during the Maturation and Enucleation of Mammalian Erythroblasts.” *Journal of Cell Biology* 109(6 I): 3005–13.

Kozar, Katarzyna et al. 2004. “Mouse Development and Cell Proliferation in the Absence of D-Cyclins.” *Cell* 118(4): 477–91.

Kuhn, Robert M., David Haussler, and W. James Kent. 2013. “The UCSC Genome Browser and Associated Tools.” *Briefings in Bioinformatics* 14(2): 144–61.

Kühnemuth, B. et al. 2015a. “CUX1 Modulates Polarization of Tumor-Associated Macrophages by Antagonizing NF-KB Signaling.” *Oncogene* 34(2): 177–87.

Kühnemuth, B et al. 2015b. “CUX1 Modulates Polarization of Tumor-Associated Macrophages by Antagonizing NF-KB Signaling.” *Oncogene* 34(2): 177–87. http://www.nature.com/doifinder/10.1038/onc.2013.530.

Lennox, W. G., F. A. Gibbs, and E.L. Gibbs. 1935. “Relationship of Unconsciousness to Cerebral Blood Flow and to Anoxemia.” *Archives of Neurology* 34(5): 1001–13.

Li, Heng et al. 2009. “The Sequence Alignment/Map Format and SAMtools.” *Bioinformatics* 25(16): 2078–79.

Li, Heng, and Richard Durbin. 2009. “Fast and Accurate Short Read Alignment with Burrows-Wheeler Transform.” *Bioinformatics* 25(14): 1754–60.

Li, Qunhua, James B. Brown, Haiyan Huang, and Peter J. Bickel. 2011. “Measuring Reproducibility of High-Throughput Experiments.” *Annals of Applied Statistics* 5(3): 1752–79.

Li, Si De et al. 1999. “Transcriptional Repression of the Cystic Fibrosis Transmembrane Conductance Regulator Gene, Mediated by CCAAT Displacement Protein/Cut Homolog, Is Associated with Histone Deacetylation.” *Journal of Biological Chemistry* 274(12): 7803–15. http://dx.doi.org/10.1074/jbc.274.12.7803.

Lin, Chyuan Sheng, Sai Kiang Lim, Vivette D’Agati, and Frank Costantini. 1996. “Differential Effects of an Erythropoietin Receptor Gene Disruption on Primitive and Definitive Erytnropoiesis.” *Genes and Development* 10(2): 154–64.

Von Lindern, Marieke et al. 2001. “Leukemic Transformation of Normal Murine Erythroid Progenitors: V- and c-ErbB Act through Signaling Pathways Activated by the EpoR and c-Kit in Stress Erythropoiesis.” *Oncogene* 20(28): 3651–64.

Lindsley, RC et al. 2017. “Prognostic Mutations in Myelodysplastic Syndrome after Stem- Cell Transplantation.” *New England Journal of Medicine* 376(6): 536–47.

Linehan, Jonathan L. et al. 2018. “Non-Classical Immunity Controls Microbiota Impact on Skin Immunity and Tissue Repair.” *Cell* 172(4): 784-796.e18. http://linkinghub.elsevier.com/retrieve/pii/S0092867417315131.

Liu, Ning et al. 2020. “CUX1, A Controversial Player in Tumor Development.” *Frontiers in Oncology* 10(May): 11–13.

Lou, Shaoke et al. 2020. “TopicNet: A Framework for Measuring Transcriptional Regulatory Network Change.” *Bioinformatics* 36: I474–81.

Love, Michael I., Wolfgang Huber, and Simon Anders. 2014. “Moderated Estimation of Fold Change and Dispersion for RNA-Seq Data with DESeq2.” *Genome Biology* 15(12): 1–21.

Luna-Fineman, S et al. 1999. “Myelodysplastic and Myeloproliferative Disorders of Childhood: A Study of 167 Patients.” *Blood* 93(2): 459–66. http://www.ncbi.nlm.nih.gov/pubmed/9885207.

Luong, M. X. et al. 2002. “Genetic Ablation of the CDP/Cux Protein C Terminus Results in Hair Cycle Defects and Reduced Male Fertility.” *Molecular and Cellular Biology* 22(5): 1424–37. http://mcb.asm.org/cgi/doi/10.1128/MCB.22.5.1424-1437.2002.

Mailly, F et al. 1996. “The Human Cut Homeodomain Protein Can Repress Gene Expression by Two Distinct Mechanisms: Active Repression and Competition for Binding Site Occupancy.” *Molecular and cellular biology* 16(10): 5346–57.

Malik, Jeffrey et al. 2017. “The Methyltransferase Setd8 Is Essential for Erythroblast Survival and Maturation.” *Cell Reports* 21(9): 2376–83. https://doi.org/10.1016/j.celrep.2017.11.011.

Martelli, Alberto M. et al. 2010. “The Emerging Role of the Phosphatidylinositol 3-Kinase/Akt/Mammalian Target of Rapamycin Signaling Network in Normal Myelopoiesis and Leukemogenesis.” *Biochimica et Biophysica Acta - Molecular Cell Research* 1803(9): 991–1002. http://dx.doi.org/10.1016/j.bbamcr.2010.04.005.

Mazzi, Stefania et al. 2018. “Megakaryocyte and Polyploidization.” *Experimental Hematology* 57: 1–13. https://doi.org/10.1016/j.exphem.2017.10.001.

McLean, Cory Y. et al. 2010. “GREAT Improves Functional Interpretation of Cis-Regulatory Regions.” *Nature Biotechnology* 28(5): 495–501.

McNerney, Megan E., Lucy A. Godley, and Michelle M. Le Beau. 2017. “Therapy-Related Myeloid Neoplasms: When Genetics and Environment Collide.” *Nature Reviews Cancer* 17(9): 513–27. http://www.nature.com/doifinder/10.1038/nrc.2017.60.

Mcnerney, Megan E et al. 2013. “CUX1 Is a Haploinsufficient Tumor Suppressor Gene on Chromosome 7 Frequently Inactivated in Acute Myeloid Leukemia.” *Blood* 444(3): 975–83.

Meers, Michael P., Terri D. Bryson, Jorja G. Henikoff, and Steven Henikoff. 2019. “Improved CUT&RUN Chromatin Profiling Tools.” *eLife* 8: 1–16.

Mei, Yang, Yijie Liu, and Peng Ji. 2021. “Understanding Terminal Erythropoiesis: An Update on Chromatin Condensation, Enucleation, and Reticulocyte Maturation.” *Blood Reviews* 46(August 2020): 100740. https://doi.org/10.1016/j.blre.2020.100740.

Monteferrario, Davide et al. 2014. “ A Dominant-Negative GFI1B Mutation in the Gray Platelet Syndrome .” *New England Journal of Medicine* 370(3): 245–53.

Nagamachi, Akiko et al. 2013. “Haploinsufficiency of SAMD9L, an Endosome Fusion Facilitator, Causes Myeloid Malignancies in Mice Mimicking Human Diseases with Monosomy 7.” *Cancer Cell* 24(3): 305–17. http://dx.doi.org/10.1016/j.ccr.2013.08.011.

Neildez-Nguyen, Thi My Anh et al. 2002. “Human Erythroid Cells Produced Ex Vivo at Large Scale Differentiate into Red Blood Cells in Vivo.” *Nature Biotechnology* 20(5): 467–72.

Nepveu, Alain. 2001. “Role of the Multifunctional CDP/Cut/Cux Homeodomain Transcription Factor in Regulating Differentiation, Cell Growth and Development.” *Gene* 270(1–2): 1–15.

Ney, Paul A. 2011. “Normal and Disordered Reticulocyte Maturation.” *Current Opinion in Hematology* 18(3): 152–57.

Novershtern, Noa et al. 2011. “Densely Interconnected Transcriptional Circuits Control Cell States in Human Hematopoiesis.” *Cell* 144(2): 296–309. http://dx.doi.org/10.1016/j.cell.2011.01.004.

Nuez, Beatriz et al. 1995. “Defective Haematopoiesis in Fetal Liver Resulting from Inactivation of the ELKF Gene.” *Nature* 375: 316–18.

Perkins, Andrew C, Arlene H Sharpet, and Stuart H Orkin. 1995. “Lethal B-Thalassaemia in Mice Lacking the Erythroid CACCC-Transcription Factor KLF.” *Nature* 375(May): 318–22.

Popova, Evgenya Y et al. 2009. “Chromatin Condensation in Terminally Differentiating Mouse Erythroblasts Does Not.” *Biochemistry* 17(1): 47–64.

Ramdzan, Zubaidah M., and Alain Nepveu. 2014. “CUX1, a Haploinsufficient Tumour Suppressor Gene Overexpressed in Advanced Cancers.” *Nature Reviews Cancer* 14(10): 673–82. http://www.nature.com/doifinder/10.1038/nrc3805.

Richmond, Terri D., Manprit Chohan, and Dwayne L. Barber. 2005. “Turning Cells Red: Signal Transduction Mediated by Erythropoietin.” *Trends in Cell Biology* 15(3): 146–55.

Ripka, S et al. 2010. “CUX1: Target of Akt Signalling and Mediator of Resistance to Apoptosis in Pancreatic Cancer.” *Gut* 59(8): 1101–10. http://gut.bmj.com/cgi/doi/10.1136/gut.2009.189720.

Rodriguez, Patrick et al. 2005. “GATA-1 Forms Distinct Activating and Repressive Complexes in Erythroid Cells.” *EMBO Journal* 24(13): 2354–66.

Rogerson, Clare, Daniele Bergamaschi, and Ryan F.L. O’shaughnessy. 2018. “Uncovering Mechanisms of Nuclear Degradation in Keratinocytes: A Paradigm for Nuclear Degradation in Other Tissues.” *Nucleus* 9(1): 56–64. https://doi.org/10.1080/19491034.2017.1412027.

Romano, Oriana et al. 2020. “GATA Factor-Mediated Gene Regulation in Human Erythropoiesis.” *iScience* 23(4): 101018. https://doi.org/10.1016/j.isci.2020.101018.

Ross-Innes, Caryn S. et al. 2012. “Differential Oestrogen Receptor Binding Is Associated with Clinical Outcome in Breast Cancer.” *Nature* 481(7381): 389–93. http://dx.doi.org/10.1038/nature10730.

Ross, Julie, Lionel Mavoungou, Emery H. Bresnick, and Eric Milot. 2012. " GATA-1 Utilizes Ikaros and Polycomb Repressive Complex 2 To Suppress Hes1 and To Promote Erythropoiesis ." *Molecular and Cellular Biology* 32(18): 3624–38.

Rowley, Janet D. 1973. "A New Consistent Chromosomal Abnormality in Chronic Myelogenous Leukaemia Identified by Quinacrine Fluorescence and Giemsa Staining." *Nature* 243: 290–93. http://www.nature.com/nature/journal/v242/n5393/abs/242117a0.html.

Salomao, Marcela et al. 2010. "Hereditary Spherocytosis and Hereditary Elliptocytosis: Aberrant Protein Sorting during Erythroblast Enucleation." *Blood* 116(2): 267–69.

Sankaran, Vijay G. et al. 2008. "Human Fetal Hemoglobin Expression Is Regulated by the Developmental Stage-Specific Repressor BCL11A." *Science* 322(5909): 1839–42.

Sankaran, Vijay G., Stuart H. Orkin, and Carl R. Walkley. 2008. "Rb Intrinsically Promotes Erythropoiesis by Coupling Cell Cycle Exit with Mitochondrial Biogenesis." *Genes and Development* 22(4): 463–75.

Schaefer, Brian C. et al. 2001. "Observation of Antigen-Dependent CD8+ T-Cell/Dendritic Cell Interactions in Vivo." *Cellular Immunology* 214(2): 110–22.

Schmidt, Dominic et al. 2014. "ChIP-Seq: Using High-Throughput Sequencing to Discover Protein-DNA Interactions." *Methods* 48(3): 240–48.

Schneider, Rebekka K., and Ruud Delwel. 2018. "Puzzling Pieces of Chromosome 7 Loss or Deletion." *Blood* 131(26): 2871–72.

Schroeder, Harry W. Jr., and Lisa Cavacini. 2010. "Structure and Function of Immunoglobulins (Author Manuscript)." *Journal of Allergy and Clinical Immunology* 125: S41–52.

Schulz, Vincent P et al. 2019. "A Unqiue Epigenomic Landscape Defines Humman Erythropoiesis." 28(11): 2996–3009.

Seto, Edward, and Minoru Yoshida. 2014. "Erasers of Histone Acetylation: The Histone Deacetylase Enzymes." *Cold Spring Harbor Perspectives in Biology* 6(4).

Sharma, Madhulika et al. 2009. "The Homeodomain Protein Cux1 Interacts with Grg4 to Repress P27kip1 Expression during Kidney Development." *Gene* 439(1–2): 87–94. http://dx.doi.org/10.1016/j.gene.2009.03.014.

Shimizu, Takafumi et al. 2016. "Loss of Ezh2 Synergizes with JAK2-V617F in Initiating Myeloproliferative Neoplasms and Promoting Myelofibrosis." *Journal of Experimental Medicine* 213(8): 1479–96.

Sinclair, Angus M. et al. 2001. "Lymphoid Apoptosis and Myeloid Hyperplasia in CCAAT

Displacement Protein Mutant Mice.” *Blood* 98(13): 3658–67.

Singleton, Belinda K. et al. 2008. “Mutations in EKLFIKLF1 Form the Molecular Basis of the Rare Blood Group In(Lu) Phenotype.” *Blood* 112(5): 2081–88.

Sivertsen, Einar Andreas et al. 2006. “PI3K/Akt-Dependent Epo-Induced Signalling and Target Genes in Human Early Erythroid Progenitor Cells.” *British Journal of Haematology* 135(1): 117–28.

Smyth, Gordon K. 2004. “Linear Models and Empirical Bayes Methods for Assessing Differential Expression in Microarray Experiments.” *Statistical Applications in Genetics and Molecular Biology* 3(1): 1–26.

Snyder, Gregory K., and Brandon A. Sheafor. 1999. “Red Blood Cells: Centerpiece in the Evolution of the Vertebrate Circulatory System.” *American Zoologist* 39(2): 189–98.

Snyder, Steven R., Jing Wang, Jeffrey F. Waring, and Gordon D. Ginder. 2001. “Identification of CCAAT Displacement Protein (CDP/Cut) as a Locus-Specific Repressor of Major Histocompatibility Complex Gene Expression in Human Tumor Cells.” *Journal of Biological Chemistry* 276(7): 5323–30.

Socolovsky, Merav et al. 1999. “Fetal Anemia and Apoptosis of Red Cell Progenitors in Stat5a-/-5b-/- Mice: A Direct Role for Stat5 in Bcl-XL Induction.” *Cell* 98(2): 181–91.

———. 2001. “Ineffective Erythropoiesis in Stat5a-/-5b-/- Mice Due to Decreased Survival of Early Erythroblasts.” *Blood* 98(12): 3261–73.

Soslau, Gerald. 2020. “The Role of the Red Blood Cell and Platelet in the Evolution of Mammalian and Avian Endothermy.” *Journal of Experimental Zoology Part B: Molecular and Developmental Evolution* 334(2): 113–27.

Spagnol, Stephen T., and Kris Noel Dahl. 2016. “Spatially Resolved Quantification of Chromatin Condensation through Differential Local Rheology in Cell Nuclei Fluorescence Lifetime Imaging.” *PLoS ONE* 11(1): 1–19.

Stark, Rory, and Gordon Brown. 2011. “DiffBind : Differential Binding Analysis of ChIP-Seq Peak Data.” : 1–27. http://bioconductor.org/packages/release/bioc/vignettes/DiffBind/inst/doc/DiffBind.pdf.

Subramanian, Aravind et al. 2005. “Gene Set Enrichment Analysis: A Knowledge-Based Approach for Interpreting Genome-Wide Expression Profiles.” *Proceedings of the National Academy of Sciences of the United States of America* 102(43): 15545–50. http://www.ncbi.nlm.nih.gov/pubmed/16199517.

Sui, Zhenhua et al. 2014. “Tropomodulin3-Null Mice Are Embryonic Lethal with Anemia Due to Impaired Erythroid Terminal Differentiation in the Fetal Liver.” *Blood* 123(5):

758–67.

Sundaravel, Sriram et al. 2015. “Reduced *DOCK4* Expression Leads to Erythroid Dysplasia in Myelodysplastic Syndromes.” *Proceedings of the National Academy of Sciences*: 201516394. http://www.pnas.org/lookup/doi/10.1073/pnas.1516394112.

———. 2019. “Loss of Function of DOCK4 in Myelodysplastic Syndromes Stem Cells Is Restored by Inhibitors of DOCK4 Signaling Networks.” *Clinical Cancer Research* 25(18): 5638–49.

Sundaravel, Sriram, Ulrich Steidl, and Amittha Wickrema. 2021. “Epigenetic Modifiers in Normal and Aberrent Erythropoeisis.” *Seminars in Hematology* 58(1): 15–26.

Swartz, Kelsey L. et al. 2017. “E2F-2 Promotes Nuclear Condensation and Enucleation of Terminally Differentiated Erythroblasts.” *Molecular and Cellular Biology* 37(1): 1–18.

Takahashi, Koichi et al. 2017. “Copy Number Alterations Detected as Clonal Hematopoiesis of Indeterminate Potential.” *Blood Advances* 1(15): 1031–36.

Tallack, Michael R. et al. 2010. “A Global Role for KLF1 in Erythropoiesis Revealed by ChIP-Seq in Primary Erythroid Cells.” *Genome Research* 20(8): 1052–63.

Thein, Swee Lay. 2013. “The Molecular Basis of β-Thalassemia.” *Cold Spring Harbor Perspectives in Medicine* 3(5): 1–24.

Thorvaldsdóttir, Helga, James T. Robinson, and Jill P. Mesirov. 2013. “Integrative Genomics Viewer (IGV): High-Performance Genomics Data Visualization and Exploration.” *Briefings in Bioinformatics* 14(2): 178–92.

Tsang, Alice P. et al. 1997. “FOG, a Multitype Zinc Finger Protein, Acts as a Cofactor for Transcription Factor GATA-1 in Erythroid and Megakaryocytic Differentiation.” *Cell* 90(1): 109–19.

Tsang, Alice P., Yuko Fujiwara, Dennis B. Horn, and Stuart H. Orkin. 1998. “Failure of Megakaryopoiesis and Arrested Erythropoiesis in Mice Lacking the GATA-1 Transcriptional Cofactor FOG.” *Genes and Development* 12(8): 1176–88.

Tufarelli, C, Y Fujiwara, D C Zappulla, and E J Neufeld. 1998. “Hair Defects and Pup Loss in Mice with Targeted Deletion of the First Cut Repeat Domain of the Cux/CDP Homeoprotein Gene.” *Developmental biology* 200(1): 69–81. http://www.ncbi.nlm.nih.gov/pubmed/9698457.

Ubukawa, Kumi et al. 2012. “Enucleation of Human Erythroblasts Involves Non-Muscle Myosin IIB.” *Blood* 119(4): 1036–44.

Velten, Lars et al. 2017. “Human Haematopoietic Stem Cell Lineage Commitment Is a Continuous Process.” *Nature Cell Biology* 19(4): 271–81.

http://www.nature.com/doifinder/10.1038/ncb3493.

Viprakasit, Vip et al. 2014. “Mutations in Krüppel-like Factor 1 Cause Transfusion-Dependent Hemolytic Anemia and Persistence of Embryonic Globin Gene Expression.” *Blood* 123(10): 1586–95.

Wadman, Isobel A. et al. 1997. “The LIM-Only Protein Lmo2 Is a Bridging Molecule Assembling an Erythroid, DNA-Binding Complex Which Includes the TAL1, E47, GATA-1 and Ldb1/NLI Proteins.” *EMBO Journal* 16(11): 3145–57.

Wagner, Brett A., Sujatha Venkataraman, and Garry R. Buettner. 2011. “The Rate of Oxygen Utilization by Cells.” *Free Radical Biology and Medicine* 51(3): 700–712. http://dx.doi.org/10.1016/j.freeradbiomed.2011.05.024.

Wang, Yaomei et al. 2021. “Impairment of Human Terminal Erythroid Differentiation by Histone Deacetylase 5 Deficiency.” *Blood*.

Wang, Zhibin et al. 2009. “Genome-Wide Mapping of HATs and HDACs Reveals Distinct Functions in Active and Inactive Genes.” *Cell* 138(5): 1019–31. http://dx.doi.org/10.1016/j.cell.2009.06.049.

Warren, Alan J. et al. 1994. “The Oncogenic Cysteine-Rich LIM Domain Protein Rbtn2 Is Essential for Erythroid Development.” *Cell* 78(1): 45–57.

Warren, Sean C. et al. 2013. “Rapid Global Fitting of Large Fluorescence Lifetime Imaging Microscopy Datasets.” *PLoS ONE* 8(8).

Watowich, Stephanie S. 2011. “The Erythropoietin Receptor: Molecular Structure and Hematopoietic Signaling Pathways.” *Journal of investigative medicine : the official publication of the American Federation for Clinical Research* 59(7): 1067–72. http://www.pubmedcentral.nih.gov/articlerender.fcgi?artid=3134576&tool=pmcentrez&rendertype=abstract.

White, Jacqueline K. et al. 2013. “Genome-Wide Generation and Systematic Phenotyping of Knockout Mice Reveals New Roles for Many Genes.” *Cell* 154(2): 452.

Wilting, Roel H. et al. 2010. “Overlapping Functions of Hdac1 and Hdac2 in Cell Cycle Regulation and Haematopoiesis.” *EMBO Journal* 29(15): 2586–97. http://dx.doi.org/10.1038/emboj.2010.136.

Witthuhn, Bruce A. et al. 1993. “JAK2 Associates with the Erythropoietin Receptor and Is Tyrosine Phosphorylated and Activated Following Stimulation with Erythropoietin.” *Cell* 74(2): 227–36.

Won, Hong Hee et al. 2009. “Comparative Analysis of the JAK/STAT Signaling through Erythropoietin Receptor and Thrombopoietin Receptor Using a Systems Approach.” *BMC Bioinformatics* 10(Supplement I): 1–10.

Wong, Chi C et al. 2013. “Inactivating CUX1 Mutations Promote Tumorigenesis.” *Nature Genetics* 46(1): 33–38. http://www.nature.com/doifinder/10.1038/ng.2846.

Wu, Hong, Xin Liu, Rudolf Jaenisch, and Harvey F. Lodish. 1995. “Generation of Committed Erythroid BFU-E and CFU-E Progenitors Does Not Require Erythropoietin or the Erythropoietin Receptor.” *Cell* 83(1): 59–67.

Yajnik, Vijay et al. 2003. “DOCK4, a GTPase Activator, Is Disrupted during Tumorigenesis.” *Cell* 112(5): 673–84.

Yamamura, Kentaro et al. 2006. “Pleiotropic Role of Histone Deacetylases in the Regulation of Human Adult Erythropoiesis.” *British Journal of Haematology* 135(2): 242–53.

Yoshida, Kenichi et al. 2011. “Frequent Pathway Mutations of Splicing Machinery in Myelodysplasia.” *Nature* 478(7367): 64–69.

Yu, Ming et al. 2009. “Insights into GATA-1-Mediated Gene Activation versus Repression via Genome-Wide Chromatin Occupancy Analysis.” *Molecular Cell* 36(4): 682–95. http://dx.doi.org/10.1016/j.molcel.2009.11.002.

Yuan, Zuo Fei et al. 2018. “EpiProfile 2.0: A Computational Platform for Processing Epi-Proteomics Mass Spectrometry Data.” *Journal of Proteome Research* 17(7): 2533–41.

Zhang, Jing et al. 2020. “DiNeR: A Differential Graphical Model for Analysis of Co-Regulation Network Rewiring.” *BMC Bioinformatics* 21(1): 1–15.

Zhang, Jing, and Harvey F. Lodish. 2007. “Endogenous K-Ras Signaling in Erythroid Differentiation.” *Cell Cycle* 6(16): 1970–73.

Zhang, Jing, Merav Socolovsky, Alec W Gross, and Harvey F Lodish. 2003. “Role of Ras Signaling in Erythroid Differentiation of Mouse Fetal Liver Cells : Functional Analysis by a Flow Cytometry – Based Novel Culture System.” *Blood* 102(12): 3938–46.

Zhang, Jiwang et al. 2006. “PTEN Maintains Haematopoietic Stem Cells and Acts in Lineage Choice and Leukaemia Prevention.” *Nature* 441(25): 518–22.

Zhang, Qi et al. 2019. “Mutations in EZH2 Are Associated with Poor Prognosis for Patients with Myeloid Neoplasms.” *Genes and Diseases* 6(3): 276–81. https://doi.org/10.1016/j.gendis.2019.05.001.

Zhang, Yong et al. 2008. “Model-Based Analysis of ChIP-Seq (MACS).” *Genome Biology* 9(9).